GLOBAL ENVIRONMENTAL CHANGE EFFECTS ON FOREST DYNAMICS: LESSONS FROM PERMANENT SAMPLE PLOT NETWORKS

By

Eric Searle

A Dissertation Submitted in

Partial Fulfillment of the Requirements for the

Degree of Doctor of Philosophy in Forest Sciences

Faculty of Natural Resources Management

Lakehead University

July 2019

ABSTRACT

Global environmental change caused by anthropogenic emissions of greenhouse gasses is a major threat to forest ecosystems globally. Before we can begin to adequately mitigate these threats, we first must understand how these systems are being affected. The purpose of this dissertation is to provide an understanding of how best to estimate these effects, investigate possible mechanisms of mitigation, and provide the first ground-based global estimate of changes in forest productivity in response to global environmental change.

In my first study, I examined how the use of size-thresholds can bias estimates of forest biomass gain, loss, and net change. Permanent sample plot networks are intensively sampled, spatially extensive, and as a result often quite costly. In an effort to reduce costs of these networks, tree size-thresholds are often used which leads to measurement of solely large trees. However, it is unclear whether these size-thresholds bias estimates of the effects of global environmental change on stand biomass gain, loss, and net change. Using a network of 141 permanent sample plots from Manitoba, Canada, with all trees of >1.3 m in height repeatedly measured, I constructed three distinct data sets: using a 10 cm, 5 cm, and no diameter at breast height threshold. These three data sets were then used to demonstrate that stand biomass gain and loss were increasingly underestimated as thresholds increased. This underestimation was particularly noticeable in the relationship between biomass gain and age: the peak productivity was estimated to be 20 years later when using a 10 cm threshold in comparison to no threshold. Despite bias in estimates of stand biomass gain and loss as stands aged, there was little evidence for any bias in estimates of global environmental change effects on forest biomass gain, loss, or net change. These results suggest that, if not properly controlled for, the use of tree size thresholds can significantly bias estimates of forest biomass gain, loss, and net change.

In my second study, I examined how tree longevity has responded to global environmental change. In particular, acceleration in tree life cycles (i.e., reduced longevity in trees with faster lifetime growth rates) has been hypothesized as a cause of increased tree mortality in response to global environmental change. However, this link has never been explicitly tested. In light of this, I defined two testable hypotheses: (i) the probability of ageing driven tree mortality increases with global change and (ii) the mortality probability associated with global change is higher for faster-growing trees. To test these hypotheses, I examined the temporal changes of tree mortality probability in 539 permanent sample plots monitored from 1960 to 2009, with ages greater than 100 years at initial censuses, across the boreal region of Alberta, Canada. I demonstrated that tree longevity has been reduced as a result of global environmental change. Further, I demonstrated that this reduction in longevity was strongest for those trees with the fastest lifetime growth rates. These reduced longevities were linked to increasing atmospheric carbon dioxide and reduced water availability, indicating that the reductions in longevity will likely continue with future global environmental change.

In my third study, I examined the potential of enhancing niche complementarity as a way to mitigate the negative effects, or enhance the positive effects, of global change on individual tree productivity. Specifically, I hypothesized that individual trees with functionally and phylogenetically dissimilar neighbours would grow more quickly and experience less

competition under global environmental change than those with functionally and phylogenetically similar neighbours. Our results showed that while competition intensity was increasing over the study period, the beneficial effects of niche complementarity were increasing more rapidly. This demonstrated that trees with functionally and phylogenetically diverse neighbourhoods were able to respond more favourably (i.e., have less reduced growth or increased growth depending on their competitive position) to global environmental change than those with functionally and phylogenetically similar neighbourhoods.

Finally, my fourth study integrated data from a global plot network with an average measurement period of 46 years per biome to estimate that forest productivity has significantly declined with ongoing global environmental change. The decline was equivalent to about 0.21% per year across the network, or about 0.06% per year when weighting for the land area represented by each plot. My results indicated that, despite some regional variability, increasing temperature was a net negative to forest productivity. Across the globe, changes in water availability were found to be a major driver of forest productivity and declines in water availability were associated with declines in forest productivity. Increasing nitrogen deposition was unable to offset the negative effects of increases in temperature and changes in water availability. Our results highlight that while forest ecosystems are still an important sink, their capacity to retain carbon is being threatened by global environmental change.

This dissertation has provided a robust investigation into how we measure global change effects on forest ecosystem dynamics and provided evidence for best practises. Further, it demonstrates direct evidence of decreased longevity in faster-growing trees. This dissertation also provides a potential avenue for mitigation of global environmental change effects on individual tree productivity: maintenance or promotion of functional and phylogenetic diversity. Finally, the dissertation provides the first ground-based estimate of the response of global forest productivity to global environmental change.

Keywords: boreal forest; climate change; competition; forest productivity; global change; global environmental change; niche complementarity; phylogenetic diversity; sampling bias; size threshold; stand development; tree growth; tree longevity; tree mortality

CONTENTS

LIST OF TABLES

LIST OF FIGURES

ACKNOWLEDGEMENTS

First and foremost, I must thank my family and friends for their love and support throughout the writing of this dissertation and my graduate studies. My erstwhile girlfriend, then fiancé, and now wife Kayla who has been the reason I was able to complete my studies and a constant source of joy. She has put up with many weekends and nights alone and times when I was physically present but mentally absent. To my parents, Mary and Bryan, who have always been there for me, who have listened as I blathered on about the vagaries of a specific statistical methodology, the wording of a particularly nettlesome hypothesis, or the difficulties that have arisen on my journey. To my sister, Kaitlynn, who is always up for a walk when I need to take a break and who has spent many nights taking care of our dogs when we were unable to. To my grandfather, Chuck, for his advice on writing and frequent engagement with my work. To my dearest grandmother, Marion, for her insightfulness, encouragement, and occasional figurative swift kick to the rear when needed. To my Opa, may you rest eternal and may His light shine perpetually on you: I will never forget the example you gave me to live up to. To my in-laws, Karen, Gilles, Logan, and all, who have welcomed me into their family and have provided me with their love and support. To all of my groomsmen: Anders, Nick, Connor, and Brad, to Ava, and to Jess, without all of whom I could not have made it. To our dogs, Winnie and Teddy who I am fairly certain have heard more about statistics and forestry than any other canines alive. And finally, to my soon-to-arrive daughter, Daphne. I can not wait to meet you.

I also wish to offer my sincere thanks and appreciation to my supervisor, Dr. Han Chen. I would not be the researcher I have become without your guidance, critique, and support. I would also like to thank my committee members, Dr. Chander Shahi and Dr. Gordon Kayahara for their useful and insightful comments. To my Graduate Assistant supervisors over the course of my PhD: Dr Shashi Shahi, Lorne Morrow, Laird Van Damme, and of course Dr. Don Henne who has been particularly helpful in aiding me to progress as an educator.

I would like to thank my lab colleagues that have had major contributions to my work and have supported me throughout: Tim, Zilong, Si, and my niece Yilin, Yong, Aaron, Masumi, Xinli, Chen, Dan, Alex, Connor, and Auldrey as well as all of my fellow labmates past and present. I would also like to thank the graduate community at Lakehead University, the members of CUPE Local 3905 for electing me as President for four years in a row, and the graduate students in Natural Resources Management for five wonderful years of Research Methods. I would also like to thank my “faith-family” at St. Paul’s Anglican Church for their support and for offering opportunities to make a difference in the community outside of research and the brethren of Shuniah Lodge for their exemplification of Brotherly Love.

Financial support for this dissertation was provided by the Natural Sciences and Engineering Research Council of Canada (RGPIN-2014-0418 and STPGP 506284). I would like to thank NSERC for an Alexander Graham Bell award. I am eternally grateful to all of the provincial forestry branches for their participation in this research.

NOTE

This is a manuscript-based thesis. The chapters were written to suit the submission requirements of the targeted journals. Formatting and reference styles may differ. Since individual chapters reflect the joint contributions of myself and my academic supervisor I use “we” instead of “I” for individual manuscripts.

Chapters:

2. Searle, E.B. & Chen, H.Y.H. (2017). Tree size thresholds produce biased estimates of forest biomass dynamics. Forest Ecology and Management, 400, 468-474.

3. Searle, E. B., & Chen, H. Y. H. (2018). Temporal declines in tree longevity associated with faster lifetime growth rates in boreal forests. Environmental Research Letters, 13(12), 125003.

4. Searle, E. B., & Chen, H. Y. H. (2019). Complementarity effects are strengthened by competition intensity and global environmental change in the central boreal forests of Canada. Submitted.

5. Searle, E. B., & Chen, H. Y. H. (2019). Weakening of the natural forest carbon sink. In preparation.

CHAPTER 1: GENERAL INRODUCTION

Anthropogenic climate change (here meant to represent increases in atmospheric carbon dioxide, increases in temperature, and alteration of precipitation cycles and water availability) is threatening ecosystems across the globe (Hoegh-Guldberg *et al.* 2018). The major driver of anthropogenic climate change is emissions of greenhouse gasses from the burning of fossil fuels (IPCC 2013) and reduction in these emissions must occur to be able to halt average global warming at 1.5°C above pre-industrial averages (de Coninck *et al.* 2018). In addition to reductions in emissions, mitigating the impact of anthropogenic climate change on forest ecosystems is important since they are responsible for at least a quarter of the total global carbon sink (Pan *et al.* 2011a). Within global forest ecosystems, the boreal forest is responsible for 49% of carbon storage (Dixon *et al.* 1994). Understanding, therefore, how global environmental change will affect forest ecosystems in general, and the boreal forest in particular, is crucial to developing strategies to mitigate the effects of anthropogenic climate change.

The effects of anthropogenic climate change on forest ecosystems are varied: increases in tree mortality have been observed across the globe (Allen *et al.* 2010; Allen *et al.* 2015), while changes in productivity reported by regional studies have been both positive (Hember *et al.* 2012; Pretzsch *et al.* 2014; Brienen *et al.* 2015) and negative (De Dios *et al.* 2007; Hogg *et al.* 2017; Zhang *et al.* 2018). In the boreal forest, responses seem to be largely dependent on water availability. In regions with lowered water availability, extensive mortality (Peng *et al.* 2011; Luo & Chen 2013; Luo *et al.* 2019) and loss in productivity (Ma *et al.* 2012; Girardin *et al.* 2016; Chen *et al.* 2018) have been reported. However, in regions without loss in water availability increases in productivity due to increasing temperature have been reported - although these effects may be transitory as warming exceeds thermal tolerances of the trees present

(D'Orangeville *et al.* 2018). These regions not experiencing loss of water availability have also been reported to be experiencing increases in tree mortality due to increasing intensity of competition (Luo & Chen 2015). These studies have been essential to shaping our understanding of how anthropogenic climate change has affected forest ecosystem dynamics at regional scales. However, in order to properly mitigate the effects of anthropogenic climate change on forest ecosystems, we need to synthesize data from multiple permanent sample plot networks that operate under different methodologies. Whether the use of different methodologies biases our estimates of climate change effects remains untested.

In regions where global environmental change has been shown to promote stand level productivity reduced longevity due to increased individual tree productivity has been highlighted as a possible driver of increased biomass loss due to mortality (Brienen *et al.* 2015). Despite the relationship between fast lifetime growth rates and shorter lifespans being well established across environmental gradients for trees (Bigler & Veblen 2009; Di Filippo *et al.* 2015) whether or not fast-growing trees are dying more quickly than slow growing trees in the face of global environmental change has not been directly tested.

Given the wide range of climate outcomes for global environmental change, and subsequent effects on forest ecosystem dynamics, the promotion or maintenance of tree diversity has been proposed as a potential mitigation strategy for forest ecosystems (Hisano *et al.* 2018; Ammer 2019). Higher tree diversity can help to buffer against the negative effects of climate change through maintenance of functional diversity and to promote the beneficial effects of climate change in areas without declining water availability through reduction in niche-overlap and competition (Hisano *et al.* 2018; Ammer 2019). Previous work has shown that increasing tree species richness leads to higher productivity and reduced mortality in stands in the western

Canadian boreal forest (Hisano *et al.* 2019), but the underlying mechanism of reduced intensity of competition in more diverse stands remains untested.

Regional estimates of forest productivity are essential to our understanding of how global environmental change will impact specific forests. Additionally, these studies support hypothesis testing of how specific global environmental change drivers will affect forest biomass dynamics. Indeed, these regional studies support the theoretical foundation of the following three chapters of this dissertation. While significant numbers of regional estimates of global environmental change effects on forest productivity using ground sourced data have been published (De Dios *et al.* 2007; Hember *et al.* 2012; Pretzsch *et al.* 2014; Brienen *et al.* 2015; Chen & Luo 2015; Chen *et al.* 2016; Hogg *et al.* 2017; Searle & Chen 2017a; Zhang *et al.* 2018), there has been no global ground-based estimate of the effect of global environmental change on forest productivity. Previous estimates at global or near-global scales have relied on satellite-derived productivity indices (Huang *et al.* 2017) or inferring changes in forest productivity from estimates of changes in atmospheric carbon dioxide fluxes (Forkel *et al.* 2016). Ground-sourced estimates of forest productivity that are able to account for endogenous processes related to stand basal area density and recovery from disturbance (Baccini *et al.* 2017) are necessary to properly estimate the impact of global environmental change on forest productivity globally. These estimates are essential to understanding how the global forest carbon sink will respond to future global environmental change.

The objective of this dissertation was to further our understanding of anthropogenic climate change effects on forest dynamics with a focus on boreal forest dynamics. To accomplish this, I first undertook an examination of whether use of size thresholds in permanent sample plot networks biased estimates of climate change effects on forest biomass gain, loss, and net change

estimates. Second, I examined whether the quickest growing trees in a stand were more susceptible to climate change-related mortality than the slowest growing trees. Third, I examined whether trees in a neighbourhood with functionally and phylogenetically dissimilar neighbours were benefitting more from climate change than those growing in a neighbourhood with functionally and phylogenetically similar neighbours. Finally, I examined how anthropogenic climate change is affecting forest productivity at a global scale.

CHAPTER 2: TREE SIZE THRESHOLDS PRODUCE BIASED ESTIMATES OF FOREST BIOMASS DYNAMICS

2.1 Abstract

Studies that examine forest biomass dynamics often rely on long-term, spatially extensive, repeatedly measured permanent sample plots. Due to the intensive cost of sampling all trees within these plots, an arbitrary size threshold is typically imposed, which leads to only larger trees being sampled. However, it remains unclear whether the sampling of only large trees is representative of the entirety of stands of diverse sizes; the sampling of only large trees may produce biased estimates of biomass dynamics (growth, ingrowth, and mortality). Using a network of 141 permanent sample plots from Manitoba, Canada, with all trees of >1.3 m in height repeatedly measured, we constructed three distinct data sets, with 10 cm, 5 cm, and no diameter at breast height threshold, to illustrate that total productivity and mortality are increasingly underestimated with increasingly larger diameter at breast height thresholds. This effect is particularly significant in young stands, where productivity estimates peak at least 20 years earlier than the determined estimates under large thresholds. We highlight the need to account for smaller trees in long-term observational studies to ensure unbiased estimates of stand level aboveground biomass productivity and loss.

2.2 Introduction

Accurate estimates of the changes in forest demographic rates (growth of surviving trees, recruits, and mortality) are essential toward understanding the contribution of forest biomass changes to the global carbon cycle (Pan *et al.* 2011a), climate change impacts on forest biomass (Ma *et al.* 2012; Brienen *et al.* 2015; Doughty *et al.* 2015; Zhang *et al.* 2015; Chen *et al.* 2016), and the relationships between tree species diversity and productivity (Liang et al. 2016). Long-

term repeatedly measured permanent sample plots (PSPs) are not only essential in the estimation of forest demographic rates, but also for the calibration of remote sensing data when mapping forest biomass distribution (Avitabile et al. 2016). However, these PSPs have been generally restricted to large trees, i.e., diameter at breast height (DBH) ≥10 cm. Accordantly, national surveys that have been developed to meet the requirements of the Kyoto Protocol often impose thresholds on plots to ease the sampling burden. In the United States of America, for example, woody plants are only considered "trees" if they attain 12.7 cm in DBH (USDA Forest Service 2010). In Canada's National Forest Inventory, only trees >9 cm in DBH are measured at the full plot size, with all other trees being measured in considerably smaller plots (Canadian Council of Forest Ministers 2008). These thresholds may lead to technical issues in the estimation of demographic rates. For example, trees that attain a threshold, but die before being measured (i.e., "unobserved recruits") may bias estimates (Talbot et al. 2014). Even studies that rely on increment coring to generate growth estimates tend to core trees >10 cm in DBH (Prior & Bowman 2014; Stephenson et al. 2014; Elliott et al. 2015). However, it remains untested whether temporal alterations in forest demographic rates observed from large trees represent those that include trees of all sizes.

When measuring stand productivity, an arbitrary DBH sampling threshold can lead to five scenarios. The first occurs when a tree is already at the threshold during the initial and second census, which is an accurate measurement of tree growth. The second is when a tree is below the threshold during the first and second census. This leads to an underestimation of tree growth, as the sampling procedure is "blind" to this tree. The third scenario occurs when the tree is absent during the first census, and achieves, or exceeds, the threshold during the second census, which is an accurate measurement of recruitment. The fourth scenario occurs when the

tree is below the threshold during the first census and achieves or exceeds the threshold during the second census. This would lead to an overestimation of tree recruitment, as the threshold measurement would count the tree as recruitment, while a no DBH threshold measurement would count the tree, properly, as growth. The final scenario occurs when a tree is absent during the first census and transitions from seedling to sapling, but does not achieve the threshold. This leads to an underestimation of recruitment using a threshold, as the threshold measurement is once again "blind" to the tree.

When using a threshold, total stand growth may only be accurately measured if all trees in a stand represent scenario one; otherwise, growth will be underestimated. Total stand recruitment will be overestimated using a threshold if the biomass from scenario four exceeds the biomass in scenario five; otherwise, if the biomass from trees representing scenario five exceeds the biomass of scenario four, recruitment will be underestimated. Recruitment may only be accurately estimated if all recruited trees represent scenario three. When measuring the biomass lost due to mortality with a threshold, there are only two possible scenarios for a tree. The first is that the tree meets or exceeds the threshold in the first census and is dead at the second census. The second is that the tree is below the threshold at the first census and is dead at the second census. If any trees in a stand align with scenario two, stand biomass lost due to mortality will be underestimated.

These arbitrary thresholds may alter our estimates of climate change driven responses of forest biomass. Similar to previous studies (Ma *et al.* 2012; Brienen *et al.* 2015; Doughty *et al.* 2015; Zhang *et al.* 2015; Chen *et al.* 2016), we consider the changes of demographic rates associated with the calendar year to be driven by climate changes as a whole. Although larger trees add significantly more biomass than do smaller trees, on an individual tree basis

(Stephenson et al. 2014), they tend to have higher mortality probabilities during drought (Bennett et al. 2015) and slower growth rates under warmer temperatures (Prior & Bowman 2014). When aggregated to the stand level, tree mortality rates associated with climate change tend to increase faster in younger forests than those in older forests (Luo & Chen 2013). It is important to note that when comparing the effects of tree sizes or stand ages, several studies (Luo & Chen 2013; Prior & Bowman 2014; Stephenson et al. 2014) have sampled trees of only >10 cm in DBH. Previous investigations using observational data from large trees have found that biomass gain from productivity increased at slower rates than did biomass loss from mortality, leading to an overall net biomass loss associated with climate change over the past thirty years in boreal and tropical forests (Brienen *et al.* 2015; Chen *et al.* 2016). If smaller trees within a stand can grow more rapidly and be less susceptible to increased mortality (Bennett et al. 2015), then studies that rely on solely large trees may be underestimating the biomass that is gained from growth, while overestimating biomass loss from increased mortality rates. This may lead to an overestimate of the negative effects of temporal trends associated with climate change on net aboveground biomass change.

The use of DBH thresholds may also alter our predictions of how forest stands respond to stand development. Generally, subsequent to a stand-replacing disturbance, stands are initiated through a high level of recruits, which grow quickly (Oliver & Larson 1990; Poorter et al. 2016). Once canopy trees attain their maximum longevity, they are replaced by understorey trees. This gap dynamics phase is theorized as biomass gain from the growth of surviving trees and recruits equaling biomass loss from mortality (Oliver & Larson 1990; Coomes et al. 2012). Sampling trees >10 cm in DBH may lead to higher underestimations of growth and mortality at younger ages. In boreal forests, for example, the majority of aboveground biomass is contained within

small trees (<10 cm in DBH) in stands younger than 27 years old, while large trees (≥10 cm in DBH) become the primary reservoirs of aboveground biomass quickly thereafter (Taylor et al. 2014). How DBH threshold use may bias estimates in the biomass dynamics of regenerating stands is critical to understand, in the face of increasing stand-replacing disturbances (Westerling et al. 2006; Millar & Stephenson 2015).

Here we used a network of 141 repeatedly measured PSPs, located throughout Manitoba, Canada to assess how DBH thresholds may alter biomass change estimates associated with each of the three demographic rates, and the predictions for their responses to temporal trends associated with climate change and stand ageing processes. These plots were established in stands that regenerated naturally following stand replacing wildfire, and underwent repeated censuses every five years, from 1985 to 2010. During each census, all trees >1.3 m in height were tagged and measured for DBH. The dataset included a total of 54,795 individual trees at least 1.3m in height and an average of 3.4 recorded measurements per stem.

2.3 Materials and Methods

2.3.1 Study area and long-term repeatedly measured sample plots

We used permanent sample plots (PSPs) established throughout Manitoba, Canada, commencing in 1985, by the Provincial Government of Manitoba (data is available upon request). The PSPs were located in visually homogenous stands of greater than 1 ha in size, at least 100 m from any openings to minimize edge effect impacts. We selected 141 plots for our study, using the following selection criteria: (*i*) PSPs had a known origin date of stand replacing wildfire, and were unmanaged; (*ii*) PSPs had all trees marked and tagged with diameter at breast height (DBH) and species identification accurately tracked over multiple censuses; and, (*iii*) PSPs had to have a minimum of three censuses with a census length of 5 years. Since the Manitoba government has

applied its own threshold of 7.1 cm DBH for all measurements after 2011, only measurements before 2011 were included in this study (i.e., measurements where all trees of ≥1.3 m in height were tagged and measured). Plots ranged from 95.3° to 101.7°W in longitude, 49.0° to 56.99°N in latitude, and from 159 to 406 m above sea level in elevation (Fig. A2-1). Plots were generally established in forests dominated by *Populus tremuloides* Michx., *Pinus banksiana* Lamb., and *Picea mariana* (Mill.) Britton, Sterns & Poggenb. Species that made up at least 1% of aboveground biomass across all plots consisted of: *Pinus banksiana* (33.6%), *Populus tremuloides* (23.7%), *Picea mariana* (21.7%), *Larix laricina* (Du Roi) K. Koch (5.4%), *Picea glauca* (Moench) Voss (3.7%), *Abies balsamea* (L.) Mill. (3.3%), *Fraxinus nigra* Marshall (3.0%), *Betula papyrifera* Marshall (2.7%), *Fraxinus pennsylvanica* Marshall (1.7%), and *Thuja occidentalis* L. (1.0%). We examined 13 trees that grew more than 2 cm yr^{-1} in DBH for measurement errors. We corrected their growth rate to the mean growth rate of the binned 10 cm growth rate (i.e., 0-10 cm, 10-20 cm, 20-30 cm, etc).

2.3.2 Biomass component calculation

Biomass for each individual stem was calculated using species specific equations for stems of below 3 cm in DBH (Bond-Lamberty *et al.* 2002), and stems above 3 cm in DBH (Lambert *et al.* 2005), at each census, and summed to obtain total stand biomass. Annual biomass growth was calculated as the amount of biomass added by surviving trees between measurements, divided by the census interval. Annual biomass added due to ingrowth was calculated as the amount of biomass added due to recruits between measurements, divided by the census interval. Annual productivity was the summation of annual growth and annual ingrowth. Annual biomass lost due to mortality was calculated as the quantity of biomass lost due to trees that had died between measurements, divided by the census interval. To derive stand-level estimates, we conducted

three separate analyses: one using only trees of ≥10 cm in DBH (hereafter 10 cm threshold), one using only trees of ≥5 cm in DBH (hereafter 5 cm threshold), and one using all trees of >1.3 m in height (hereafter no DBH threshold).

2.3.3 Explanatory variables

We used mid-calendar year (i.e., average of initial and final measurements during a census period) to represent temporal trends associated with climate change (van Mantgem *et al.* 2009; Chen & Luo 2015), corresponding to each census period of each plot. This encompassed not only the systematic increases in atmospheric CO_2 concentrations and temperatures throughout our study region (IPCC 2013), but also non-climatic drivers, such as temporal trends relating to insect outbreaks (Michaelian *et al.* 2011).

We employed stand age to account for stand ageing processes, interpretable as time since fire (years), as all selected stands originated from stand replacing wildfires. The stand age for each PSP was determined by coring at least four dominant/co-dominant trees outside the plot at the time of plot establishment, and using the average age of the oldest species. While stand age and calendar year necessarily increased at the same rate, there was a wide distribution of stand ages sampled across the study period (Fig. A2-1).

2.3.4 Data analysis

To examine whether the DBH thresholds of surveyed trees led to changes in coefficient estimates for endogenous ageing processes and temporal trends associated with climate change, we used the following linear mixed effects model for biomass productivity and loss due to mortality, and changes in stems per hectare, calculated with a 5 cm and 10 cm threshold, and without a threshold:

$$AGB_{ij} = \beta_0 + \beta_1 \cdot Y_{ij} + \beta_2 \cdot f(A_{ij}) + \pi_j \qquad (1)$$

where AGB_{ij} is biomass growth, loss, or stem change, observed at the *i*th census in the *j*th plot; Y_{ij} is the mid-calendar year at the *i*th census in the *j*th plot; $f(A_{ij})$ is the best fit function of age, selected by Akaike Information Criterion (AIC, Table A1-2); and π_j is the random plot error accounting for the random effects of local site conditions and initial stand characteristics, including species composition; and the βs are coefficients to be estimated.

We conducted the mixed effect analysis using maximum likelihood with the *lme4* package (Bates *et al.* 2016). Due to departures in normality, and to improve coefficient estimates, we bootstrapped each model using 10000 iterations to produce 95% confidence intervals, based on the 2.5 % and 97.5% quantiles of the bootstrapped distributions. Model coefficients from the no DBH threshold and threshold models were assumed to be significantly different if their confidence intervals did not overlap the other's mean. To remove any bias from the use of allometric equations, we also fit models using basal area demographics. The outputs were similar (Figs. S3 & S4) and the biomass dynamics are presented in the main text for clarity. Models were fit with the *lmer* function and 95% CIs were determined using the *confint* and *bootMer* functions within *lme4*.

2.4 Results

Across all stand age and census intervals, the estimated annual growth was 1.7 ± 0.04 (mean ± 95% confidence intervals of the bootstrapped distribution) Mg ha^{-1} yr^{-1} using a 10 cm DBH threshold, 2.6 ± 0.06 using a 5 cm DBH threshold, and 2.8 ± 0.06 using no DBH threshold (Fig. 2-1). Using 10 cm and 5 cm thresholds underestimated annual growth, on average, by 37% and 6%, respectively. This was due to the exclusion of approximately 4244 stems ha^{-1} when using a 10 cm threshold, and 2527 stems ha^{-1} when using a 5 cm threshold (Table 2-1). Estimated annual

ingrowth was 1.0 ± 0.06 Mg ha^{-1} yr^{-1} using 10 cm DBH threshold, 0.3 ± 0.02 using a 5 cm DBH threshold, and 0.1 ± 0.02 using no DBH threshold, respectively (Fig. 2-1). This indicated that the use of 10 cm and 5 cm thresholds overestimated annual ingrowth biomass, on average, by 900% and 200%, respectively. The estimated annual loss from mortality was 0.7 ± 0.1 Mg ha^{-1} yr^{-1} using a 10 cm DBH threshold, 1.2 ± 0.12 using a 5 cm DBH threshold, and 1.5 ± 0.12 using no DBH threshold (Fig. 2-1). Using 10 cm and 5 cm thresholds underestimated annual loss from mortality, on average, by 51% and 20%, respectively. These underestimations were a direct result of the 10 cm and 5 cm thresholds, which missed approximately 705 and 506 dead stems ha^{-1}, respectively (Table 2-1). The major underestimations in growth were not entirely made up by the overestimations of ingrowth when estimating stand productivity: estimated annual productivity was 2.7 ± 0.08, 2.8 ± 0.06, and 2.9 ± 0.06 Mg ha^{-1} yr^{-1} using the 10 cm, 5 cm, and no DBH threshold, respectively (Fig. 2-1). This represented, on average, an underestimation of 7% and 2%, by 10 cm and 5 cm thresholds.

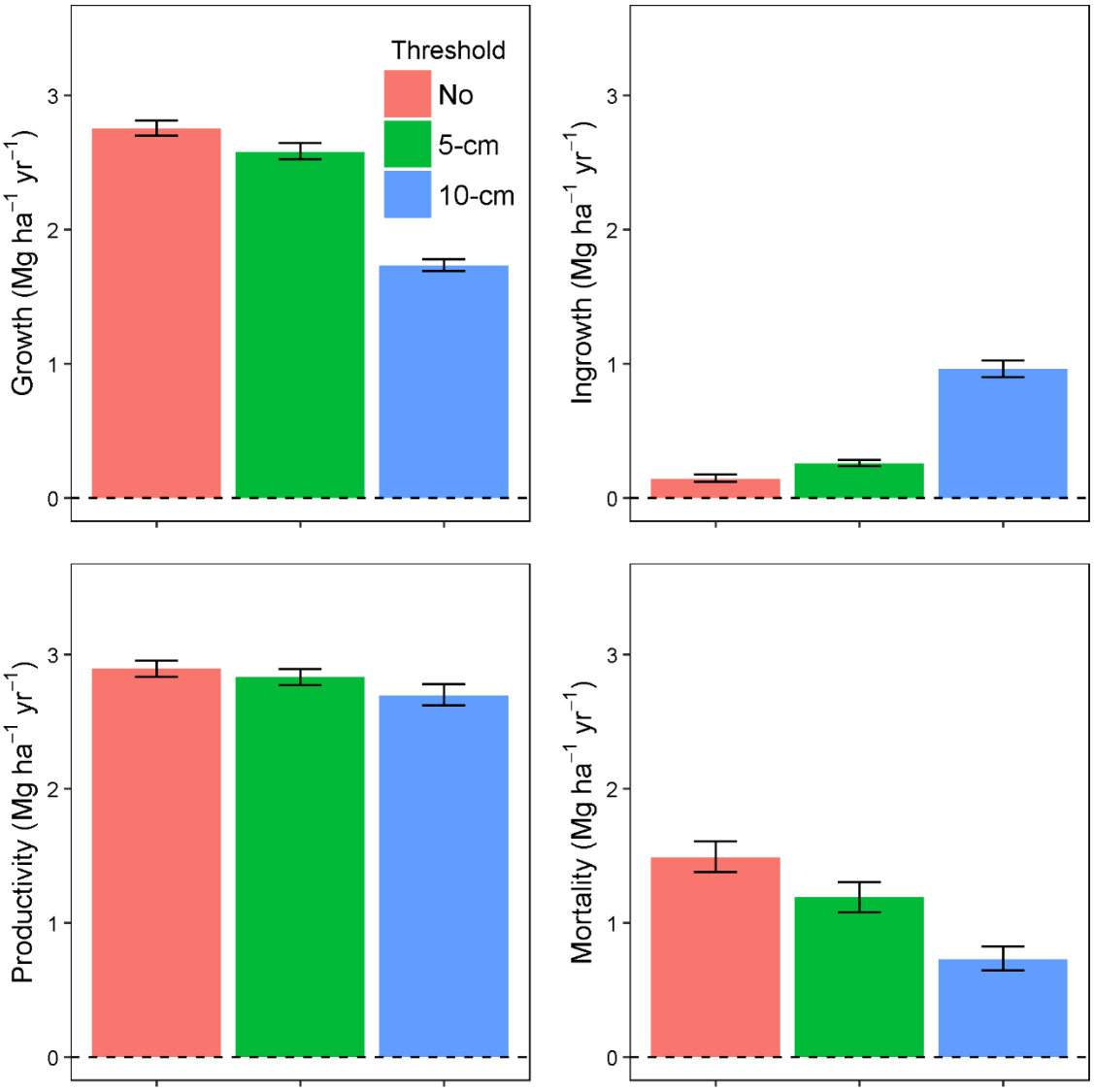

Figure 2-1: Bootstrapped mean and associated 95% confidence interval of each biomass component following the removal of the mean effects of age and calendar year.

Table 2-1: Number of stems per hectare measured and missed at each census, across all sites, years, and ages, by each DBH threshold for stand productivity and biomass lost due to mortality. Values presented are the means and bootstrapped 95% confidence intervals in brackets.

Scenario	10 cm threshold (stems ha^{-1})	5 cm threshold (stems ha^{-1})	No DBH threshold (stems ha^{-1})
Productivity			
Scenario 1 *Stems above threshold both censuses*	922.9 (869.8 - 975.7)	2609.3 (2489.4 - 2735.7)	5326.1 (4831.9 - 5848.1)
Scenario 2 *Stems below threshold both censuses*	4243.5 (3727.1 - 4790.5)	2526.9 (2091.3 - 2996.6)	0.0 (0.0 - 0.0)
Scenario 3 *Stem absent, then recruited above threshold*	0.0 (0.0 - 0.0)	1.3 (0.7 - 2.0)	326.8 (233.8 - 442.3)
Scenario 4 *Stem below threshold first census, above threshold second census*	159.7 (144.9 - 175.5)	190.0 (159.2 - 223.0)	0.0 (0.0 - 0.0)
Scenario 5 *Stem absent, then recruited below threshold*	326.8 (232.3 - 438.3)	325.5 (231.5 - 435.8)	0.0 (0.0 - 0.0)
Mortality			
Scenario 1 *Stems die above threshold and are counted*	57.6 (49.0 - 66.9)	256.9 (227.2 - 290.3)	762.7 (686.2 - 843.1)

Scenario 2 *Stems die below threshold and are missed*	705.1 (628.0 - 787.7)	505.9 (438.8 - 577.6)	0.0 (0.0 - 0.0)

Our predictions in differences between estimates of temporal trends in biomass dynamics across the three DBH thresholds were not supported. Temporal responses of growth and productivity to calendar year were comparable between no DBH threshold and 5 and 10 cm threshold stand measurements, with all being significantly positive (Fig. 2-2a&c, Table A1-1). Temporal trends in biomass gained through recruitment associated with calendar year were also similar between no DBH threshold and 5- and 10 cm threshold stand measurements (Fig. 2-2b). However, annual biomass loss due to mortality increased more rapidly without a threshold (Fig. 2-2d, Table A1-1), which was likely driven by significantly higher loss of smaller stems (Table 2-1), in contrast to using a threshold.

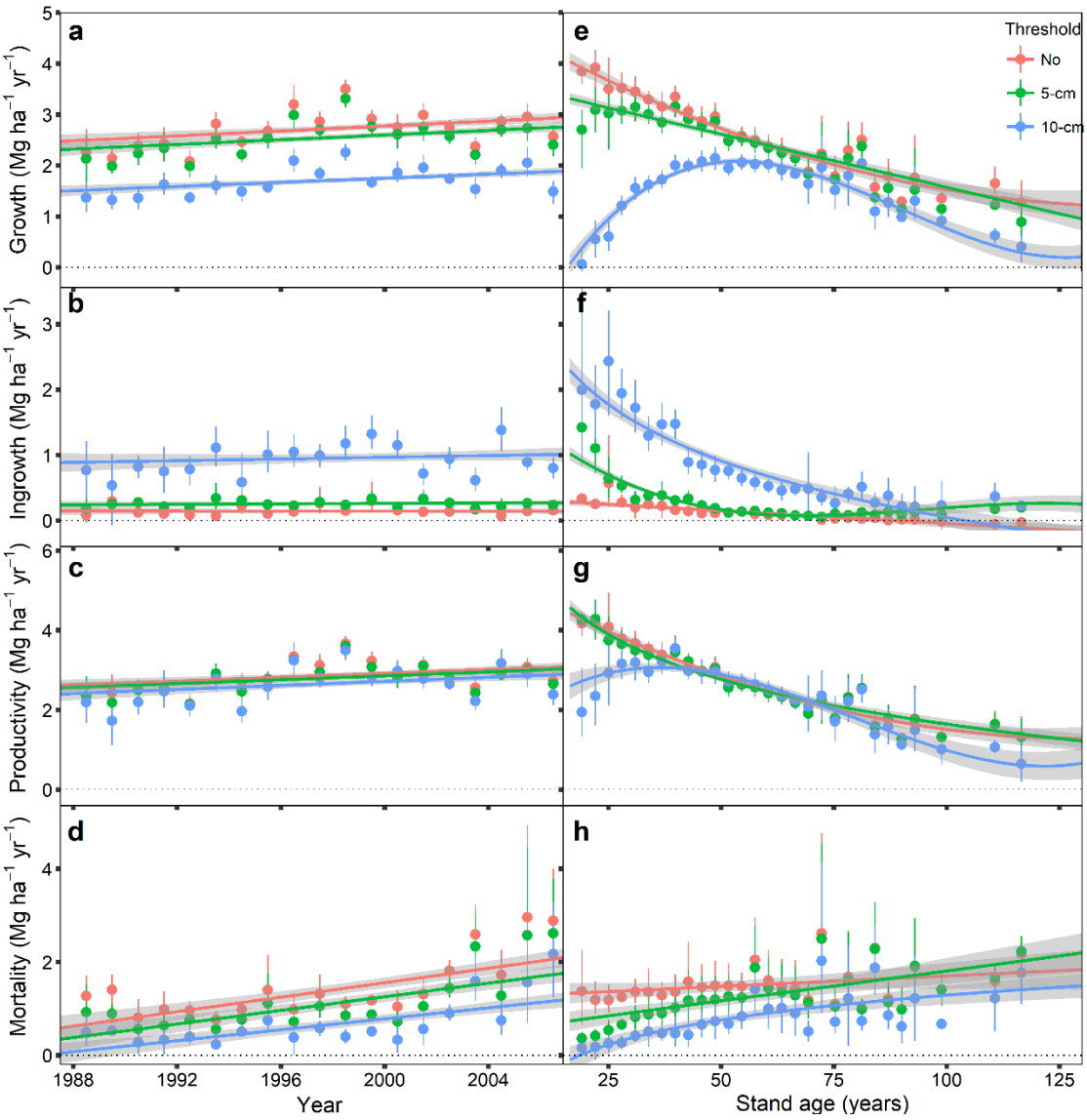

Figure 2-2 Partial regression plots of variables included in plot level analysis of growth, ingrowth, productivity, and mortality by threshold: Calendar year effect **(a-d)** Stand age effect **(e-h)**. Shaded lines are 95% confidence intervals.

The largest estimate discrepancies occurred in endogenous ageing processes. Our predictions for biomass growth and ingrowth estimates were largely supported. Growth was initially higher when no DBH threshold was imposed, compared to estimates using either threshold, eventually tapering off and meeting 5 cm threshold estimates, as expected, but remaining consistently higher than the 10 cm threshold estimates (Fig. 2-2e). Biomass loss was

higher for no DBH threshold samples in younger stands; however, with the estimates converging around 75 and 125 years, for 5 cm and 10 cm thresholds, respectively (Fig. 2-2h).

While the use of increasingly larger thresholds led to increasingly large numbers of missed dead stems (Table 2-1), biomass loss estimates converged at older ages. As anticipated, estimates without a threshold demonstrated a significant and consistent decline in productivity with stand age (Fig. 2-2g), which indicated that the maximum productivity of a stand was younger than the ages sampled.

2.5 Discussion

The mean underestimates in growth and mortality were driven by the number of stems missed by threshold sampling (Table 2-1). While more trees were considered recruits without a threshold than with (Table 2-1), those trees that were considered ingrowth using thresholds were much larger and added more biomass, leading to an overall overestimation of ingrowth (i.e., the biomass of scenario four was much higher than the biomass of scenario five).

The similar temporal trends in the responses of biomass growth or productivity at the stand level between sampling thresholds suggests that climate change effects were similarly positive for large and small trees. However, significantly more stems were lost at smaller thresholds than larger thresholds (Table 2-1), leading to a slightly increased estimated rate of biomass loss (Fig. 2-2d, Table A1-1). This may have been due to the fact that our study area had not experienced significant droughts over the study period (Luo & Chen 2015), which has been highlighted as a driver of large tree death (Bennett *et al.* 2015). A possible driver for the increased loss of smaller trees compared to larger trees may be increased competition, which had been shown to have increased within our study region for trees greater than 5 cm in DBH (Luo & Chen 2015). Smaller trees have been shown to be more adversely affected by competition for

certain resources than larger trees (Coomes & Allen 2007; Luo & Chen 2011), and as a result may experience greater rates of climate change-induced increased competition. Future observational studies should be cautious of estimates of the magnitude of biomass loss from mortality due to temporal trends associated with climate change if they include only large trees. The consistent underestimates in growth through stand development supported out initial hypothesis. However, biomass added by ingrowth was always higher in threshold measurements, likely because the trees that were observed as recruits were much larger. The large quantity of early ingrowth (i.e., approximately 17 to 65 years old) was likely due to the recruitment of the initial cohort to the threshold DBH. Our expectations for mortality were met, with initially significantly higher estimates without a threshold, eventually converging with threshold estimates. The convergence of mortality estimates indicates that sampling only large trees may be a good representative of total biomass lost due to mortality only at late stages in stand development.

Estimates of stand level productivity were significantly underestimated for approximately the first 45 years following a stand replacing disturbance using a 10 cm threshold. This was consistent with previous study estimates, where the majority of the biomass of young stands was found to be stored in smaller trees (Taylor *et al.* 2014). The functions of productivity also differed strongly: 5 cm and no DBH threshold productivity estimates were highest at the youngest age sampled, while 10 cm productivity increased from approximately 17 to 38 years before decreasing in a similar manner to the other estimates. This indicated that underestimates of biomass growth using 10 cm thresholds were not corrected for by the overestimation of ingrowth in young stands. Our results emphasized the importance of productivity from young stands (Poorter *et al.* 2016), which may have been even higher in stands that were younger than

our sample. In order to correct these age-related biases, studies using sites without available small tree plots should consider developing region-specific models that provide estimated corrections (Fig. A1-1).

2.6 Conclusion

Overall, we have provided evidence that using a DBH threshold significantly underestimates biomass productivity and loss due to mortality, with significantly larger underestimates as the threshold increases. Further, using a threshold may lead to underestimations in temporal accelerations of biomass loss from mortality. Finally, we demonstrated that the use of an artificial threshold leads to drastically different estimated relationships between stand biomass dynamics and stand ageing – with a greater deviation when using larger thresholds and sampling younger ages. Future studies based on PSPs should endeavour to use the smallest threshold possible, especially when estimating biomass dynamics at younger ages. Trees smaller than the required threshold should be accounted for through modelling biases once responses between large trees and smaller trees are correctly determined or through extrapolations based on smaller sampling plots.

CHAPTER 3: TEMPORAL DECLINES IN TREE LONGEVITY ASSOCIATED WITH FASTER LIFETIME GROWTH RATES IN BOREAL FORESTS

3.1 Abstract

Global change has been linked to significant increases in tree mortality in the world's forests. Reduced tree longevity through increased growth rates has been suggested as one of the mechanisms responsible for the temporal increases in tree mortality, but this idea has not been directly tested. Here we explicitly defined two testable hypotheses: (i) the probability of ageing driven tree mortality increases with global change and (ii) the mortality probability associated with global change is higher for faster-growing trees. To test these hypotheses, we examined the temporal changes of tree mortality probability in 539 permanent sample plots monitored from 1960 to 2009, with ages greater than 100 years at initial censuses, across the boreal region of Alberta, Canada. As expected, we found an overall temporal increase in tree mortality probability, indicating a loss in tree longevity with global change. We also found that trees with faster lifetime growth rates experienced higher temporal increases in mortality probability compared to slower growing trees. An analysis of the responses of tree mortality probability to increasing atmospheric carbon dioxide and temperature and decreases in water availability indicated that increasing atmospheric carbon dioxide and decreasing water availability were the major drivers of declining longevity. Our results suggest that tree longevity may further decline with the expected increase of atmospheric carbon dioxide and decreasing water availability in the region.

3.2 Introduction

Anthropogenic global change has been linked to extensive tree mortality worldwide (Allen *et al.* 2010; Allen *et al.* 2015). The major interdependent mechanisms causing this increase include hydraulic failure and carbon starvation, often attributed to direct heat stress, lowered water availability, pest and pathogen outbreaks, or intensified tree-to-tree competition, with their relative importance dependent on tree species and region-specific temporal climatic trends (McDowell *et al.* 2011; Peng *et al.* 2011; Anderegg *et al.* 2012; Luo & Chen 2013; Luo & Chen 2015; McDowell *et al.* 2015; Rowland *et al.* 2015; Hember *et al.* 2017; Chen *et al.* 2018). Reduced tree longevity due to global change has been hypothesized as a mechanism for increased biomass loss associated with global change at the stand level (Brienen *et al.* 2015). While studies have shown temporally increasing tree mortality rates (van Mantgem *et al.* 2009; Peng *et al.* 2011), the hypothesis that global change reduces tree longevity (here defined as the lifespan of an organism) has yet to be directly tested. Examining whether mortality probability has increased (i.e., longevity has decreased) for stems in older stands where trees are reaching their longevity (Burns & Honkala 1990; Chen & Popadiouk 2002; Luo & Chen 2011), would enable directly testing if global change has reduced tree longevity.

The negative relationship between lifetime tree growth rates and longevities has been well documented. Among plant species, longevities are negatively related to lifetime growth rates due to the investment tradeoff between defense and growth (Herms & Mattson 1992) or smaller sizes at older ages being less susceptible to stresses (Mencuccini *et al.* 2005). Size tends to have a greater impact on tree mortality probabilities than age (Mencuccini *et al.* 2005; Thomas 2013; Mencuccini & Munné-Bosch 2017; Schmid-Siegert *et al.* 2017). At larger sizes, trees are more susceptible to hydraulic and mechanical constraints (Ryan *et al.* 2006) and pest and

pathogen outbreaks (Haas *et al.* 2016). It is plausible that faster lifetime growth rates lead to trees reaching larger sizes more quickly, leaving them more exposed to size-related mortality, and reducing their longevities. This relationship holds within species across spatial gradients of environmental conditions, where tree longevity also has been negatively associated with quicker early (Bigler & Veblen 2009) and lifetime tree growth rates (Di Filippo *et al.* 2015).

Under a temporally changing climate, modelling studies suggest that global change-induced growth stimulation leading to greater sizes more quickly may reduce tree longevity (Bugmann & Bigler 2011; Hember & Kurz 2018). Global change events such as droughts that coincide with bark beetle outbreaks have been shown to cause larger reductions in short-term growth and higher mortality probabilities in larger trees compared to smaller trees (Bennett *et al.* 2015), although evidence of taller trees having higher mortality probabilities during droughts without co-occurrence of bark beetle outbreaks is mixed and species-specific (Hember *et al.* 2017). Since trees can increase their growth rates in response to positive global change drivers such as warming, increased atmospheric CO_2, and nitrogen deposition (Pretzsch *et al.* 2014; Brienen *et al.* 2015; Chen *et al.* 2016; Schulte-Uebbing & de Vries 2018) when not limited by water availability (Jump *et al.* 2006; Korner 2015; Girardin *et al.* 2016), reduced longevity due to increased lifetime growth rates may contribute to the observed global change-induced increases in tree mortality. While previous studies have inferred reduced longevity from positive relationships between stand-level productivity and mortality (Brienen *et al.* 2015), direct proof of this mechanism should come from individual stem level data. We note that trees that eventually die from long-term accumulated stresses have reduced recent growth rates prior to death (Cailleret *et al.* 2017).

The boreal forest is an ideal candidate to examine how tree longevity might have been affected by global change since the prevalence of stand-replacing wildfires, and consistent seasonality, allows for accurate tree age determination. In western North American boreal forests, trees of all species are recruited simultaneously following wildfire (Gutsell & Johnson 2002). This leads to evenly-aged, though not evenly-sized, stands that can be used to exclude age effects while analyzing growth-mortality relationships. Evidence for global change-induced alterations in growth rates are mixed in the boreal forest with no change or declines at the individual tree level reported in dendrochronological studies (Girardin *et al.* 2016; Chen *et al.* 2017; Hogg *et al.* 2017; Chen *et al.* 2018) and increases in young stands but no change in older stands (*i.e.,* 140 years and older) at the stand level (Luo & Chen 2015; Chen *et al.* 2016). Here, we use data from 539 permanent sample plots established in the western boreal forest of Canada to examine whether tree longevities have been shortened in the past 50 years. We specifically tested whether: (i) annual mortality probabilities have increased temporally for trees in stands older than 100 years, when boreal tree species begin to reach their longevity (Chen & Popadiouk 2002; Luo & Chen 2011); and, (ii) relatively larger trees within a stand (i.e., trees with faster lifetime growth rates) have higher increases in global-change related mortality probabilities than relatively smaller trees. To understand whether a specific global change driver was the cause of differences in temporal longevity, we examined the relationships between tree mortality and changes in atmospheric CO_2, temperature, and water availability.

3.3 Datasets and methods

3.3.1 Study area and long-term repeatedly measured sample plots

The permanent sample plots (PSPs) used in this study were established throughout Alberta starting in 1958 by the provincial government. The PSP data is available upon request to the

forestry department of the Alberta government. The PSPs were established in visually homogenous well-stocked stands greater than 1 ha in size, at least 100 m from any openings to minimize the impacts of edge effects. A total of 539 PSPs were compiled from the networks for use in our study, using the following data selection criteria: (*i*) PSPs with a known origin date of stand-replacing wildfire, and unmanaged; (*ii*) PSPs with all trees marked and tagged with diameter at breast height (DBH) and species identification tracked accurately over multiple censuses (stems with any negative growth observations were removed from all analyses); (*iii*) plot spatial location was available and plots were within the boreal zone as defined by Natural Resources Canada (Brandt 2009); and, (*iv*) plots had a minimum of three censuses and a minimum of two censuses with an average age greater than 100 years. These plots range in latitude from 51.5° to 59.6° N, in longitude from 119.7° to 114.0° W, and in elevation from 291 to 1784 metres above sea level (see Fig. A2-1). Across space and time, annual temperatures ranged from -5.74 to 11.67 °C, and annual precipitation ranged from 187 mm to 881.9 mm between 1957 and 2009, obtained by using the BioSIM 10 software (Réginère *et al.* 2014).

Wildfire is the dominant forest-replacing disturbance with fire return intervals that vary temporally and spatially, from 15 to 90 years in the study area (Weir *et al.* 2000). To examine whether longevity has been reduced (through higher mortality probability in older organisms) and to minimize the effects of competition-induced mortality, which is a driving factor for individuals smaller than the average tree size in a stand particularly in young boreal forests (Chen *et al.* 2008; Luo & Chen 2011, 2015), we selected only stands older than 100 years, when boreal tree species begin to reach their longevity (Burns & Honkala 1990; Chen & Popadiouk 2002).

Tree species left after selection for age included *Picea glacua* ((Moench) Voss.) (41.9% of total stems), *Pinus contorta* (Douglas) (24.6%), *Populus tremuloides* (Michx.) (13.2%), *Abies balsamea* ((L.) Mill) (8.2%), *Picea mariana* (Mill.) (7.4%), *Populus balsamifera* (L.) (3.0%), and other species including *Betula papyrifera* (Marshall), *Picea engelmannii* (Parry ex Engelm), *Abies lasiocarpa* ((Hooker) Nuttall), *Larix laricina* ((Du Roi) Koch), and *Pinus banskiana* (Lamb.), accounting for a total of 1.7% of the total number of stems (Table A2-1).

3.3.2 Explanatory variables

We used the midpoint year of a census (i.e., the average of initial and final measurement years during a census period) to represent overall climatic conditions (van Mantgem *et al.* 2009; Chen & Luo 2015; Chen *et al.* 2016), corresponding to each census period of each plot. Using the midpoint year as a proxy for global change encompassed not only the systematic increases in atmospheric CO_2 concentrations and temperatures and declines in water availability throughout our study region (IPCC 2013), but also increases in other global change drivers such as insect outbreaks (Chen *et al.* 2018).

We used the relative basal area of each stem to the average stem basal area in the prior census period to quantify relative lifetime growth rates within a stand (Luo & Chen 2011). Since all stems are recruited simultaneously following stand-replacing wildfire (Gutsell & Johnson 2002), the larger stems within a stand were also, the faster growing over their lifetime. We also examined absolute size in the prior census period as a potential covariate.

To investigate the sensitivity of tree mortality to increases in temperature and decreases in water availability, we examined the response to climate change drivers by using the annual temperature anomaly (ATA), the annual standardised precipitation-evapotranspiration index (SPEI), and atmospheric carbon dioxide (CO_2) concentration averaged over the census period.

The annual temperature anomaly was defined as the average difference between observed mean annual temperatures over the census period and its long-term mean (1957-2013, the length of our study period) at each plot. Similarly, we used the average annual SPEI for each census period as a measure of water availability; SPEI is an excellent indicator of drought conditions and is sensitive to changes in water availability due to global warming (Vicente-Serrano *et al.* 2010). We calculated SPEI using the *SPEI* package in R (Vicente-Serrano *et al.* 2010) using the annual climate moisture index as our measurement of water availability. Both mean annual temperature and the annual climate moisture index (used to calculate SPEI) were generated using BioSIM 10 (Réginère *et al.* 2014) for the length of our study period. BioSIM uses historical weather data from the nearest weather station to a location and adjusts predictions for differences in elevation, latitude, and longitude (Réginère *et al.* 2014). Atmospheric CO_2 concentration was derived from the Manua Loa Earth System Research Laboratory (http://www.esrl.noaa.gov/gmd/ ccgg/trends/co2_data_mlo.html) and from the Law Dome DE08 and DE08-2 ice cores (http://cdiac.ornl.gov/ftp/tren- ds/co2/lawdome.smoothed.yr20) for measurements before 1959. CO_2 values were the average values for each measurement period for each plot. To ensure our use of annual climate variables was appropriate, we also examined the average growing season (May 1st to Sept 1st) temperature anomaly and SPEI over the measurement period. Since coefficient estimates were similar (Fig. A2-2), we retained annual variables for clarity and to remain consistent with previous literature (van Mantgem *et al.* 2009; Peng *et al.* 2011; Luo & Chen 2013).

3.3.3 Statistical analysis

Because our measurement intervals varied, similar to Luo and Chen (2013), we scaled the annual mortality probability using the following function:

$$p_{ijk} = 1 - (1 - p_{ijk,t=1})^{\Delta t} \quad \textbf{(1)}$$

where p_{ijk} is the mortality probability of an individual stem for the *i*th tree during the *j*th census period in the *k*th plot, Δt is the length of the census period in years, and $p_{ijk,\ t=1}$ is the annual mortality probability of the *i*th tree of *j*th census period in *k*th plot.

We used a generalized mixed-effects logistic model (Chen *et al.* 2008; Hulsmann *et al.* 2018) to investigate whether trees with faster lifetime growth rates were more susceptible to global change-induced mortality.

$$\log it(p_{ijkl,t=1}) = \beta_0 + \beta_1 \times Y_{ijkl} + \beta_2 \times f(R_{ij-1kl}) + \beta_3 \times Y_{ijkl} \times R_{ij-1kl} + \pi_k + \rho_l + \varepsilon_{ijkl} \quad \textbf{(2)}$$

where: $p_{ijk,t=1}$ is the annual probability of mortality of the *i*th tree of *j*th census period in the *k*th plot of the *l*th species; Y_{ijkl} is the middle calendar year of census; $f(R_{ij\text{-}1k\,l})$ is the best fit function (i.e., linear or logarithmic) of annual tree mortality probability to the previous relative basal area; π_k is the random effect of the *k*th plot; ρ_l is the random effect of the *l*th species. We determined the best fit function for relative basal area using a general additive model and AIC selection (Table A2-2). To ensure that our estimate of increasing mortality probabilities with increasing relative size was robust, we also examined initial absolute size as a covariate. Since size-dependent mortality is often U-shaped (Hember *et al.* 2017), we determined that a linear function for absolute size produced a better model than a quadratic function for absolute size through AIC selection. All variables were centred and scaled prior to analysis to aid in interpretation and convergence.

We implemented our model using the *glmer* function in the *lme4* package (Bates *et al.* 2015). We fit the above model to the dataset including all trees and then by the six major species. We then examined the response to climate change drivers by substituting *Y* in eqn. 2 by atmospheric CO_2, ATA, and SPEI in order to determine which climactic drivers were responsible

for temporal trends. Because these drivers have changed concurrently during the past six decades in the study region (Luo & Chen 2013; Chen & Luo 2015; Chen *et al.* 2016), we ran the analysis with all climate variables simultaneously by the generalized mixed-effects logistic model. To ensure that the correlation between climate drivers did not bias estimates, we also modelled annual tree mortality probability by ridge regression using the *lm.ridge* function from the *MASS* package and a non-parametric model using the *rfit* function in the *Rfit* package. For the ridge regression and non-parametric model, we removed the random effects estimated by the simultaneous model prior to model fits and bootstrapped confidence intervals from 1000 bootstrap iterations. To ensure our model specification was correct, we also examined a model including all interactions between each climate driver and relative size (Fig. A2-3). Since this did not affect our parameter estimates, we present the two-way interaction model in the Results. Parameter significance for *glmer* models was assessed using an analysis of deviance with Type II sum of squares through the *Anova* function in the *car* package. Alternative to the models with global change drivers simultaneously included, we also ran models with each driver considered separately, similar to previous analyses (van Mantgem *et al.* 2009; Peng *et al.* 2011; Luo & Chen 2013).We generated 95% confidence intervals using the Wald method of the *confint* function within the *lme4* package. To determine if the models properly discriminated trees that died from trees the survived, we used the Area Under the Receiver Operating Characteristic Curve (AUC). A value of AUC > 0.8 indicates that a model has excellent discriminatory power, and a value > 0.7 indicates good discriminatory power (Hosmer & Lemeshow 2000). The AUC was calculated using the *pROC* package (Robin *et al.* 2011). All analyses were implemented in R statistical software, version 3.5.0.

3.4 Results

Across all individuals, annual mortality probability increased significantly over time (0.471 ± 0.016, scaled coefficient estimate ± 95% confidence interval, $P < 0.001$) but decreased on average with increasing relative size (-0.349 ± 0.016, $P < 0.001$) (Table 3-1, Fig. 3-1). Temporal increases in mortality probability increased with increasing relative basal area (0.092 ± 0.014, $P < 0.001$), but this increase was not large enough to cause larger trees to have higher mortality probabilities than smaller trees by the end of the study period (Fig. 3-1). The AUC of the model was 0.736 indicating a good fit. Temporal trends by individual species were consistent with the model of all trees except for *A. balsamea*. For *A. balsamea*, larger individuals on average had higher mortality probabilities than smaller individuals, and there was no significant interaction effect of relative size and year (Fig. A2-4). Alternative models with the diameter at breast height as a predictor yielded similar coefficient estimates for the effects of the calendar year, relative tree basal area and their interactions (Table 3-1).

Table 3-1: Effects of relative size, year, and absolute size on annual tree mortality probability for two alternative models. Values are parameter estimates with 95% confidence interval in brackets. *logR* is natural log transformed relative tree basal area, *Y* is calendar year, *D* is diameter at breast height. Model is defined in eqn. 2.1

Parameter	Model from eqn. 2	Model with *D*
Intercept	-3.948 (-4.24 - -3.656)	-3.967 (-4.247 - -3.687)
logR	-0.349 (-0.366 - -0.333)	-0.592 (-0.635 - -0.548)
Y	0.471 (0.455 - 0.486)	0.448 (0.432 - 0.464)
D	-	0.320 (0.267 - 0.372)
D^2	-	-
logR × *Y*	0.092 (0.079 - 0.106)	0.086 (0.073 - 0.100)
AIC	97746.5	97609.2
AUC	0.736	0.737

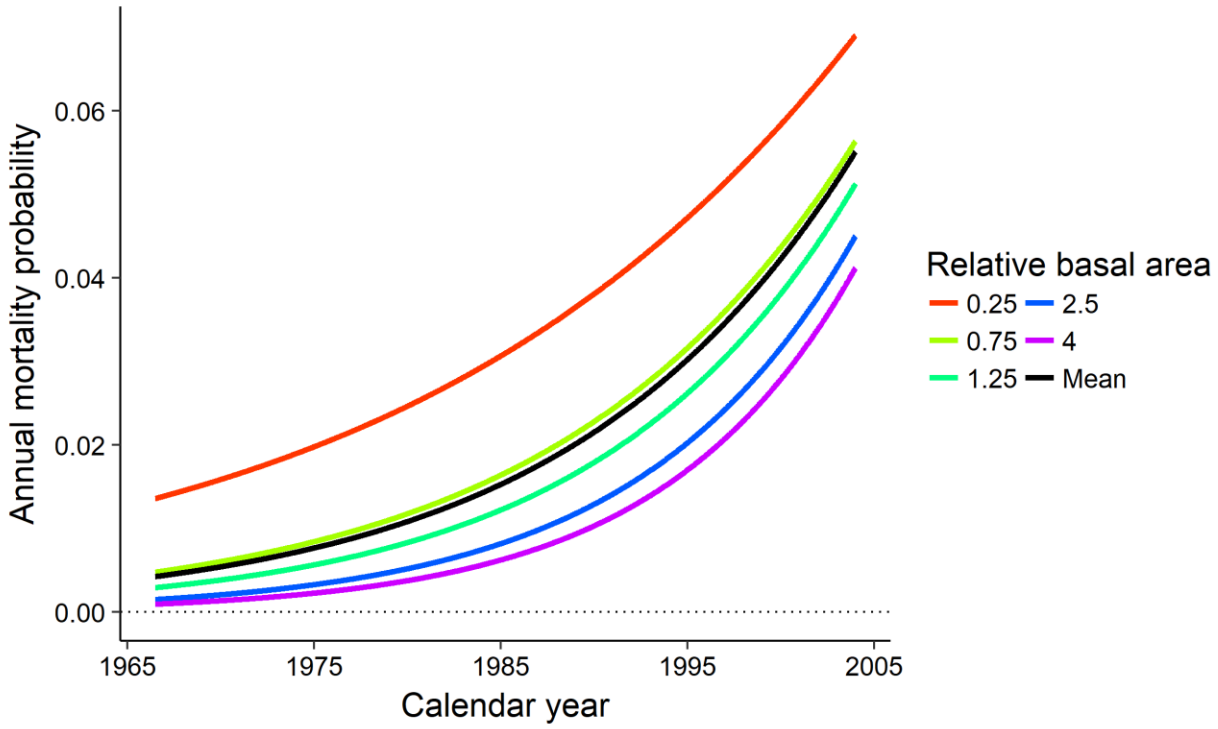

Figure 3-1: Temporal trends in annual mortality probability by relative basal area. Black line represents the response at mean relative basal area.

During the study period, atmospheric CO_2 and temperature increased, while water availability decreased (Fig. 3-2 a-c). The linear mixed effect model that included atmospheric CO_2, ATA and SPEI simultaneously as predictors showed that with rising atmospheric CO_2 and decreasing SPEI led to on average higher mortality probabilities, while increasing ATA led to on average lower tree mortality probability (Table 3-2, Fig. 3-2d-f). Similar to the response to calendar year, increasing atmospheric CO_2 and decreasing SPEI led to higher mortality probability in larger trees than in smaller trees, but the effect of ATA was independent of relative tree size, indicated by the insignificant interaction of ATA and relative basal area (Table 3-2, Fig. 3-2d-f). Ridge regression and non-parametric regression yielded similar coefficient estimates to those of the linear mixed effect model. However, the results from the models that tested global change drivers individually yielded a contrasting effect of ATA (Fig. 3-3). In the

ATA model, the effect of ATA was confounded with the effect of atmospheric CO_2 and SPEI since ATA and CO_2 were correlated (Spearman correlation, r = 0.297, $P < 0.001$) and ATA and SPEI were also correlated (r = -0.369, $P < 0.001$). The model examining the response to climate drivers was a good fit to the data by AUC (Table 3-2).

Table 3-2: Effects of relative basal area, atmospheric carbon dioxide concentration (CO2), annual temperature anomaly (ATA) and standardized precipitation-evapotranspiration index (SPEI) on annual tree mortality probability. Values are parameter estimates with 95% confidence interval in brackets, Chi-square test statistic, and associate P value. logR refers to the natural logarithm of the relative basal area.

Model terms	Parameter estimate	χ^2	*P*
Intercept	-3.952 (-4.245 - -3.659)	-	-
CO_2	0.463 (0.447 - 0.48)	3072.7	<0.001
ATA	-0.083 (-0.105 - -0.062)	57.2	<0.001
SPEI	-0.077 (-0.1 - -0.054)	30.3	<0.001
logR	-0.351 (-0.367 - -0.334)	1572.7	<0.001
logR × CO_2	0.076 (0.062 - 0.089)	115.3	<0.001
logR × SPEI	-0.051 (-0.067 - -0.035)	39.2	<0.001
logR × ATA	-0.007 (-0.024 - 0.009)	0.8	0.364
AUC			0.738

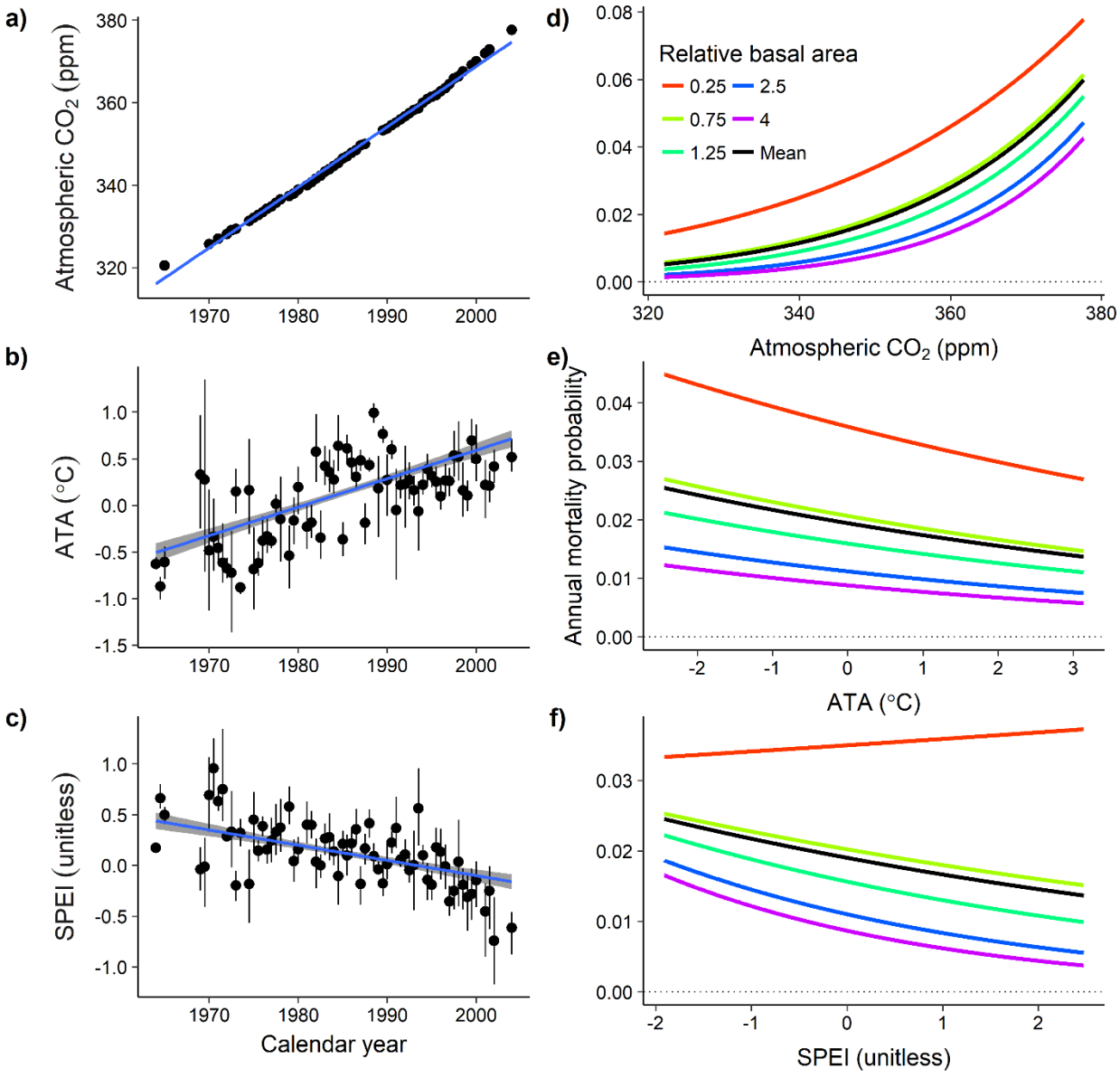

Figure 3-2: Trends in global change drivers and the response of annual mortality probabilities. (a) Atmospheric CO2 concentration, (b) mean annual temperature anomaly (ATA), and (c) mean standardized precipitation-evapotranspiration index (SPEI) in relation to calendar year. Dots and error bars show the mean and their 95% bootstrapped confidence intervals. Blue line is a fitted linear model with 95% confidence bands in grey. (d-f) Change in annual mortality probability according to global change drivers by relative basal area: (d) atmospheric CO_2, (e) ATA; and (f) SPEI. Black line represents the response at mean relative basal area.

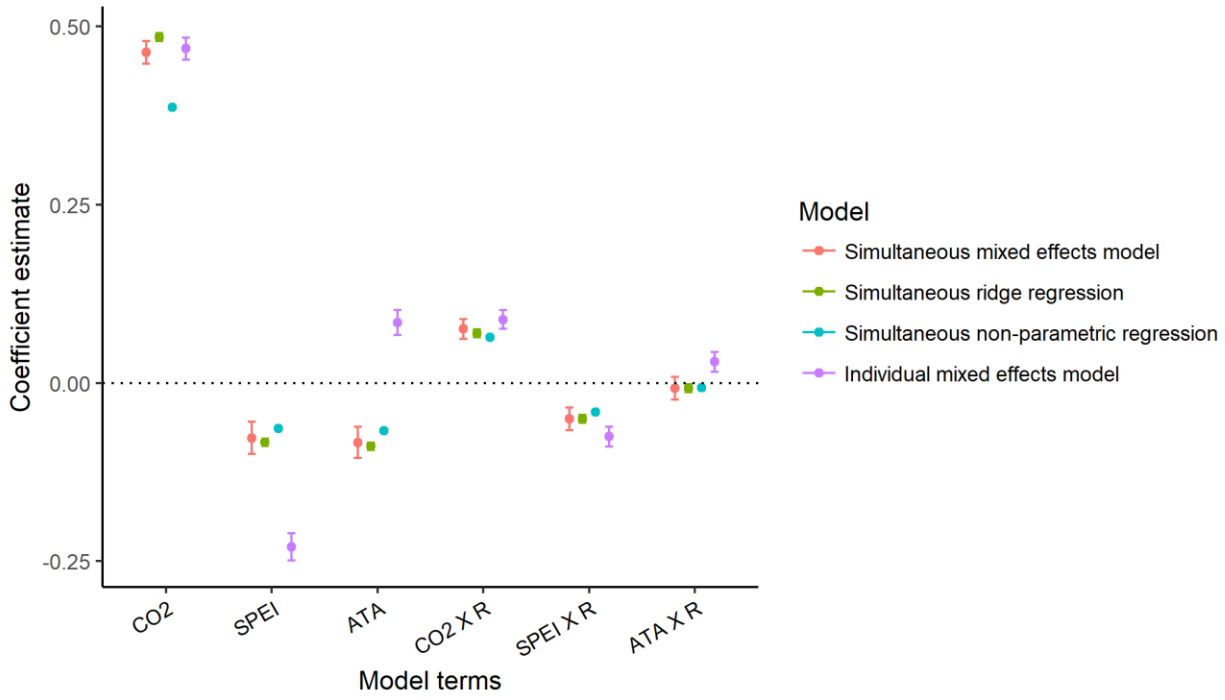

Figure 3-3: Coefficient estimates of global change driver effects on annual tree mortality probability using four modelling approaches: simultaneous modelling of all drivers using generalised linear mixed effect model, simultaneous ridge regression of all drivers, simultaneous non-parametric regression of all drivers, and individual modelling of drivers.

3.5 Discussion

Our results show consistent temporal increases in annual mortality probabilities (i.e., reduction in survival probabilities) for trees older than 100 years during the past half-century in our study region, indicating that tree longevity declined over time. We found that annual mortality probabilities increased temporally faster for larger trees although larger trees on average had lower annual mortality probabilities. Lower mortality probabilities for dominant trees is consistent with previous literature in the boreal forest (Luo & Chen 2011). This suggests that some suppression still occurs in these stands and is significant enough to outweigh increases in mortaltiy due to faster lifetime growth rates on average. Species-level responses were similar with the exception of *A. balsamea*. Large individuals of *A. balsamea* died more frequently than smaller individuals of the species, and there was no difference in temporal trends between large

and small individuals. This may be attributable to the fact that *A. balsamea* rarely grows to dominate these stands (average relative basal area across all stands was 0.700 ± 0.009) and is highly susceptible to insect outbreaks (Fleming & Volney 1995).

Our climate change driver analysis suggests that rising atmospheric CO_2 and decreasing water availability increased annual tree mortality probabilities, confirming work done by other studies in the region (Peng *et al.* 2011; Luo & Chen 2013; Hember *et al.* 2017). Our analysis with global change drivers individually modelled corroborated the result that warming increased tree mortality probability (van Mantgem *et al.* 2009; Peng *et al.* 2011; Luo & Chen 2013). However, with all three global change drivers accounted simultaneously, our mixed effect model, non-parametric model, and ridge regression model, all of which equally split the shared variations among correlated predictors (Legendre & Legendre 2012) showed that increasing temperature on average decreased annual tree mortality probability. It remains unknown whether warming by 1°C (Fig. 3-2b) during the past decades in our region has led to an effect on tree mortality independent from rising atmospheric CO_2 and decreasing water availability since our observational data showed that changes in temperature correlated positively with atmospheric CO_2 and decreasing water availability. A study to the east of our region, using a space-for-time methodology, shows that warming at higher than 2° C had a negative effect on trees, but warming at a lower temperature could have a positive effect (D'Orangeville *et al.* 2018).

In agreement with our second hypothesis, we found that reductions in longevity due to increasing atmospheric CO_2 and decreases in water availability were stronger in trees with faster lifetime growth rates. Reduced longevity due to increasing CO_2 could be attributable to an acceleration in tree life cycles: higher atmospheric CO_2 promotes tree growth, causing trees to grow larger, and leading them to be more susceptible to size-related mortality (Brienen *et al.*

2015). On the other hand, it could be related to concurrent increases in pest and pathogen pressures, which are expected to affect larger trees more than smaller trees (Haas *et al.* 2016). Increasing mortality probabilities as water availability declines and trees grow larger could be caused by requirements of larger investments in rebuilding xylem post-drought in bigger than in smaller trees (Trugman *et al.* 2018) or due to increases in path length putting increased hydrological pressure on larger individuals (Hember *et al.* 2017).

We demonstrate that decreases in tree longevity in the western boreal forests of Canada are associated with trees that have higher lifetime growth rates. Our climate change driver analysis suggests that rising atmospheric CO_2 and reduced water availability are the major drivers of reduced longevity for larger trees in our study area, and that tree longevity may be further reduced with an expected on-going increase in atmospheric CO_2 and decrease in water availability in the region.

CHAPTER 4: COMPLEMENTARITY EFFECTS ARE STRENGTHENED BY COMPETITION INTENSITY AND GLOBAL ENVIRONMENTAL CHANGE IN THE CENTRAL BOREAL FORESTS OF CANADA.

4.1 Abstract

Increases in niche complementarity have been hypothesized to reduce the intensity of inter-specific competition within natural forests. In regions currently experiencing potentially enhanced growth under global environmental change, niche complementarity may become even more beneficial. However, few studies have provided direct evidence of this mechanism. Here, we use data from 180 permanent sample plots in Manitoba, Canada, with full spatial mapping of all stems, to show that complementarity effects on average increased with neighbourhood competition intensity and temporally rising CO2, warming, and water availability. Importantly, complementarity effects increased with both shade tolerance and phylogenetic dissimilarity between the focal tree and its neighbours when modelling these effects individually and simultaneously. Our results provide further evidence that increasing stand functional and phylogenetic diversity can improve individual tree productivity, especially for individuals experiencing intense competition and may offer an avenue to maintain productivity under global environmental change.

4.2 Introduction

Competition for limited resources is a major driver of forest demographic dynamics (Oliver & Larson 1996) and especially in the boreal forest of North America (Chen & Popadiouk 2002; Luo & Chen 2011). With ongoing global environmental change, in areas of the North American boreal forest where soil moisture is not limiting, competition has become more intense (Luo & Chen 2015; Nicklen et al. 2019). Within terrestrial plant communities, the effect of plant species

diversity on growth is likely positive (Zhang et al. 2012; Grace et al. 2016) and higher tree species diversity can lead to reductions in competition (Forrester & Bauhus 2016). This effect of plant diversity on growth has led to speculation that increasing diversity can promote tree productivity under global environmental change and offset increases in tree mortality (Hisano et al. 2018; Ammer 2019). If stands with higher tree species richness experience higher niche complementarity, then individuals within the stand should also experience lower competition (Ammer 2019). However, studies examining the effects of tree competition normally rely on intraspecific *versus* interspecific designations or a summation of broadleaf *versus* conifer basal area within a stand (Luo & Chen 2015; González de Andrés et al. 2018; Nicklen et al. 2019). While useful to examine general trends, this methodology tends to reduce mechanistic interpretability by neglecting variation in intensity of interspecific competition for limited resources.

Tree-to-tree competition occurs when individuals compete with one another for a sufficient amount of shared resources. Individuals can succeed in acquiring sufficient resources by either gathering or using resources more quickly or by tolerating lowering levels of resource availability than other individuals (Kunstler *et al.* 2016). Consequently, tree species develop specific traits that result in a tradeoff, allowing them to maximise access to one resource while reducing their access to another. Light is one of the most limiting resource in forests (Pacala et al. 1996) and competition for this resource provides stark contrasts in life-history traits. For example, lower wood density has been linked to quicker growth (and therefore more access to light) but has also been linked to a lower ability to tolerate competitive pressures from other trees (Kunstler *et al.* 2016). In forests, positive tree diversity effects on stand-level productivity occur only when constituent species exhibit shade tolerance heterogeneity (Zhang et al. 2012),

suggesting that increased light utilization complementarity drives overyielding in tree species mixtures. Previous studies have demonstrated higher productivity in plots with shade tolerance dissimilarity (Toigo et al. 2018) but direct evidence of reduced competition should come from the individual tree level. If tree-to-tree competition is the determinant for tree growth, we would expect that trees neighbouring individuals with contrasting shade tolerance would grow more than those neighbouring with similar shade tolerance since they would experience less intense competition. Furthermore, if tree growth increases with global environmental change and intensifies the effect of competition in our study area (Luo & Chen 2015), growth rates of the trees neighbouring individuals with contrasting shade tolerance would be expected to increase more than those neighbouring with similar shade tolerance.

Phylogenetic dissimilarity within a tree's neighbourhood may also provide benefits to individual tree growth through increasing complementarity or facilitation. Within temperate and boreal forests, many traits are phylogenetically conserved (Paquette et al. 2015), suggesting that species with close evolutionary relatedness may occupy similar niche space. Further, phylogenetic dissimilarity can affect tree growth through reduction in susceptibility to species-specific pests, pathogens, and/or predators. Originally developed to describe patterns of seedling recruitment (Janzen 1970; Connell 1978), this theory has been extended to mature plants in the form of the resource concentration hypothesis (Parker et al. 2015; Grossman et al. 2018). The theory stipulates that mature plant communities with high abundances of host species are more susceptible to specialised pest and pathogen outbreak than those with higher phylogenetic dissimilarity. Thus, a tree with phylogenetically distant neighbours may experience less intense competition and be better able avoid exposure to specialised pest and pathogen outbreaks and maintain higher growth rates than a tree with phylogenetically similar neighbours.

Here we set out to test whether: (i) focal trees with functionally and phylogenetically diverse neighbourhoods would grow more on average than those with functionally and phylogenetically diverse neighbourhoods; (ii) focal trees with functionally and phylogenetically diverse neighbourhoods experienced less intensity of competition; and, (iii) focal trees with functionally and phylogenetically diverse neighbourhoods would grow more in the face of beneficial global environmental change (i.e., rising atmospheric CO_2, temperatures, and water availability), than trees with less functionally and phylogenetically diverse neighbourhoods. We utilized 180 permanent sample plots established by the provincial government of Manitoba, Canada in 1985 and remeasured every five years. These plots represent a range of forest conditions and species mixtures. At the individual tree level, there are wide ranges of competition intensity, shade tolerance dissimilarity, and phylogenetically dissimilarity. The spatial location of each individual tree within the plot was recorded which enabled us to estimate spatially explicit competition, neighbourhood shade tolerance dissimilarity and phylogenetic dissimilarity indices.

4.3 Materials and Methods

4.3.1 Study area

Permanent sample plots (PSPs) were established across Manitoba, Canada (Fig. A3-1) starting in 1985 and were re-measured every 5 years after establishment. The PSPs are in visually homogenous well-stocked stands greater than 1 ha in size, at least 100 m from any openings to minimize the impacts of edge effects and were all circular in shape with a 12.6m radius or 500.34 m^2 in size. Plots from the network were compiled in our study using the following data selection criteria: (*i*) PSPs originating from a known stand replacing wildfire, and were unmanaged; (*ii*) PSPs with all trees marked and tagged with diameter at breast height (DBH),

position within the plot, and species identification tracked accurately over multiple censuses; and, (iii) PSPs had a minimum of three remeasurements. Primary tree species included in the network included: *Picea mariana* (Mill.) B.S.P. (40.4% of all stems measured), *Pinus banksiana* Lamb. (25.7%), *Populus tremuloides* Michx. (19.2%), *Abies balsamea* (L.) Mill. (5.2%), *Betula papyrifera* Marsh. (2.8%), *Fraxinus nigra* Marsh. (2.1%), *Picea glauca* (Moench) Voss (2.0%), *Larix laricina* (Du Roi) K. Koch (1.4%), *Thuja occidentalis* L. (1.1%); and, minor species included: *Ulmus Americana* L., *Acer negundo* L., *Quercus macrocarpa* Michx., and *Pinus resinosa* Ait. (total approximately 0.05%).

4.3.2 Estimates of growth rates

We estimated individual tree growth as annual basal area increment ($cm^2\ year^{-1}$). Annual basal area increment was obtained by taking the difference between basal area at the end of the census period and basal area at the beginning of the census period and dividing by the time between measurements.

4.3.3 Global environmental change drivers

We used the midpoint year of a census (i.e., the average of initial and final measurement years) to represent the overall effects of global environmental change (van Mantgem *et al.* 2009; Chen *et al.* 2016; Searle & Chen 2017b). This corresponded to not only the increase in atmospheric CO_2 and temperature in the region (IPCC 2013) but also increases in any other global change drivers. To investigate the sensitivity of tree growth to increases in atmospheric carbon dioxide (CO_2), temperature, and water availability, we examined the response to global environmental change drivers by using the annual temperature anomaly (ATA), the annual standardised precipitation-evapotranspiration index (SPEI), and CO_2 averaged over the census period. The annual temperature anomaly was defined as the average difference between observed mean

annual temperatures over the census period and its long-term mean (1985-2011, the length of our study period) at each plot. Similarly, we used the average annual SPEI for each census period as a measure of water availability; SPEI is an excellent indicator of drought conditions and is sensitive to changes in water availability due to global warming (Vicente-Serrano et al. 2010). We calculated SPEI by using annual climate moisture index (defined as potential evapotranspiration minus precipitation) as our measurement of water availability and the *SPEI* package in R (Vicente-Serrano et al. 2010). Both annual temperature and the annual climate moisture index were generated using BioSIM 10 (Réginère et al. 2014) for the length of our study period. BioSIM uses historical weather data from the nearest weather station to a location and adjusts predictions for differences in elevation, latitude, and longitude (Réginère et al. 2014). Atmospheric CO_2 concentration was derived from the Manua Loa Earth System Research Laboratory (http://www.esrl.noaa.gov/gmd/ ccgg/trends/co2_data_mlo.html). CO_2 values were the average values for each measurement period for each plot.

4.3.4 Competition, shade tolerance dissimilarity, and phylogenetic dissimilarity indices

Because light competition is a strong determinant for tree growth, we calculated Hegyi competition index (Hegyi 1974) based on the focal tree size, the tree sizes and distances of its neighbours using the following equation:

$$H_{ijk} = \sum_{n \neq i} \left(\frac{DBH_{njk}}{DBH_{ijk}} * \frac{1}{\left(Dist_{in}\right)_{jk}} \right) \qquad (1)$$

where H_{ijk}, is the Hegyi competition index for the *i*th tree, in the *j*th plot during the *k*th census; DBH_{njk}, DBH_{ijk}, and $(Dist_{in})_{jk}$, were the DBH of the neighbouring trees, the DBH of the focal tree *i*, and the distance between the neighbouring tree and the focal tree, respectively. We considered all trees within 12.6 m radius as the neighbours of a focal tree (Luo & Chen 2015). For tree's

which neighbourhood was not completely sampled, we divided the competition index by the area of overlap. For example, if 25% of the focal tree's neighbourhood fell outside of the plot, estimates of competition were divided by 0.75. We assumed that the stands were homogenous in that size of neighbourhood would not produce significantly different estimates of competition intensity (Luo & Chen 2015). In order to ensure our use of the full plot radius was not biasing model estimates, we calculated the Hegyi's index, shade tolerance dissimilarity, and phylogenetic dissimilarity using 10, 7.5, and 5 metre radii. Model estimates for all neighbourhood radii are presented in Fig. A3-2.

We used shade tolerance as our measure of functional niche. We adopted values of shade tolerance from Niinemets and Valladares (2006) which assign values from approximately 1 to 5 that correspond to the minimum light availability required for an individual to grow. A level of 1 corresponds to highly shade intolerant (i.e., requires at least 50% of full sunlight) and a level of 5 corresponds to highly shade tolerant (i.e., requires less than 5% of full sunlight). We estimated average neighbourhood shade tolerance dissimilarity between the focal tree and its neighbours using the following equation:

$$S_{ijk} = \frac{\sum_{n \neq i} abs(T_i - T_{nj}) \times \frac{B_{njk}}{D_{nj}}}{\sum_{1}^{n} \frac{B_{njk}}{D_{nj}}} \qquad (2)$$

where S_{ijk} is the weighted mean of neighbourhood shade tolerance dissimilarity for the *i*th focal tree in the *j*th neighbourhood at the *k*th census with *n* neighbours; and *T*, *B,* and *D* are the shade tolerance, basal area, and distance to the neighbours of the focal tree. We also estimated the phylogenetic dissimilarity for each focal tree from each surrounding neighbour. We produced a phylogeny for our study species using the Phylomatic V3 software web client

(http://phylodiversity.net/phylomatic/) and the *cophenetic* package in R statistical software, version 3.5.2 (Swenson 2014; Parker et al. 2015). We produced a dissimilarity matrix for the study species where maximum dissimilarity was set to 1 and maximum similarity (i.e., neighbour of the same species as the focal tree) to 0. Similar to shade tolerance dissimilarity, we produced a weighted neighbourhood average phylogenetic similarity by substituting phylogenetic similarity for shade tolerance in eqn. (2) (Chen *et al.* 2016). If a tree's entire neighbourhood was not sampled, we assumed the sampled region was representative of its neighbourhood since previous studies in the region found the stands to be largely homogenous (Luo & Chen 2015). Histograms of all explanatory variables across the plot network are presented in Fig. A3-3 and functional and phylogenetic similarity are presented for *Pinus banksiana* in Fig. A3-4.

4.3.5 Statistical analyses

We used the following maximum likelihood linear mixed effect model to assess whether neighbourhood dissimilarity and temporal change in the environment (represented by calendar year) interacted to improve individual tree growth rates in our study region:

$$\begin{aligned}\ln G_{ijk} = {} & \beta_0 + \beta_1 \cdot C_{ij-1k} + \beta_2 \cdot Y_{ijk} + \beta_3 \cdot D_{ijk} + \beta_4 \cdot P_{ijk} + \\ & + \beta_5 \cdot C_{ij-1k} \times Y_{ijk} + \beta_6 \cdot C_{ij-1k} \times D_{ijk} + \beta_7 \cdot Y_{ijk} \times D_{ijk} \\ & + \beta_8 \cdot C_{ij-1k} \times P_{ijk} + \beta_9 \cdot P_{ijk} \times Y_{ijk} + \beta_{10} \cdot D_{ijk} \times C_{ij-1k} \times Y_{ijk} \\ & + \beta_{11} \cdot P_{ijk} \times C_{ij-1k} \times Y_{ijk} + \beta_{12} \cdot A_{ijk} \\ & + \alpha_k + \alpha_{(k)i} + \alpha_{(k)l} + \varepsilon_{ijkl}\end{aligned} \qquad (3)$$

where lnG_{ijk} is the natural logarithm of the growth rate for the *i*th tree, at the *j*th census, within the *k*th plot; C_{ijk}, Y_{ijk}, D_{ijk}, P_{ijk}, A_{ijk}, are the competition index, calendar year, shade tolerance dissimilarity, phylogenetic dissimilarity, and age for the *i*th tree, at the *j*th census, within the *k*th plot; and, α_k, $\alpha_{(k)i}$, and $\alpha_{(k)l}$, are random intercept terms representing the effects of plot, individual tree nested within plot, and tree species nested within plot. Basal area increment was

logarithmically transformed to conform to the assumption of normality. Since the age of the tree can affect its growth rates (Poage & Tappeiner 2002), we included log-transformed stand age as a covariate in the model since all individuals recruit simultaneously post-fire in boreal stands leading to evenly-aged, though not evenly-sized, stands (Gutsell & Johnson 2002). We also estimated species level slopes by nesting the fixed effects of eqn. (3) into tree species and removing the random species term; however, Akaike Information Criterion (AIC) selection identified the model with species as a random intercept effect as the most parsimonious model.

Coefficient estimates from species level modelling are presented in Fig. A3-5 for the three major species in our study region. To ensure that any correlation between shade tolerance dissimilarity and phylogenetic similarity did not affect model interpretation, we refit eqn. (3) by modelling shade tolerance dissimilarity and phylogenetic similarity separately (Fig. A4-4). Akaike Information Criterion selection identified the combined model as the most parsimonious and variance inflation factors were less than 3 for all coefficients (Zuur et al. 2010).To investigate individual tree growth response to increased atmospheric CO_2, temperature, and water availability, we replaced the year term in eqn (3) with the individual climate drivers. While simultaneous modelling of the climate drivers would be preferable, variance inflation factors were in excess of 10 when including all three drivers, which could cause spurious coefficient estimates (Zuur et al. 2010; Dormann et al. 2013). We bootstrapped each model 1000 times to produce coefficient estimates and 95% confidence intervals.

We assessed the effects of neighbourhood dissimilarity at a radius of 12.6 m (i.e., the radius of all plots). All independent variables were standardised to speed convergence and aid in interpretability. All analyses were performed in R package *lme4* (Bates et al. 2015).

4.4 Results

Competition explained the largest amount of variation in the model, followed by the interaction between shade tolerance dissimilarity and competition, and the main effects of shade tolerance dissimilarity and temporal trends; overall, the simultaneous model accounted for 64.5% of variation in the data from the fixed effects and 86.9% of variation in the data from the random effect (Table A3-1). On average, across all species, annual basal area increment increased at 0.54 ± 0.03cm^2 $year^{-1}$ per tree (mean ± 95% bootstrapped confidence intervals). Growth decreased strongly as competition intensity increased on average (Fig. 4-1a) and decreased throughout the duration of the study period (Fig. 4-1b). Growth increased with increasing shade tolerance dissimilarity (Fig. 4-1c) but did not respond on average with increasing phylogenetic dissimilarity (Fig. 4-1d). On average, growth declined as trees aged (Fig. A3-6).

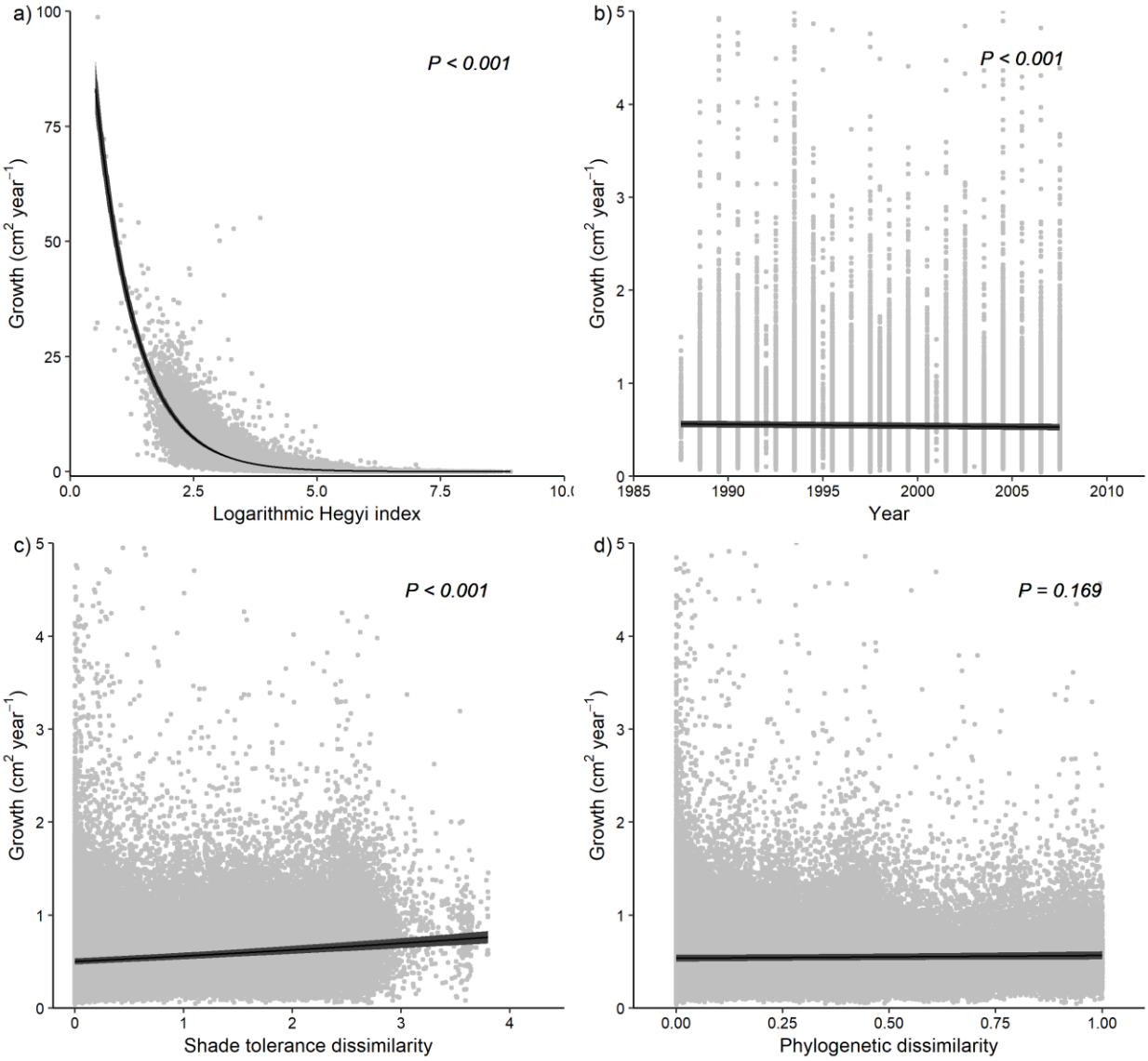

Figure 4-1: Trends in individual focal tree growth and the effects of (a) competition, (b) calendar year, and (c & d) neighbourhood dissimilarity. Solid black lines show average effects, with 95% confidence bands in grey generated by coefficient estimates from simultaneous model fit presented in Table A3-1. Background points are individual measurements of tree growth with the effects of all other predictors removed.

The effect of competition intensity on growth became more negative over the study period (Fig. 4-2). Increasing competition intensity enhanced complementarity effects; the response of growth to both shade tolerance and phylogenetic dissimilarity improved as competition intensity increased (Fig. 4-3). The improvement in the effect of shade tolerance dissimilarity on individual tree growth was particularly strong: a tree experiencing relatively low

intensity of competition had a negative response to increasing shade tolerance dissimilarity of neighbours whereas a tree experiencing relatively high intensity of competition had a positive response to increasing shade tolerance dissimilarity of its neighbours (Fig. 4-3a). Growth did not significantly respond to increases in neighbourhood phylogenetic dissimilarity until a relatively high intensity of competition (Fig. 4-3b). Complementarity effects also increased during the study period with the effects of both shade tolerance dissimilarity and phylogenetic dissimilarity increasing (Fig. 4-4). Notably, the average effect of phylogenetic dissimilarity changed directionality from initially negative at the start of the study period to positive by the end of the study period (Fig. 4-4b). The enhancement of the positive effect of shade tolerance dissimilarity by increasing competition intensity was consistent across the study period (i.e., a non-significant three-way interaction), while enhancement of the positive effect of phylogenetic dissimilarity by increasing competition intensity was increased over the study period (i.e., a significantly positive three-way interaction; Table A3-1).

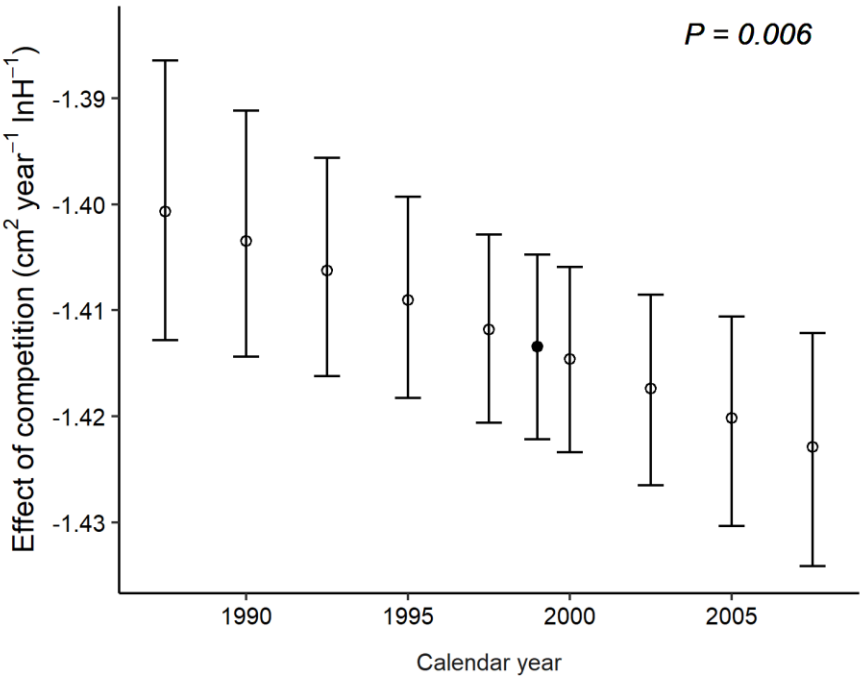

Figure 4-2: Year-dependent effect of competition intensity on growth. Values are mean and bootstrapped 95% confidence intervals generated by coefficient estimates from simultaneous model fit presented in Table A3-1; filled circles indicate mean effects for each coefficient.

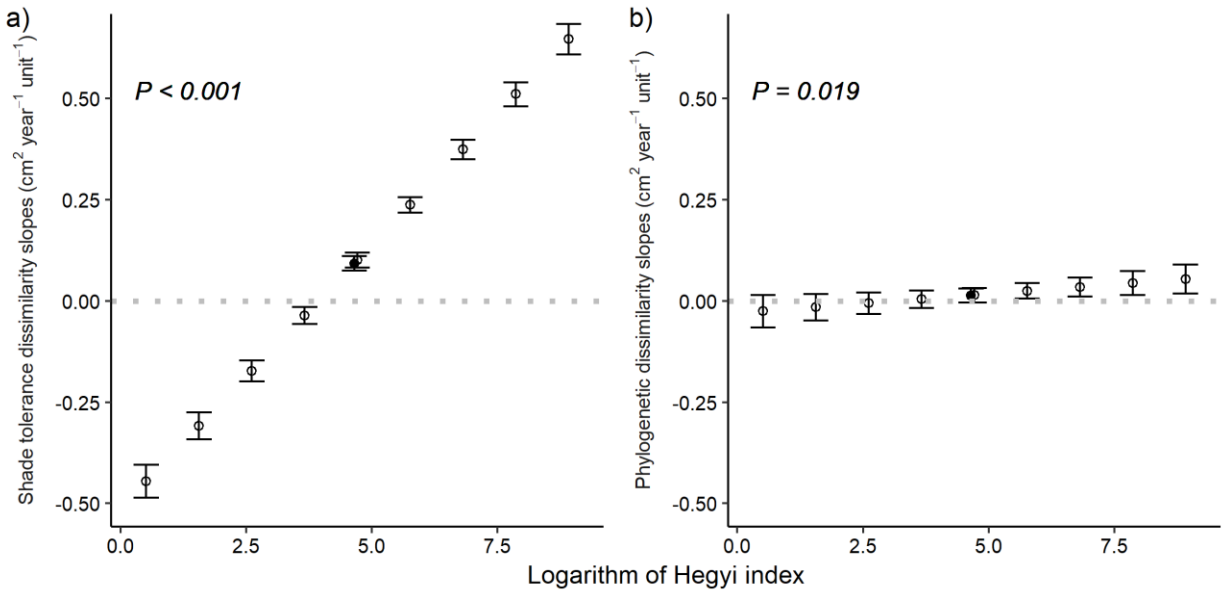

Figure 4-3: Competition-dependent effect of niche complementarity on growth. Panels depict: (a) shade tolerance dissimilarity and (b) phylogenetic dissimilarity. Values are mean and bootstrapped 95% confidence intervals generated by coefficient estimates from simultaneous model fit presented in Table A3-1; filled circles represent the effect of complementarity at the average competition intensity experienced by an individual in this study.

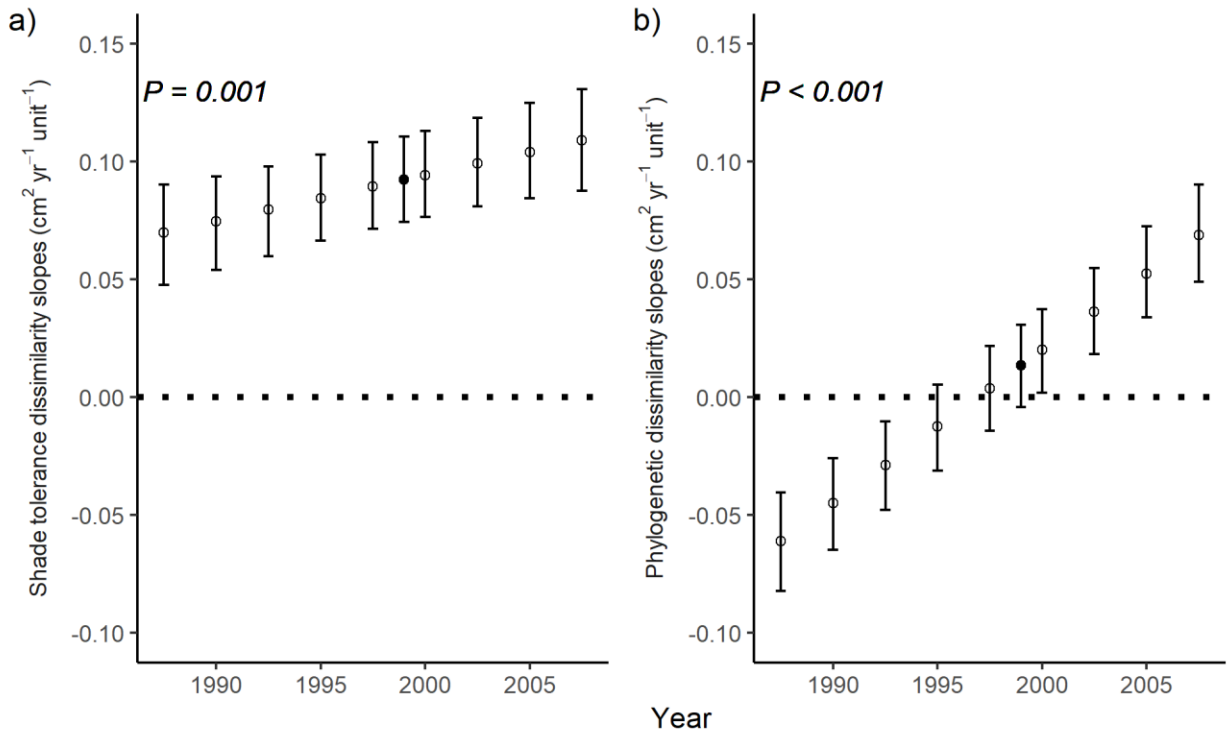

Figure 4-4: Year-dependent effect of niche complementarity on growth. Panels depict: (a) shade tolerance dissimilarity and (b) phylogenetic dissimilarity. Values are mean and bootstrapped 95% confidence intervals generated by coefficient estimates from simultaneous model fit presented in Table A3-1; filled circles represent the average effect of complementarity.

Individually modelling shade tolerance and phylogenetic dissimilarity produced similar coefficient estimates to the simultaneous model (Table A3-1). When shade tolerance dissimilarity was not accounted for, coefficient estimates of phylogenetic dissimilarity were larger and accounted for more variance suggesting that the two parameters had shared variation that was best explained by shade tolerance dissimilarity. However, there was some variation attributable to solely phylogenetic dissimilarity, particularly in the two-way interactions, as increasing phylogenetic dissimilarity still moderated the effect of competition, and enhanced response to global environmental change, after accounting for shade tolerance dissimilarity (Table A3-1).

During the study period, atmospheric CO_2, temperature, and water availability increased (Fig. 4-5 a-c). On average, similar to temporal trends, increases in both atmospheric CO_2 and

temperature led to declines in focal tree growth; however, contrary to temporal trends, increases in water availability increased focal tree growth (Table A3-2). Increases in all three climate drivers led to increases in the negative effect of competition on tree growth (Fig. 4-5 d-f). The most pronounced increase in the negative effect of competition occurred with increasing temperature, then increasing atmospheric CO_2 and finally with increasing water availability. The positive effect of shade tolerance dissimilarity was enhanced by increasing atmospheric CO_2 and water availability but reduced by increasing temperature (Fig. 4-6 a-c). The positive effect of phylogenetic dissimilarity was enhanced by increasing atmospheric CO_2 and temperature but reduced by increasing water availability (Fig. 4-6 d-f). All three climate models explained approximately 64% of the variation in growth from their fixed effects and 87% of the variation in growth when including the random effects.

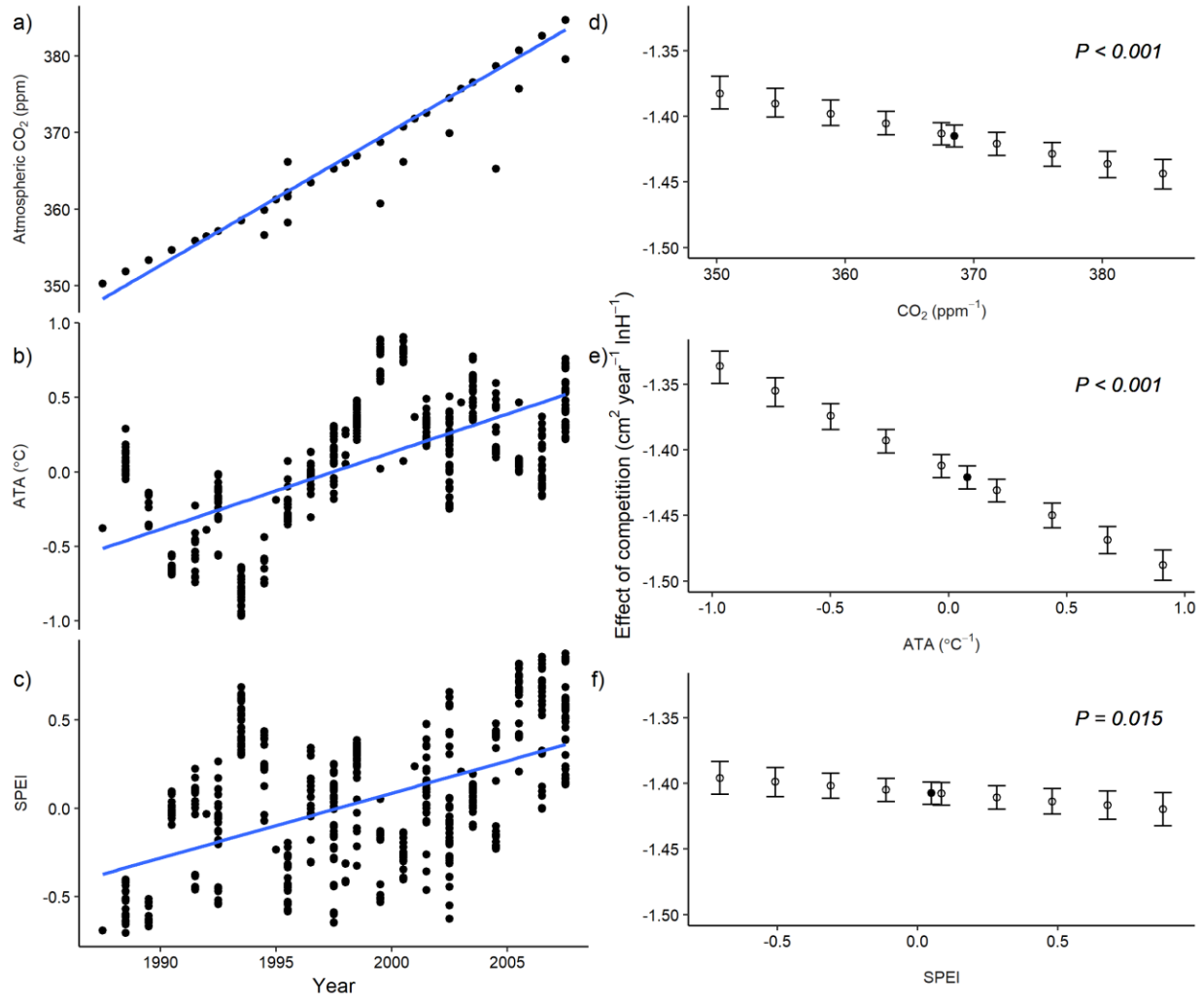

Figure 4-5: Trends in climate drivers (a-c) and their effect on the response of growth to competition (d-f). Background points in (a-c) are the climate driver for each measurement of each tree while blue lines represent linear fits. Points and error bars in (d-f) represent the average and associated 95% bootstrap confidence limits of the response of growth to competition, dependent on (d) atmospheric CO2, (e) annual temperature anomaly, and (f) standardised precipitation-evapotranspiration index generated by coefficient estimates from model fits presented in Table A3-2. Filled circles represent the average competition intensity experienced by a tree in this study.

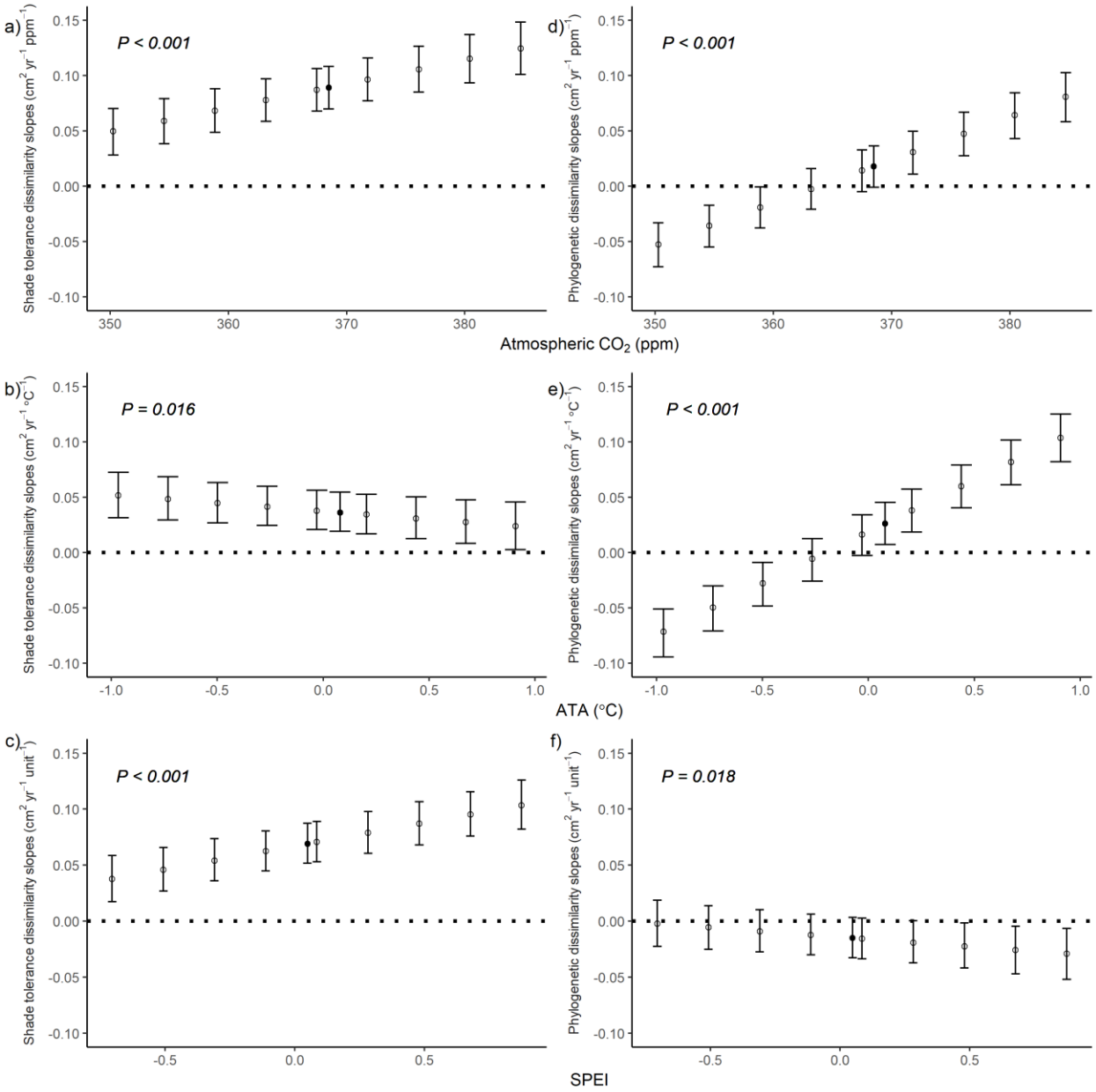

Figure 4-6: Climate driver-dependent effect of (a-c) shade tolerance dissimilarity and (d-f) phylogenetic dissimilarity. Points and error bars represent the average and associated 95% bootstrap confidence limits of (a&d) atmospheric CO_2, (b & e) annual temperature anomaly, and (c & f) standardised precipitation-evapotranspiration index dependent effects. Filled circles represent mean effects of each driver. Values are generated by coefficient estimates from model fits presented in Table A3-2.

4.5 Discussion

Our results provide evidence that the positive effect of niche complementarity on individual tree growth increases with competition intensity. Further, the positive effects of niche

complementarity on growth were enhanced during the study period and in response to increases in atmospheric CO_2, temperature, and water availability. For individuals experiencing relatively high intensity of competition, promotion of neighbours with dissimilar shade tolerance and high amount of phylogenetic resistance could help to promote growth under global environmental change.

Unsurprisingly, we found that intensity of competition was the most important predictor for tree growth rates (Oliver & Larson 1996). However, the interaction between competition intensity and neighbourhood shade tolerance dissimilarity was the second most important predictor in the full model. This interaction suggests that both the magnitude and directionality of complementarity effects on tree growth are strongly dependent on the intensity of competition being experienced by an individual tree. This dependency may help to explain discrepancies in the estimates of biodiversity-productivity relationships. In fact, on average, in neighbourhoods with low intensity of competition, trees with dissimilar neighbours grew less quickly than in stands with similar neighbours. Previous studies have suggested that smaller trees benefit more from increased diversity than larger trees (Jucker et al. 2014), and here we present direct evidence that this pattern is driven by spatial distribution of shade tolerance. Mixed stands have been shown to have higher light use efficiency (Sapijanskas et al. 2014) and crown complementarity (Pretzsch 2014; Williams et al. 2017); however, these complementarity effects are only important when light is limiting (Forrester & Bauhus 2016). Future studies examining biodiversity-productivity relationships in natural forests need to ensure that they include trees experiencing a wide-range of light availability and competitive intensities.

Complementarity effects were also strengthened during the study period providing evidence that maintaining tree species diversity can enhance positive responses, or mitigate

negative responses, of tree productivity to global environmental change (Hisano et al. 2018; Ammer 2019; Hisano et al. 2019). The effects of phylogenetic dissimilarity became significantly positive over the study period, even after accounting for differences in shade tolerance, which could be a result of two mechanisms. First, it may reflect increasing complementarity effects with global environmental change dependent on dispersion of functional traits not correlated with shade tolerance dissimilarity (Paquette et al. 2015). Second, higher phylogenetic dissimilarity may buffer tree's against the negative effects of specialist pest and pathogen outbreaks (Parker et al. 2015; Grossman et al. 2018). Studies have suggested that outbreaks of pests such as spruce budworm have increased in intensity in our study region (Boucher et al. 2018) and regions previously inaccessible to the pest due to cold temperatures will become more susceptible as the climate warms (Pureswaran et al. 2015). Further studies in areas of ongoing pest-outbreak that integrate local neighbourhood diversity and landscape level diversity are required to determine if the second mechanism is occurring at ecologically relevant magnitudes.

Despite increases in atmospheric CO_2, temperature, and water-availability, we found an average decrease in growth during our study period. The decline was strongest with increasing temperature, suggesting that these forests may be experiencing heat-stress which has been predicted to reduce growth of *Picea mariana* in the area (Girardin *et al.* 2016) and seedlings of other boreal species (Reich et al. 2015). Despite the potential heat-stress effect, trees experiencing more intense competition were even more disadvantaged than trees experiencing lower rates of competition. Our average stand was less than 45 years old which is a time of intense competition in boreal forests (Chen & Popadiouk 2002) and the majority of growth is accounted for in smaller trees at this age in this study region (Searle & Chen 2017b). It is possible that these smaller trees were more susceptible to global environmental change, or that

the previously observed increases in mortality rates with higher competition (Luo & Chen 2015) are being preceded by reduced growth rates in smaller suppressed trees (Cailleret et al. 2017), leading to an average decline in growth rates in our sample. However, this increase in competition intensity could be entirely offset by conservation and promotion of niche complementarity within stands.

CHAPTER 5: WEAKENING OF THE NATURAL FOREST CARBON SINK

5.1 Abstract

Understanding the effects of long-term global environmental change on forest productivity, estimated as growth of live trees plus volume added by recruited trees, is essential to properly estimate changes in the global terrestrial carbon sink. Here we use 293,580 ground-measured observations of forest productivity, from across the globe, representing a time series of 1951 to 2018 with the best coverage from 1985, to show that forest productivity after accounting for endogenous processes has declined by 0.016 ± 0.001 m3 ha-1 yr-2 or about a 1.9% loss per decade. By weighting biome-level estimates by their forested area to better reflect a global response, we identified a persistent decline of global forest productivity of -0.011 m3 ha-1 yr-2 or about 1.3% per decade. Further, we found that increases in temperature and declines in water availability were associated with losses in global forest productivity suggesting shifts to warmer and drier climates are at least partly responsible for our observed loss in forest productivity. Our results highlight the threat global environmental change poses to the future ability of forest ecosystems to sequester carbon.

5.2 Main body

Established forests are responsible for more than a quarter of the total global carbon sink (Pan *et al.* 2011a) but they are being threatened by increased frequency of catastrophic events as well as long-term stress associated with global environmental change (Trumbore *et al.* 2015). Until now estimates of how long-term global environmental change affects the productivity of established forests at near-global scales have been dependent on satellite-derived productivity indices (Huang *et al.* 2017) or down-scaling from measurements of atmospheric carbon dioxide fluxes

(Forkel *et al.* 2016). These studies are important in understanding overall global trends in forest productivity and carbon sequestration. However, without ground-sourced information, these studies are not able to incorporate endogenous processes associated with changes in forest regrowth or structure quantitatively into modelling frameworks (Baccini *et al.* 2017) and thereby tease apart whether overall trends in forest productivity are being driven by endogenous processes or long-term environmental change. For example, younger forests are typically more productive than older forests (Chen *et al.* 2016; Poorter *et al.* 2016) and may benefit more from global environmental change in some regions (Chen *et al.* 2016). Further, site-specific characteristics linked to total aboveground biomass, which itself is tied to time since disturbance, have a strong control on forest productivity (Michaletz *et al.* 2014). Consequently, large ground sourced networks containing plots in a variety of stages of regrowth and site conditions are required to properly disentangle the effect of long-term global environmental change from that of endogenous processes in natural forests. Previous reports from regional studies have observed both increases (Hember *et al.* 2012; Pretzsch *et al.* 2014; Brienen *et al.* 2015) and decreases (De Dios *et al.* 2007; Hogg *et al.* 2017; Zhang *et al.* 2018) in forest productivity, making global patterns hard to infer. To address this, we sought to provide a comprehensive assessment of the effects of global environmental change on the productivity of established forests, while accounting for endogenous processes, to provide better information on how this critical carbon sink is responding to long-term global environmental change.

Trends in forest response to global environmental change appear to be dependent on spatially varying factors such as regional climates and their rate of change (Girardin *et al.* 2016; Luo *et al.* 2019). Typically, four major drivers of long-term global environmental change (i.e., not catastrophic events such as drought, fire, or windstorms) are often cited as affecting forest

biomass dynamics: increasing atmospheric CO_2, increasing temperature, changes in water availability, and nitrogen deposition. Increasing atmospheric CO_2 is a global phenomena so is unlikely to be directly driving region-dependent changes in forest productivity but has been linked to increases in forest productivity through increases in water use efficiency (Keenan *et al.* 2013; Pretzsch *et al.* 2014). Alternatively, increases in temperature are occurring more quickly in regions closer to the pole than the equator (Diffenbaugh & Field 2013). These increases can improve forest productivity and lengthen growing seasons (Keenan *et al.* 2014); but may leave plants more susceptible to frost (Liu *et al.* 2018) and cause water stress in regions where precipitation has not increased. Changes in water availability are highly regional (Sheffield *et al.* 2012), but in areas where water availability is decreasing, it has often been cited as a critical driver of increased mortality (Allen *et al.* 2015) and reduced growth (Girardin *et al.* 2016), especially in those regions that were already water-limited (Luo *et al.* 2019). Similar to water availability, nitrogen deposition is also spatially variable, with the highest rates typically concentrated near large population centers and areas with high agricultural development. Nitrogen deposition increases forest productivity in areas that are nitrogen limited (Schulte-Uebbing & de Vries 2018) and may also help alleviate water stress on plants in areas that are drying (Ibanez *et al.* 2018). While regional studies of permanent sample plot networks have focussed on examining the global change driver operating within their region, there has been no investigation to determine which of the three regionally dependent environmental factors are most important to forest productivity response to long-term environmental change at global scales.

Here we used a global network of permanent sample plots to: 1) assess how long-term global environmental change has affected forest productivity; and, 2) to better understand the

drivers (i.e., increasing temperature, changes in water availability, and nitrogen deposition) of divergent responses to long-term global environmental change across the globe. Our data set consists of a total of 293,580 observations of forest productivity. The observations were recorded between 1951 and 2018 with good coverage after 1980; total measurement period within biomes was on average 38 years (Table A4-1 & Fig. A4-1). The longest coverage was within temperate, boreal, and Mediterranean biomes. For each plot, all trees were tagged and repeatedly measured. Annual forest productivity was the sum of growth in volume of all trees alive at the second census date plus the volume added by stems that recruited during two successive censuses (i.e., grew larger than the measurement threshold) divided by the length of the census period. We used a two-step modelling framework to achieve our two objectives. First, we used linear mixed effects models to estimate the change in forest productivity within each biome over our study period (represented by calendar year (Brienen *et al.* 2015)). Second, we modelled the responses of forest productivity to both calendar year and stand basal area. We used stand basal area in our models as a direct measure of stand density, and as a proxy for aboveground biomass, since both stand density and aboveground biomass are positively correlated to the age of a stand and to site quality (Michaletz *et al.* 2014; Liang *et al.* 2016). This allowed us to more accurately estimate the response of forest productivity to long-term environmental change, rather than overall change during the study period, by removing some of the confounding variation due to endogenous processes associated with stand development (Chen *et al.* 2016). To examine whether changes in forest productivity were related to rising temperatures, changes in water availability, and nitrogen deposition, we substituted each climate driver for calendar year in the model.

On average, across our global plot network, forest productivity was estimated to be 8.9 $m^3\ ha^{-1}\ yr^{-1}$. Overall, forest productivity increased significantly by 0.008 ±0.001 $m^3\ ha^{-1}\ yr^{-2}$

during our study period. The estimated increase in forest productivity was not consistent across the globe: notably, temperate conifer forests (largely located on the western coast of North America) experienced a significant decline in forest productivity over the study period (Fig. 5-1a). Models used to estimate the overall trend in forest productivity over the study period explained 16% of the variation in forest productivity from the fixed effects alone, increasing to 90% when including the random effects.

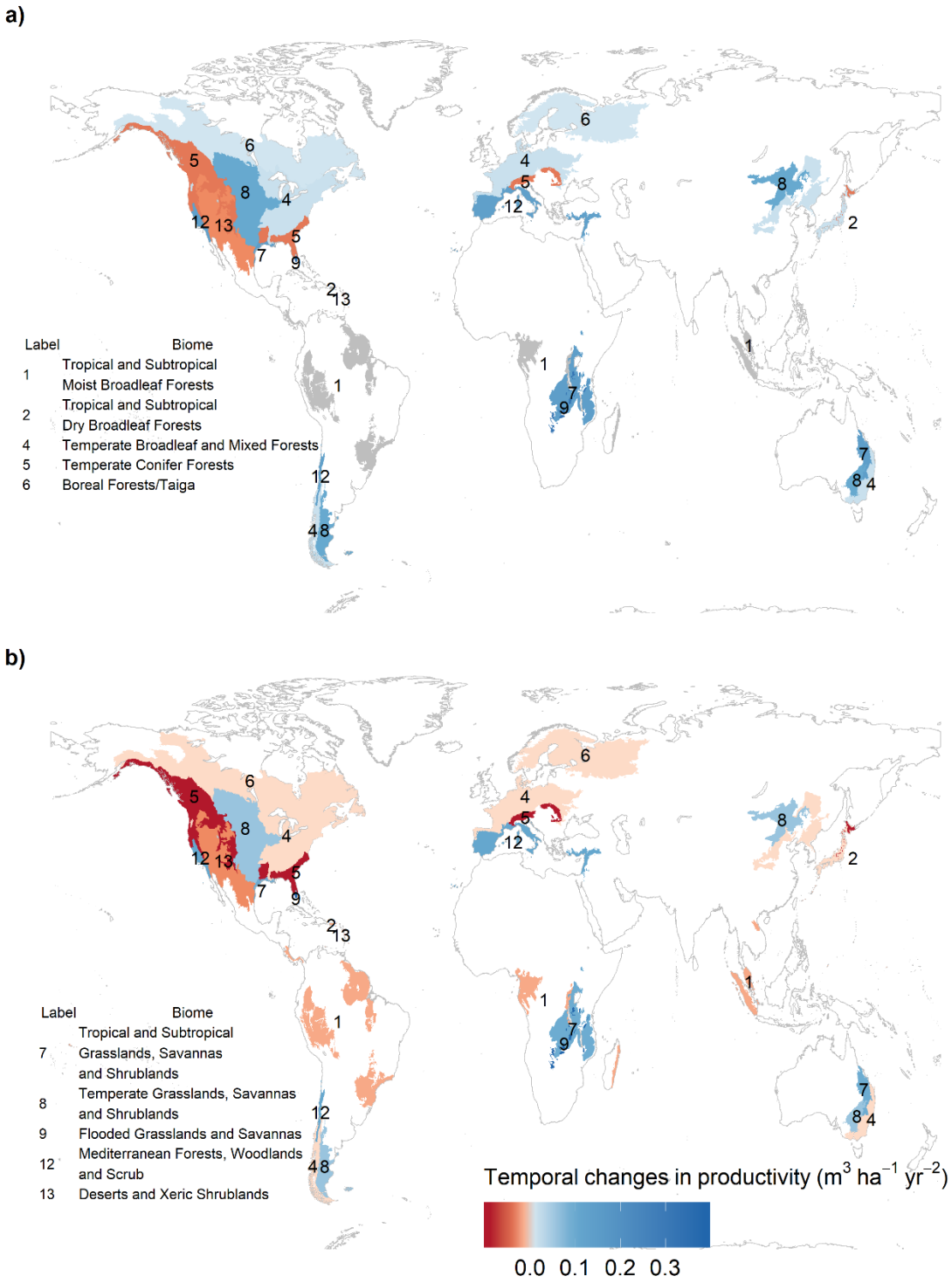

Figure 5-1: Temporal trends in annual forest productivity. The figure depicts coefficient estimates of change in forest productivity over our study period of 1951 to 2018, with the best coverage from 1985 onwards, for each biome: (a) without simultaneous modelling of stand basal area (i.e., model in eqn. (1)) (b) with simultaneous modelling of stand basal area (i.e., model in eqn. (2)). Colours represent coefficient estimates of calendar year fit by biome from linear mixed

effects models presented in eqn. 1 & 2. Polygons are the subset of each biome that represent ecoregions where plots were established, extracted from shapefiles provided by the Nature Conservatory at http://maps.tnc.org/gis_data.html, based on World Wildlife Fund estimates (37). Biome-level estimates were not visualised on forested regions where our data did not have coverage.

This overall increase in forest productivity during our study period seems to be largely attributable to endogenous processes. Simultaneous modelling of stand basal area and calendar year led to an average forest productivity estimate of 8.2 m^3 ha^{-1} yr^{-1} and a significant decline in forest productivity across our plots of 0.016 ± 0.001 m^3 ha^{-1} yr^{-2} or about a 1.9% loss per decade. This decline in forest productivity after accounting for endogenous processes was largely driven by temperate coniferous forests, temperate broadleaf and mixed forests, and boreal forests, all of which responded negatively to global environmental change. Mediterranean forests and flooded savannahs continued to have significant increases in forest productivity after accounting for endogenous processes (Fig. 5-1b). Other biomes with large magnitudes of estimates in changes in forest productivity had large uncertainty around the estimates (Fig. A4-2). Models estimating forest productivity over the study period including both calendar year and stand basal area explained 21% of the variation in forest productivity from the fixed effects alone, increasing to 92% when including the random effects.

To produce more robust estimates of changes in forest productivity over the forest areas that our plots represent, rather than within the plots themselves, we weighted the biome level estimates by their forested area. Average forest productivity when weighting by forested area was estimated to be 9.2 m^3 ha^{-1} yr^{-1} for the total forest area represented by our plot network of 1.6 *10^9 ha, and a temporal increase of forest productivity of 0.011 m^3 ha^{-1} yr^{-2}, or about a 1.2% gain per decade.

From the model with both calendar year and stand basal area as predictors, we estimated that global forest productivity declined by 0.011 m^3 ha^{-1} yr^{-2} or about 1.3% per decade. Once

again this was driven by the increased importance of boreal forests which responded less negatively than temperate conifer forests (Fig. 5-1b). Our estimates for the negative long-term effect of global change on forest productivity were less severe when weighted by forest area represented by each biome. The increase in the estimate of global forest productivity change over our study period is attributable to the large forested area and more precise positive estimate of the temporal trend in boreal forests compared to the slightly smaller forested area and large variation around the negative estimate of the temporal trend in temperate conifer forests (Table A4-1, Fig. 5-1a).

The opposing trends of forest productivity estimates when omitting or including stand basal area highlight key mechanisms underpinning global changes in forest productivity. Endogenous processes dominate patterns in forest productivity – for instance, recovery from a stand-replacing disturbance is more important than half-century shifts in climate (Chen *et al.* 2016). On aggregate across our plot network, stands were continuing to regrow from major disturbances in the past and thus would experience accelerations in forest productivity as aboveground biomass recovered to pre-disturbance levels (Michaletz *et al.* 2014; Poorter *et al.* 2016; Pugh *et al.* 2019) leading to an overall increase in forest productivity over our study period. This pattern of regrowth is likely a major driver of the reported increases of carbon uptake in northern forests (Ciais *et al.* 2019), where stand-replacing disturbances are common and the youngest stands are often the most productive (Chen *et al.* 2016). After accounting for these endogenous processes, however, global forest productivity is overall in decline. This suggests that while continued regrowth will maintain positive trends in global forest productivity for some time, the rate is slowing. Recent estimates for an upper bound on biomass storage in North American temperate and boreal forest ecosystems due to long-term global environmental

change (D'Orangeville *et al.* 2018; Zhu *et al.* 2018) indicate that this may already be occurring. Established forests are still a major carbon sink (Pan *et al.* 2011a) but such broad-scale reductions in forest productivity are likely to present a threat to forest ecosystems globally, and any decrease in their capacity to store carbon provides a negative feedback loop to ongoing global environmental change.

The next step in our analysis involved disentangling, to the degree possible, impacts of different global change drivers. Responses to increasing temperature were, on average, significantly negative. Declines in forest productivity across North America, Australia, Asia, and some tropical areas in Africa were observed (Fig. 5-2d). Whether this decline is due to increases in heat stress as temperatures exceed physiological optima (Huang *et al.* 2019), indirect impacts on soil moisture, insects, or diseases, or through simultaneous increases in other negative drivers is unclear. The forest productivity of four biomes responded negatively to increasing annual temperature anomaly (temperate broadleaf and mixed forests, temperate conifer forests, boreal forests, and tropical savannas and shrublands) while only Mediterranean forests responded significantly positively to increases in temperature. Responses in other biomes had large magnitudes (e.g., tropical regions) but the uncertainty around these estimates was also large (Fig. A-3). Increases in water availability, as measured by the standardised precipitation-evapotranspiration index, were significantly associated with increases in forest productivity; put another way, declines in water availability were associated with declines in forest productivity. At the biome level, forest productivity in five biomes was positively associated with increases in water availability (temperate conifer forests, boreal forests, tropical savannas and shrublands, temperate savannas and shrublands, and Mediterranean forests) while only flooded savannas had a negative relationship to increases in water availability (Fig. 5-2e). Water availability has been

highlighted as a major driver of forest productivity in North American boreal (Girardin *et al.* 2016) and temperate forests (Zhang *et al.* 2018). Strong declines in overall water availability in parts of these regions, particularly western North America (Fig. 5-2b), may be responsible for our estimated declines in forest productivity over the study period. Further, droughts in tropical areas have been linked to major losses in forest productivity (Doughty *et al.* 2015), suggesting that even in these regions water availability has a tight link to forest productivity. Finally, increases in nitrogen deposition had an overall positive effect on forest productivity but the trend was not statistically significant (Fig. A4-3). While the forest productivity of temperate conifer forests, boreal forests, and temperate savannas had a significantly positive response to nitrogen deposition, tropical and subtropical moist broadleaf forests, temperate broadleaf and mixed forests, and Mediterranean forests had declines in forest productivity associated with higher nitrogen deposition. However, given these forests' proximity to population centers (especially on the eastern coast of North America and throughout Western Europe), this pattern may track more closely to direct anthropogenic disturbance, or co-varying ozone pollution, than to nitrogen deposition itself.

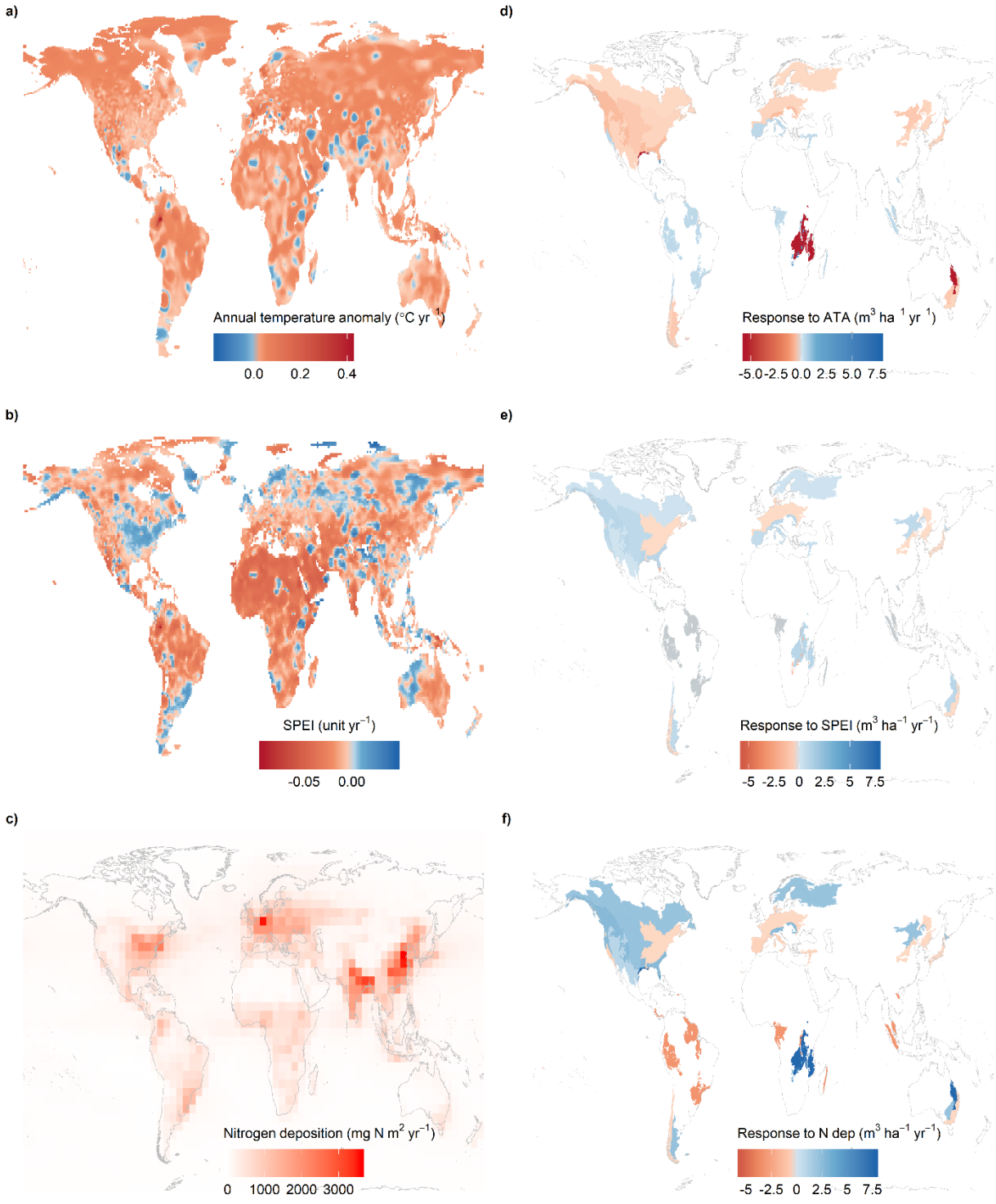

Figure 5-2: Temporal trends in global environmental change drivers and their effects on forest productivity. The figure depicts (a) temporal trends in annual temperature anomaly in 1° by 1° grids from 1948 to 2018; (b) temporal trends standardized precipitation-evapotranspiration index in 1° by 1° grids from 1954 to 2018; and, (c) annual nitrogen deposition as of 1993 in 5° by 3.75° grids. Changes in forest productivity due to: (d) increasing annual temperature

anomalies; (e) increases in water availability (i.e., a positive slope means decreasing forest productivity in regions with decreasing water availability); and, (f) increases in nitrogen deposition. Trends in annual temperature anomaly were derived from UDel_AirT_Precip data (38) provided by the NOAA/OAR/ESRL PSD, Boulder, Colorado, USA, from their Web site at http://www.esrl.noaa.gov/psd/ and averaged to a yearly value from 1948 to 2018. Trends in SPEI were derived from a global dataset of 12-month average SPEI values at http://spei.csic.es/index.html from 1954 to 2018. was extracted from an estimate of annual nitrogen deposition in the year 1993 (41). Colours represent coefficient estimates of drivers of global environmental change in (d-f) by biome from linear mixed effects models. All variables were scaled prior to analysis so colour intensity is directly comparable across all global environmental change drivers.

Our analysis reveals an overall global decline in forest productivity under long-term global environmental change, when controlling for endogenous processes. These striking trends alter our perception of the global forest sink under global change. First, these trends suggest that while current forests are gaining in productivity, these gains are likely due to recovery from disturbance and increases in stand density and not from global environmental change making these gains unlikely to persist. Second, these trends suggest that changes in forest productivity may in fact cause a potential negative feedback loop: declines in overall forest productivity will reduce the ability forests to sequester carbon under global environmental change, which would further compromise forest productivity. Finally, given the expected intensification of global environmental change with ongoing increases in carbon emissions (IPCC 2013) our reported declines in forest productivity may only increase in severity.

5.3 Materials and Methods

5.3.1 Forest productivity data

We compiled data from two major sources. Since data processing methodologies were varied, we designated these two data as “Tier 1” and “Tier 2”. Tier 1 data was compiled directly from twelve different forest surveys across Canada and the United States. Data of individual tree

measurements were obtained from the Canadian provincial governments of British Columbia, Alberta, Saskatchewan, Manitoba, Ontario, Nova Scotia, and Newfoundland and Labrador, as well as from the federal government of the United States Forest Inventory Analysis program and from the University of Alaska Fairbanks. While each forest survey had its own methodology, we selected only plots that met the following criteria: (i) were fixed in area; (ii) had all trees tagged and repeatedly measured with species identification and diameter at breast height recorded; and (iii) had a minimum of two censuses so that volume productivity could be accurately estimated. The plots in the Tier 1 data set are well distributed throughout Canada and the United States and represent a continental spatial gradient (Fig. A4-1). Tier 1 plots were measured between 1951 and 2018 with good coverage from 1970 onwards (Fig. A4-4). Tier 1 plots had a mean interval length of 7.3 ±3.4 (standard deviation) years, an average total monitoring length of 13.9 ±10.2 years, and a mean plot size of 0.25 ± 0.24 ha. When possible, allometric equations for gross stem volume provided by the data provider were used; when unavailable (only the case in Canada) national volume estimates or neighboring province estimates were used. Tier 1 data were examined for typographical errors (e.g., misreported decimal places in DBH measurements) and further examined for missed observations. Stems with a missed observation (e.g., present and live in census 1 and in census 3 onwards but not present in census 2) had the missing DBH interpolated as the average between the successive and previous census DBH. Dead trees without measured DBHs were assigned their previous live DBH. Negative growth rates were allowed so long as they were reasonable (i.e., within measurement error), but large negative changes were examined for typographical errors and corrected if found. Measurement errors could have resulted from different positions measured for DBH between censuses, and weather conditions that affect tree bark swell due to available moisture. We considered these errors to be random,

causing small negative or positive changes in growth estimates. Tier 1 data included 136,273 observations of annual forest productivity and 71,247 fixed plots, with over 20,750 ha and 200,000 ha years-worth of monitoring.

Tier 2 data was collected from the Global Forest Biodiversity Initiative database for forest inventories outside of North America. This database includes estimates of stand-level annual forest productivity (net change in standing live volume between censuses plus volume lost due to mortality), stand basal area, and plot locations. Data for this database were obtained from national and sub-national governments and research institutions with a variety of collection methodologies (full details provided in (Liang *et al.* 2016)). We excluded estimates of forest productivity that were not estimated by at least two census points and removed 6 observations that occurred before 1951 (the start of our Tier 1 data set) due to the long period between remeasurements (50 or more years in all cases). Tier 2 stands did not always have unique plot identifications meaning that re-measurements of the same plot could not be reliably identified within the data set. Tier 2 data represented 157,307 observations of annual forest volume productivity with an average census period of 7.5±2.9 years. Observations in Tier 2 data began in 1970 but was best representative of 1985 onwards with most observations occurring after 2000 (Fig. A4-4). The total dataset combined (i.e., Tier 1 and Tier 2) represented 293,580 observations of annual forest volume productivity. Number of observations, first and last year of census, and forested area by biome for the total dataset are presented in Table S1.

5.3.2 Explanatory variables

We used the middle calendar year of a census period for each observation as a proxy to represent global environmental change as a whole (van Mantgem *et al.* 2009; Peng *et al.* 2011; Pretzsch *et al.* 2014; Brienen *et al.* 2015; Chen & Luo 2015; Chen *et al.* 2016; Searle & Chen 2017a).

Biomes were extracted from shapefiles provided by the Nature Conservatory at http://maps.tnc.org/gis_data.html, based on World Wildlife Fund estimates (Olson *et al.* 2001), using plot spatial locations, similar to previous global forest inventory studies (Liang *et al.* 2016). For mapping purposes, only ecoregions that contained plots were graphed to emphasize the spatial extent of our network (i.e., no 'boreal biome' presence in Eastern Russia because of no established plots in that ecoregion).

To estimate the impact of endogenous processes related to stand density, time since disturbance, and site quality we used stand basal area (Michaletz *et al.* 2014; Liang *et al.* 2016). Stand basal area was calculated as the sum of the basal area of every living tree divided by the plot area. To generate an average for the census period we averaged stand basal area at the initial measurement with stand basal area at the second measurement. Temperature data was acquired from UDel_AirT_Precip data (Willmott *et al.* 2001) provided by the NOAA/OAR/ESRL PSD, Boulder, Colorado, USA, from their Web site at http://www.esrl.noaa.gov/psd/ and averaged to a yearly value from 1948 to 2018. Climate anomalies allow for direct comparison of differences from long-term climates across large spatial and climactic scales (Clark *et al.* 2011). The annual temperature anomaly (ATA) was calculated as the difference between an observed annual temperature and the mean temperature for the entirety of the study period. The ATA was then averaged across all years of a census period for each remeasurement of each plot. It increased across the globe over the study period (Fig. 5-2a). Monthly global standardized precipitation-evapotranspiration index (SPEI) data was acquired from http://spei.csic.es/index.html and was averaged across each year. Yearly SPEI data was then averaged across all years of a census period for each remeasurement of each plot. SPEI is scaled to each location and sensitive to changes in both temperature and precipitation, making it an ideal index of changes in long-term

water availability (Vicente-Serrano *et al.* 2010). SPEI changes were highly regional (Fig. 5-2b). Nitrogen deposition data was extracted from an estimate of annual nitrogen deposition in the year 1993 (Dentener 2006). Nitrogen deposition was greatest around large population centers (Fig. 5-2c).

5.3.3 Statistical analyses

To examine changes in global forest productivity due to global environmental change, we used two modelling approaches. First, we examined overall temporal trends in forest productivity without accounting for stand basal area. We accounted for effects of regional climate and forest structures by modelling forest response within biomes (Crowther *et al.* 2015; Liang *et al.* 2016). As we use data from multiple data sources with different thresholds, which can lead to biased mean estimates of forest productivity (Searle & Chen 2017b), we included data provider in the model as a fixed factor. Further, to account for local site conditions and non-independence of remeasurements we also included plot identity as a random intercept effect. This produced the following linear mixed effect model:

$$P_{ijklm} = B_i + B_i \times Y_{(i)jm} + T_k + P_l + \pi_m + \varepsilon \qquad (1)$$

where P_{ijklm} was the forest productivity, observed at the jth census period in the mth plot. B_i was the biome and $Y_{(j)jm}$ was the mid calendar year for the jth census in the kth plot, nested in biome. T_k was the data Tier (i.e., Tier 1 or Tier 2 data) and P_l is the data provider. π_m is the random effect of plot identity.

The second modelling approach was to examine the response of forest productivity to global environmental change after accounting for the effect of endogenous processes represented by stand basal area. To do this, we modified eqn. (1) to include the stand basal area per hectare (Liang *et al.* 2016):

$$P_{ijklmno} = B_i + B_i \times Y_{(i)jm} + B_i \times \ln(G)_{(i)jm} + T_k + P_l + \pi_m + \varepsilon \qquad (2)$$

where all terms are identical to eqn. (1) except for the addition of $\ln(G)_{(i)jo}$ which was the standing basal area observed at the *j*th census in the oth plot. Basal area and year were standardised by subtracting their mean and dividing by their standard deviation prior to analysis. R^2 values were determined using the *r.squaredGLMM* function from the package *MuMIn* and methods described in Nakagawa and Schielzeth (2013).

To estimate the average temporal trend in forest productivity across our plot network we modified eqn. (2) by removing the interaction between calendar year and biome. Since we assumed a normal error distribution the maximum likelihood algorithm simplifies to be a least-squares algorithm for estimating the fixed effects (Zuur *et al.* 2009), making the overall slope estimate an average of all biome level responses weighted by the reciprocal of each biome estimate's variance (Neter *et al.* 1996). To produce a forest area weighted global estimate of the temporal trend in forest productivity, we weighted the average of biome-level estimates obtained by eqn. (1) and (2) by the forest area contained within each polygon in Fig. 5-1 for each biome multiplied by the reciprocal of the variance of the biome estimate. Forest areas were retrieved from a forest cover database that represents forest cover as of 2000 (Hansen *et al.* 2013); we defined forest to be any area with vegetation at least 5 m high covering at least 20% of the area (DeFries *et al.*). To reduce computation time we aggregated the initial rasters of 900 m^2 to 1 km^2. We obtained areas of each raster cell, correcting for differences in latitude, by using the *area* function in the *raster* package.

We also compared estimates of forest productivity by modelling both Tier 1 and Tier 2 data and then modelling estimates of forest productivity using just Tier 1 data. Since estimates were largely consistent (Fig. A4-5), we report on the total dataset in the main text. We also examined

whether basal area was a good proxy for stand age in determining stand development. Following previous studies (Luo & Chen 2013; Pretzsch *et al.* 2014; Chen & Luo 2015; Chen *et al.* 2016; Searle & Chen 2017a) we used the natural logarithm of stand age instead of the natural logarithm of stand basal area to account for endogenous processes. To estimate ages in Canadian data dendrochronological ageing was used, with appropriate correction factors (Huang *et al.* 2009) and stands were assigned the average age of the oldest present species. For data from the United States, stand age was also determined by dendrochronological techniques with local correction factors, but stands were assigned the average age of all selected ageing trees across species. For data from the Alaskan database, North American forest age maps (Pan *et al.* 2011b) were used to extract ages for each stand. Since stand age information was only available for 42,999 plots, and using stand basal area in the models as a proxy for stand age and other endogenous processes produced similar coefficient estimates to using stand age directly (Fig. A4-6), we present the analysis including stand basal area in the main text. Finally, to ensure our use of allometric equations to estimate individual tree volume did not bias our estimates of global environmental change effects on forest productivity, we re-fit eqn. (2) using only Tier 1 data and forest productivity determined by basal area. Since coefficient estimates between forest productivity estimated by basal area and forest productivity estimate by volume were similar (Fig. A4-7), and Tier 2 data did not contain estimates of forest productivity from basal area, we presented results derived from forest productivity estimated by volume in the main text.

To further examine how global change drivers (annual temperature anomaly, standardized-precipitation evapotranspiration index, and nitrogen deposition) were affecting forest productivity, we replaced calendar year in eqn. (2) with each global environmental change

driver. Since variance inflation factors were over 10 for a model with all drivers included, we modelled each driver independently (Zuur *et al.* 2010).

CHAPTER 6: GENERAL CONCLUSION

Anthropogenic global environmental is a major threat to ecosystems across the globe. While cutting emissions of so-called greenhouse gasses is the most efficient way to curb anthropogenic global environmental change, promoting and maintaining carbon storage in forest ecosystems is also an important avenue for mitigation. However, before we can fully realise the carbon-storing potential of these ecosystems, we must understand how these ecosystems have responded to past and present anthropogenic climate change and how they are likely to respond to future anthropogenic climate change.

By using permanent sample plot networks from across the globe, I have furthered our understanding of how anthropogenic global environmental change has affected forest ecosystem dynamics. I have demonstrated that using large size thresholds can bias estimates of age-related trends in stand level biomass gain, loss, and net change but does not bias estimates of climate change effects on biomass dynamics. Further, I have demonstrated that trees with faster lifetime growth rates have shortened longevities due to higher mortality rates compared to trees with slower lifetime growth rates. Moreover, I have also shown that both functional and phylogenetic dissimilarity to neighbours can benefit individual tree growth and reduce the increasingly negative effects of competition under global change. Finally, I have shown that global environmental change has led to an overall decline in global forest productivity. A summary of the key findings of each chapter of this dissertation are as follows:

1. Use of a diameter at breast height threshold significantly underestimated biomass productivity and loss due to mortality. These underestimates are exacerbated as the threshold size increases since surveys become “blind” to an increasing number of smaller trees. There was some indication that use of a threshold might underestimate temporal

increases in biomass loss due to mortality but no indication of biases in estimates of productivity or net change. However, there was a large effect of thresholds on estimates of age effects on biomass dynamics. Mortality was always underestimated and, notably, the peak productivity was incorrectly estimated using a 10 cm threshold. Without a threshold, the most productive stands were the youngest stands. Use of a 10 cm threshold estimated peak productivity to occur at about 48-years post-fire. Future studies seeking to estimate forest recovery need to properly account for the effects of tree-size thresholds in their sampling designs.

2. My results show consistent temporal increases in annual mortality probabilities for trees older than 100 years during the past half-century in Alberta indicating that tree longevity declined over time. These reductions in tree longevity were strongest in trees with faster lifetime growth rates suggesting that tree life cycles were accelerated. The reduced longevity was associated with increasing atmospheric carbon dioxide concentrations and reduced water availability. With ongoing environmental change in the region expected to continue to increase carbon dioxide concentrations and reduce water availability the reductions in tree longevity are expected to continue.
3. In my examination of how functional and phylogenetic dissimilarity of a focal tree to its neighbours might affect individual tree growth, I found that both functional and phylogenetic dissimilarity to neighbours reduced the negative effect of competition for light on growth and the negative effect of global environmental change. Importantly, this reduction was accomplished when modelling each measure individually and combined suggesting functional and phylogenetic dissimilarity operate on different elements of tree growth. These results provide a potential mechanism to explain how promoting or

maintaining tree species richness can improve or mitigate forest response to global environmental change. These findings also provide two dimensions on which forest managers can maintain this diversity: both functionally and phylogenetically.

4. By using 228,545 plots from across the globe sampled from 1916 to 2018, I estimated that forest productivity after accounting for forest regrowth has declined by -0.019 ± 0.001 m3 ha-1 yr-2 or about a 0.21% loss per year. When these estimates were weighted by land area they represented, I estimated a decline of global forest productivity of -0.005 m3 ha-1 yr-2 or about 0.06% per year. The major drivers of this decline appear to be increases in temperature and changes in water availability, which were both net negatives at the global scale. These results highlight that the global terrestrial carbon sink is weakening and that future global environmental change may be exacerbated.

REFERENCES

Allen, C.D., Breshears, D.D. & McDowell, N.G. (2015). On underestimation of global vulnerability to tree mortality and forest die-off from hotter drought in the Anthropocene. *Ecosphere*, 6, 1-55.

Allen, C.D., Macalady, A.K., Chenchouni, H., Bachelet, D., McDowell, N., Vennetier, M., Kitzberger, T., Rigling, A., Breshears, D.D., Hogg, E.H., Gonzalez, P., Fensham, R., Zhang, Z., Castro, J., Demidova, N., Lim, J.H., Allard, G., Running, S.W., Semerci, A. & Cobb, N. (2010). A global overview of drought and heat-induced tree mortality reveals emerging climate change risks for forests. *For. Ecol. Manage.*, 259, 660-684.

Ammer, C. (2019). Diversity and forest productivity in a changing climate. *New Phytol.*, 221, 50-66.

Anderegg, W.R., Berry, J.A., Smith, D.D., Sperry, J.S., Anderegg, L.D. & Field, C.B. (2012). The roles of hydraulic and carbon stress in a widespread climate-induced forest die-off. *Proc Natl Acad Sci U S A*, 109, 233-237.

Avitabile, V., Herold, M., Heuvelink, G.B., Lewis, S.L., Phillips, O.L., Asner, G.P., Armston, J., Ashton, P.S., Banin, L., Bayol, N., Berry, N.J., Boeckx, P., de Jong, B.H., DeVries, B., Girardin, C.A., Kearsley, E., Lindsell, J.A., Lopez-Gonzalez, G., Lucas, R., Malhi, Y., Morel, A., Mitchard, E.T., Nagy, L., Qie, L., Quinones, M.J., Ryan, C.M., Ferry, S.J., Sunderland, T., Laurin, G.V., Gatti, R.C., Valentini, R., Verbeeck, H., Wijaya, A. & Willcock, S. (2016). An integrated pan-tropical biomass map using multiple reference datasets. *Glob Chang Biol*, 22, 1406-1420.

Baccini, A., Walker, W., Carvalho, L., Farina, M., Sulla-Menashe, D. & Houghton, R.A. (2017). Tropical forests are a net carbon source based on aboveground measurements of gain and loss. *Science*, 358, 230-234.

Bates, D., Bolker, B., Walker, S., Christensen, R.H.B., Singmann, H., Dai, B. & Grothendieck, G. (2016). lme4: Linear mixed-effects models using Eigen and S4. R package version 1.1-10. Available at: https://cran.r-project.org/web/packages/lme4/index.html Last accessed 1 September 2016.

Bates, D., Machler, M., Bolker, B.M. & Walker, S.C. (2015). Fitting Linear Mixed-Effects Models Using lme4. *Journal of Statistical Software*, 67, 1-48.

Bennett, A.C., McDowell, N.G., Allen, C.D. & Anderson-Teixeira, K.J. (2015). Larger trees suffer most during drought in forests worldwide. *Nat Plants*, 1, 15139.

Bigler, C. & Veblen, T.T. (2009). Increased early growth rates decrease longevities of conifers in subalpine forests. *Oikos*, 118, 1130-1138.

Bond-Lamberty, B., Wang, C. & Gower, S.T. (2002). Aboveground and belowground biomass and sapwood area allometric equations for six boreal tree species of northern Manitoba. *Canadian Journal of Forest Research-Revue Canadienne De Recherche Forestiere*, 32, 1441-1450.

Boucher, D., Boulanger, Y., Aubin, I., Bernier, P.Y., Beaudoin, A., Guindon, L. & Gauthier, S. (2018). Current and projected cumulative impacts of fire, drought, and insects on timber volumes across Canada. *Ecol. Appl.*, 28, 1245-1259.

Brandt, J.P. (2009). The extent of the North American boreal zone. *Environ. Rev.*, 17, 101-161.

Brienen, R.J., Phillips, O.L., Feldpausch, T.R., Gloor, E., Baker, T.R., Lloyd, J., Lopez-Gonzalez, G., Monteagudo-Mendoza, A., Malhi, Y., Lewis, S.L., Vasquez Martinez, R., Alexiades, M., Alvarez Davila, E., Alvarez-Loayza, P., Andrade, A., Aragao, L.E.,

Araujo-Murakami, A., Arets, E.J., Arroyo, L., Aymard, C.G., Banki, O.S., Baraloto, C., Barroso, J., Bonal, D., Boot, R.G., Camargo, J.L., Castilho, C.V., Chama, V., Chao, K.J., Chave, J., Comiskey, J.A., Cornejo Valverde, F., da Costa, L., de Oliveira, E.A., Di Fiore, A., Erwin, T.L., Fauset, S., Forsthofer, M., Galbraith, D.R., Grahame, E.S., Groot, N., Herault, B., Higuchi, N., Honorio Coronado, E.N., Keeling, H., Killeen, T.J., Laurance, W.F., Laurance, S., Licona, J., Magnussen, W.E., Marimon, B.S., Marimon-Junior, B.H., Mendoza, C., Neill, D.A., Nogueira, E.M., Nunez, P., Pallqui Camacho, N.C., Parada, A., Pardo-Molina, G., Peacock, J., Pena-Claros, M., Pickavance, G.C., Pitman, N.C., Poorter, L., Prieto, A., Quesada, C.A., Ramirez, F., Ramirez-Angulo, H., Restrepo, Z., Roopsind, A., Rudas, A., Salomao, R.P., Schwarz, M., Silva, N., Silva-Espejo, J.E., Silveira, M., Stropp, J., Talbot, J., ter Steege, H., Teran-Aguilar, J., Terborgh, J., Thomas-Caesar, R., Toledo, M., Torello-Raventos, M., Umetsu, R.K., van der Heijden, G.M., van der Hout, P., Guimaraes Vieira, I.C., Vieira, S.A., Vilanova, E., Vos, V.A. & Zagt, R.J. (2015). Long-term decline of the Amazon carbon sink. *Nature*, 519, 344-348.

Bugmann, H. & Bigler, C. (2011). Will the CO2 fertilization effect in forests be offset by reduced tree longevity? *Oecologia*, 165, 533-544.

Burns, R.M. & Honkala, B.H.J.A.H. (1990). Silvics of North America: 1. Conifers; 2. Hardwoods. USDA Forest Service. 654, 1970-2002.

Cailleret, M., Jansen, S., Robert, E.M., Desoto, L., Aakala, T., Antos, J.A., Beikircher, B., Bigler, C., Bugmann, H., Caccianiga, M., Cada, V., Camarero, J.J., Cherubini, P., Cochard, H., Coyea, M.R., Cufar, K., Das, A.J., Davi, H., Delzon, S., Dorman, M., Gea-Izquierdo, G., Gillner, S., Haavik, L.J., Hartmann, H., Heres, A.M., Hultine, K.R., Janda, P., Kane, J.M., Kharuk, V.I., Kitzberger, T., Klein, T., Kramer, K., Lens, F., Levanic, T., Linares Calderon, J.C., Lloret, F., Lobo-Do-Vale, R., Lombardi, F., Lopez Rodriguez, R., Makinen, H., Mayr, S., Meszaros, I., Metsaranta, J.M., Minunno, F., Oberhuber, W., Papadopoulos, A., Peltoniemi, M., Petritan, A.M., Rohner, B., Sanguesa-Barreda, G., Sarris, D., Smith, J.M., Stan, A.B., Sterck, F., Stojanovic, D.B., Suarez, M.L., Svoboda, M., Tognetti, R., Torres-Ruiz, J.M., Trotsiuk, V., Villalba, R., Vodde, F., Westwood, A.R., Wyckoff, P.H., Zafirov, N. & Martinez-Vilalta, J. (2017). A synthesis of radial growth patterns preceding tree mortality. *Glob Chang Biol*, 23, 1675-1690.

Canadian Council of Forest Ministers (2008). Canada's National Forest Inventory ground sampling guidelines: specifications for ongoing measurement. (ed. Force, NT).

Chen, H.Y.H., Fu, S., Monserud, R.A. & Gillies, I.C. (2008). Relative size and stand age determine *Pinus banksiana* mortality. *For. Ecol. Manage.*, 255, 3980-3984.

Chen, H.Y.H. & Luo, Y. (2015). Net aboveground biomass declines of four major forest types with forest ageing and climate change in western Canada's boreal forests. *Glob Chang Biol*, 21, 3675-3684.

Chen, H.Y.H., Luo, Y., Reich, P.B., Searle, E.B. & Biswas, S.R. (2016). Climate change-associated trends in net biomass change are age dependent in western boreal forests of Canada. *Ecol. Lett.*, 19, 1150-1158.

Chen, H.Y.H. & Popadiouk, R.V. (2002). Dynamics of North American boreal mixedwoods. *Environ. Rev.*, 10, 137-166.

Chen, L., Huang, J.G., Alam, S.A., Zhai, L., Dawson, A., Stadt, K.J. & Comeau, P.G. (2017). Drought causes reduced growth of trembling aspen in western Canada. *Glob Chang Biol*, 23, 2887-2902.

Chen, L., Huang, J.G., Dawson, A., Zhai, L., Stadt, K.J., Comeau, P.G. & Whitehouse, C. (2018). Contributions of insects and droughts to growth decline of trembling aspen mixed boreal forest of western Canada. *Glob Chang Biol*, 24, 655-667.

Ciais, P., Tan, J., Wang, X., Roedenbeck, C., Chevallier, F., Piao, S.-L., Moriarty, R., Broquet, G., Le Quéré, C. & Canadell, J. (2019). Five decades of northern land carbon uptake revealed by the interhemispheric CO 2 gradient. *Nature*, 1.

Clark, J.S., Bell, D.M., Hersh, M.H. & Nichols, L. (2011). Climate change vulnerability of forest biodiversity: climate and competition tracking of demographic rates. *Global Change Biol.*, 17, 1834-1849.

Connell, J.H. (1978). Diversity in tropical rain forests and coral reefs. *Science*, 199, 1302-1310.

Coomes, D.A. & Allen, R.B. (2007). Effects of size, competition and altitude on tree growth. *J. Ecol.*, 95, 1084-1097.

Coomes, D.A., Holdaway, R.J., Kobe, R.K., Lines, E.R. & Allen, R.B. (2012). A general integrative framework for modelling woody biomass production and carbon sequestration rates in forests. *J. Ecol.*, 100, 42-64.

Crowther, T.W., Glick, H.B., Covey, K.R., Bettigole, C., Maynard, D.S., Thomas, S.M., Smith, J.R., Hintler, G., Duguid, M.C., Amatulli, G., Tuanmu, M.N., Jetz, W., Salas, C., Stam, C., Piotto, D., Tavani, R., Green, S., Bruce, G., Williams, S.J., Wiser, S.K., Huber, M.O., Hengeveld, G.M., Nabuurs, G.J., Tikhonova, E., Borchardt, P., Li, C.F., Powrie, L.W., Fischer, M., Hemp, A., Homeier, J., Cho, P., Vibrans, A.C., Umunay, P.M., Piao, S.L., Rowe, C.W., Ashton, M.S., Crane, P.R. & Bradford, M.A. (2015). Mapping tree density at a global scale. *Nature*, 525, 201-205.

D'Orangeville, L., Houle, D., Duchesne, L., Phillips, R.P., Bergeron, Y. & Kneeshaw, D. (2018). Beneficial effects of climate warming on boreal tree growth may be transitory. *Nat Commun*, 9, 3213.

de Coninck, H., Revi, A., Babiker, M., Bertoldi, P., Buckeridge, M., Cartwright, A., Dong, W., Ford, J., Fuss, S. & Hourcade, J.-C. (2018). Strengthening and implementing the global response. In: *Global Warming of 1.5°C. An IPCC Special Report on the impacts of global warming of 1.5°C above pre-industrial levels and related global greenhouse gas emission pathways, in the context of strengthening the global response to the threat of climate change, sustainable development, and efforts to eradicate poverty* (ed. Masson-Delmotte, V, P. Zhai, H.-O. Pörtner, D. Roberts, J. Skea, P.R. Shukla, A. Pirani, W. Moufouma-Okia, C. Péan, R. Pidcock, S. Connors, J.B.R. Matthews, Y. Chen, X. Zhou, M.I. Gomis, E. Lonnoy, T. Maycock, M. Tignor,T. Waterfield) In Press.

De Dios, V.R., Fischer, C. & Colinas, C. (2007). Climate change effects on Mediterranean forests and preventive measures. *New forests*, 33, 29-40.

DeFries, R., Hansen, M., Townshend, J., Janetos, A. & Loveland, T. Kilometer Tree Cover Continuous Fields, 1.0. Department of Geography, University of Maryland. College Park, Maryland, 1992–1993.

Dentener, F.J. (2006). Global Maps of Atmospheric Nitrogen Deposition, 1860, 1993, and 2050. ORNL Distributed Active Archive Center.

Di Filippo, A., Pederson, N., Baliva, M., Brunetti, M., Dinella, A., Kitamura, K., Knapp, H.D., Schirone, B. & Piovesan, G. (2015). The longevity of broadleaf deciduous trees in Northern Hemisphere temperate forests: insights from tree-ring series. *Frontiers in Ecology and Evolution*, 3.

Diffenbaugh, N.S. & Field, C.B. (2013). Changes in ecologically critical terrestrial climate conditions. *Science*, 341, 486-492.
Dixon, R.K., Solomon, A.M., Brown, S., Houghton, R.A., Trexier, M.C. & Wisniewski, J. (1994). Carbon pools and flux of global forest ecosystems. *Science*, 263, 185-190.
Dormann, C.F., Elith, J., Bacher, S., Buchmann, C., Carl, G., Carre, G., Marquez, J.R.G., Gruber, B., Lafourcade, B., Leitao, P.J., Munkemuller, T., McClean, C., Osborne, P.E., Reineking, B., Schroder, B., Skidmore, A.K., Zurell, D. & Lautenbach, S. (2013). Collinearity: a review of methods to deal with it and a simulation study evaluating their performance. *Ecography*, 36, 27-46.
Doughty, C.E., Metcalfe, D.B., Girardin, C.A., Amezquita, F.F., Cabrera, D.G., Huasco, W.H., Silva-Espejo, J.E., Araujo-Murakami, A., da Costa, M.C., Rocha, W., Feldpausch, T.R., Mendoza, A.L., da Costa, A.C., Meir, P., Phillips, O.L. & Malhi, Y. (2015). Drought impact on forest carbon dynamics and fluxes in Amazonia. *Nature*, 519, 78-82.
Elliott, K.J., Miniat, C.F., Pederson, N. & Laseter, S.H. (2015). Forest tree growth response to hydroclimate variability in the southern Appalachians. *Glob Chang Biol*, 21, 4627-4641.
Fleming, R.A. & Volney, W.J.A. (1995). Effects of climate change on insect defoliator population processes in Canada's boreal forest: Some plausible scenarios. *Water, Air, Soil Pollut.*, 82, 445-454.
Forkel, M., Carvalhais, N., Rodenbeck, C., Keeling, R., Heimann, M., Thonicke, K., Zaehle, S. & Reichstein, M. (2016). Enhanced seasonal CO2 exchange caused by amplified plant productivity in northern ecosystems. *Science*, 351, 696-699.
Forrester, D.I. & Bauhus, J. (2016). A Review of Processes Behind Diversity-Productivity Relationships in Forests. *Current Forestry Reports*, 2, 45-61.
Girardin, M.P., Bouriaud, O., Hogg, E.H., Kurz, W., Zimmermann, N.E., Metsaranta, J.M., de Jong, R., Frank, D.C., Esper, J., Buntgen, U., Guo, X.J. & Bhatti, J. (2016). No growth stimulation of Canada's boreal forest under half-century of combined warming and CO2 fertilization. *Proc Natl Acad Sci U S A*, 113, E8406-E8414.
González de Andrés, E., Camarero, J.J., Blanco, J.A., Imbert, J.B., Lo, Y.-H., Sangüesa-Barreda, G., Castillo, F.J. & Turnbull, M. (2018). Tree-to-tree competition in mixed European beech-Scots pine forests has different impacts on growth and water-use efficiency depending on site conditions. *J. Ecol.*, 106, 59-75.
Grace, J.B., Anderson, T.M., Seabloom, E.W., Borer, E.T., Adler, P.B., Harpole, W.S., Hautier, Y., Hillebrand, H., Lind, E.M., Partel, M., Bakker, J.D., Buckley, Y.M., Crawley, M.J., Damschen, E.I., Davies, K.F., Fay, P.A., Firn, J., Gruner, D.S., Hector, A., Knops, J.M., MacDougall, A.S., Melbourne, B.A., Morgan, J.W., Orrock, J.L., Prober, S.M. & Smith, M.D. (2016). Integrative modelling reveals mechanisms linking productivity and plant species richness. *Nature*, 529, 390-393.
Grossman, J.J., Cavender-Bares, J., Reich, P.B., Montgomery, R.A., Hobbie, S.E. & Shefferson, R. (2018). Neighborhood diversity simultaneously increased and decreased susceptibility to contrasting herbivores in an early stage forest diversity experiment. *J. Ecol.*, 107, 1492-1505.
Gutsell, S.L. & Johnson, E.A. (2002). Accurately ageing trees and examining their height-growth rates: implications for interpreting forest dynamics. *J. Ecol.*, 90, 153-166.
Haas, S.E., Cushman, J.H., Dillon, W.W., Rank, N.E., Rizzo, D.M. & Meentemeyer, R.K. (2016). Effects of individual, community, and landscape drivers on the dynamics of a wildland forest epidemic. *Ecology*, 97, 649-660.

Hansen, M.C., Potapov, P.V., Moore, R., Hancher, M., Turubanova, S.A., Tyukavina, A., Thau, D., Stehman, S.V., Goetz, S.J., Loveland, T.R., Kommareddy, A., Egorov, A., Chini, L., Justice, C.O. & Townshend, J.R. (2013). High-resolution global maps of 21st-century forest cover change. *Science*, 342, 850-853.

Hegyi, F. (1974). A simulation model for managing jack-pine standssimulation. *RoyalColl. For, Res. Notes*, 30, 74-90.

Hember, R.A. & Kurz, W.A. (2018). Low Tree-Growth Elasticity of Forest Biomass Indicated by an Individual-Based Model. *Forests*, 9, 21.

Hember, R.A., Kurz, W.A. & Coops, N.C. (2017). Relationships between individual-tree mortality and water-balance variables indicate positive trends in water stress-induced tree mortality across North America. *Glob Chang Biol*, 23, 1691-1710.

Hember, R.A., Kurz, W.A., Metsaranta, J.M., Black, T.A., Guy, R.D. & Coops, N.C. (2012). Accelerating regrowth of temperate-maritime forests due to environmental change. *Global Change Biol.*, 18, 2026-2040.

Herms, D.A. & Mattson, W.J. (1992). The Dilemma of Plants: To Grow or Defend. *The Quarterly Review of Biology*, 67, 283-335.

Hisano, M., Chen, H.Y.H., Searle, E.B. & Reich, P.B. (2019). Species-rich boreal forests grew more and suffered less mortality than species-poor forests under the environmental change of the past half-century. *Ecol. Lett.*, 22, 999-1008.

Hisano, M., Searle, E.B. & Chen, H.Y.H. (2018). Biodiversity as a solution to mitigate climate change impacts on the functioning of forest ecosystems. *Biol. Rev. Camb. Philos. Soc.*, 93, 439-456.

Hoegh-Guldberg, O., Jacob, D., Taylor, M., Bindi, M., Brown, S., Camilloni, I., Diedhiou, A., Djalante, R., Ebi, K. & Engelbrecht, F. (2018). Impacts of 1.5 ºC global warming on natural and human systems. In: *Global Warming of 1.5°C. An IPCC Special Report on the impacts of global warming of 1.5°C above pre-industrial levels and related global greenhouse gas emission pathways, in the context of strengthening the global response to the threat of climate change, sustainable development, and efforts to eradicate poverty* (ed. Masson-Delmotte V., PZ, H.-O. Pörtner, D. Roberts, J. Skea, P.R. Shukla, A. Pirani, W. Moufouma-Okia, C. Péan, R. Pidcock, S. Connors, J.B.R. Matthews, Y. Chen, X. Zhou, M.I. Gomis, E. Lonnoy, T. Maycock, M. Tignor, T. Waterfield) In Press.

Hogg, E.H., Michaelian, M., Hook, T.I. & Undershultz, M.E. (2017). Recent climatic drying leads to age-independent growth reductions of white spruce stands in western Canada. *Glob Chang Biol*, 23, 5297-5308.

Hosmer, D.W. & Lemeshow, S. (2000). *Applied Logistic Regression*. 2nd edn. John Wiley & Sons, Inc., New York, New York, USA.

Huang, M., Piao, S., Ciais, P., Penuelas, J., Wang, X., Keenan, T.F., Peng, S., Berry, J.A., Wang, K., Mao, J., Alkama, R., Cescatti, A., Cuntz, M., De Deurwaerder, H., Gao, M., He, Y., Liu, Y., Luo, Y., Myneni, R.B., Niu, S., Shi, X., Yuan, W., Verbeeck, H., Wang, T., Wu, J. & Janssens, I.A. (2019). Air temperature optima of vegetation productivity across global biomes. *Nat Ecol Evol*, 3, 772-779.

Huang, M., Piao, S., Janssens, I.A., Zhu, Z., Wang, T., Wu, D., Ciais, P., Myneni, R.B., Peaucelle, M., Peng, S., Yang, H. & Penuelas, J. (2017). Velocity of change in vegetation productivity over northern high latitudes. *Nat Ecol Evol*, 1, 1649-1654.

Huang, S., Meng, S.X. & Yang, Y. (2009). A growth and yield projection system (GYPSY) for natural and post-harvest stands in Alberta. Edmonton, Alberta, Canada.

Hulsmann, L., Bugmann, H., Cailleret, M. & Brang, P. (2018). How to kill a tree: empirical mortality models for 18 species and their performance in a dynamic forest model. *Ecol. Appl.*, 28, 522-540.
Ibanez, I., Zak, D.R., Burton, A.J. & Pregitzer, K.S. (2018). Anthropogenic nitrogen deposition ameliorates the decline in tree growth caused by a drier climate. *Ecology*, 99, 411-420.
IPCC (2013). Climate Change 2013: The Physical Science Basis. Contribution of Working Group I to the Fifth Assessment Report of the Intergovernmental Panel on Climate Change. Cambridge University Press, Cambridge, UK and New York, NY, USA.
Janzen, D. (1970). Herbivores and the number of tree species in tropical forests. *Am. Nat.*, 104, 501-528.
Jucker, T., Bouriaud, O., Avacaritei, D., Danila, I., Duduman, G., Valladares, F. & Coomes, D.A. (2014). Competition for light and water play contrasting roles in driving diversity-productivity relationships in Iberian forests. *J. Ecol.*, 102, 1202-1213.
Jump, A.S., Hunt, J.M. & Penuelas, J. (2006). Rapid climate change-related growth decline at the southern range edge of Fagus sylvatica. *Global Change Biol.*, 12, 2163-2174.
Keenan, T.F., Gray, J., Friedl, M.A., Toomey, M., Bohrer, G., Hollinger, D.Y., Munger, J.W., O'Keefe, J., Schmid, H.P., SueWing, I., Yang, B. & Richardson, A.D. (2014). Net carbon uptake has increased through warming-induced changes in temperate forest phenology. *Nature Climate Change*, 4, 598-604.
Keenan, T.F., Hollinger, D.Y., Bohrer, G., Dragoni, D., Munger, J.W., Schmid, H.P. & Richardson, A.D. (2013). Increase in forest water-use efficiency as atmospheric carbon dioxide concentrations rise. *Nature*, 499, 324-327.
Korner, C. (2015). Paradigm shift in plant growth control. *Curr. Opin. Plant Biol.*, 25, 107-114.
Kunstler, G., Falster, D., Coomes, D.A., Hui, F., Kooyman, R.M., Laughlin, D.C., Poorter, L., Vanderwel, M., Vieilledent, G., Wright, S.J., Aiba, M., Baraloto, C., Caspersen, J., Cornelissen, J.H., Gourlet-Fleury, S., Hanewinkel, M., Herault, B., Kattge, J., Kurokawa, H., Onoda, Y., Penuelas, J., Poorter, H., Uriarte, M., Richardson, S., Ruiz-Benito, P., Sun, I.F., Stahl, G., Swenson, N.G., Thompson, J., Westerlund, B., Wirth, C., Zavala, M.A., Zeng, H., Zimmerman, J.K., Zimmermann, N.E. & Westoby, M. (2016). Plant functional traits have globally consistent effects on competition. *Nature*, 529, 204-207.
Lambert, M.C., Ung, C.H. & Raulier, F. (2005). Canadian national tree aboveground biomass equations. *Canadian Journal of Forest Research*, 35, 1996-2018.
Legendre, P. & Legendre, L. (2012). *Numerical Ecology*. 2 edn. Elsevier, New York.
Liang, J., Crowther, T.W., Picard, N., Wiser, S., Zhou, M., Alberti, G., Schulze, E.D., McGuire, A.D., Bozzato, F., Pretzsch, H., de-Miguel, S., Paquette, A., Herault, B., Scherer-Lorenzen, M., Barrett, C.B., Glick, H.B., Hengeveld, G.M., Nabuurs, G.J., Pfautsch, S., Viana, H., Vibrans, A.C., Ammer, C., Schall, P., Verbyla, D., Tchebakova, N., Fischer, M., Watson, J.V., Chen, H.Y., Lei, X., Schelhaas, M.J., Lu, H., Gianelle, D., Parfenova, E.I., Salas, C., Lee, E., Lee, B., Kim, H.S., Bruelheide, H., Coomes, D.A., Piotto, D., Sunderland, T., Schmid, B., Gourlet-Fleury, S., Sonke, B., Tavani, R., Zhu, J., Brandl, S., Vayreda, J., Kitahara, F., Searle, E.B., Neldner, V.J., Ngugi, M.R., Baraloto, C., Frizzera, L., Balazy, R., Oleksyn, J., Zawila-Niedzwiecki, T., Bouriaud, O., Bussotti, F., Finer, L., Jaroszewicz, B., Jucker, T., Valladares, F., Jagodzinski, A.M., Peri, P.L., Gonmadje, C., Marthy, W., O'Brien, T., Martin, E.H., Marshall, A.R., Rovero, F., Bitariho, R., Niklaus, P.A., Alvarez-Loayza, P., Chamuya, N., Valencia, R., Mortier, F., Wortel, V., Engone-Obiang, N.L., Ferreira, L.V., Odeke, D.E., Vasquez, R.M., Lewis, S.L. & Reich, P.B.

(2016). Positive biodiversity-productivity relationship predominant in global forests. *Science*, 354.
Liu, Q., Piao, S., Janssens, I.A., Fu, Y., Peng, S., Lian, X., Ciais, P., Myneni, R.B., Penuelas, J. & Wang, T. (2018). Extension of the growing season increases vegetation exposure to frost. *Nat Commun*, 9, 426.
Luo, Y. & Chen, H.Y. (2013). Observations from old forests underestimate climate change effects on tree mortality. *Nat Commun*, 4, 1655.
Luo, Y. & Chen, H.Y.H. (2011). Competition, species interaction and ageing control tree mortality in boreal forests. *J. Ecol.*, 99, 1470-1480.
Luo, Y. & Chen, H.Y.H. (2015). Climate change-associated tree mortality increases without decreasing water availability. *Ecol. Lett.*, 18, 1207-1215.
Luo, Y., Chen, H.Y.H., McIntire, E.J.B. & Andison, D.W. (2019). Divergent temporal trends of net biomass change in western Canadian boreal forests. *J. Ecol.*, 107, 69-78.
Ma, Z., Peng, C., Zhu, Q., Chen, H., Yu, G., Li, W., Zhou, X., Wang, W. & Zhang, W. (2012). Regional drought-induced reduction in the biomass carbon sink of Canada's boreal forests. *Proc Natl Acad Sci U S A*, 109, 2423-2427.
McDowell, N.G., Beerling, D.J., Breshears, D.D., Fisher, R.A., Raffa, K.F. & Stitt, M. (2011). The interdependence of mechanisms underlying climate-driven vegetation mortality. *Trends Ecol Evol*, 26, 523-532.
McDowell, N.G., Williams, A.P., Xu, C., Pockman, W.T., Dickman, L.T., Sevanto, S., Pangle, R., Limousin, J., Plaut, J., Mackay, D.S., Ogee, J., Domec, J.C., Allen, C.D., Fisher, R.A., Jiang, X., Muss, J.D., Breshears, D.D., Rauscher, S.A. & Koven, C. (2015). Multi-scale predictions of massive conifer mortality due to chronic temperature rise. *Nature Climate Change*, 6, 295-300.
Mencuccini, M., Martinez-Vilalta, J., Vanderklein, D., Hamid, H.A., Korakaki, E., Lee, S. & Michiels, B. (2005). Size-mediated ageing reduces vigour in trees. *Ecol. Lett.*, 8, 1183-1190.
Mencuccini, M. & Munné-Bosch, S. (2017). 13 Physiological and Biochemical Processes Related to Ageing and Senescence in Plants. *The Evolution of Senescence in the Tree of Life*, 257.
Michaelian, M., Hogg, E.H., Hall, R.J. & Arsenault, E. (2011). Massive mortality of aspen following severe drought along the southern edge of the Canadian boreal forest. *Global Change Biol.*, 17, 2084-2094.
Michaletz, S.T., Cheng, D., Kerkhoff, A.J. & Enquist, B.J. (2014). Convergence of terrestrial plant production across global climate gradients. *Nature*, 512, 39-43.
Millar, C.I. & Stephenson, N.L. (2015). Temperate forest health in an era of emerging megadisturbance. *Science*, 349, 823-826.
Nakagawa, S. & Schielzeth, H. (2013). A general and simple method for obtaining R2 from generalized linear mixed-effects models. *Methods in Ecology and Evolution*, 4, 133-142.
Neter, J., Kutner, M.H., Nachtsheim, C.J. & Wasserman, W. (1996). *Applied linear statistical models*. Irwin Chicago.
Nicklen, E.F., Roland, C.A., Csank, A.Z., Wilmking, M., Ruess, R.W. & Muldoon, L.A. (2019). Stand basal area and solar radiation amplify white spruce climate sensitivity in interior Alaska: Evidence from carbon isotopes and tree rings. *Glob Chang Biol*, 25, 911-926.
Niinemets, U. & Valladares, F. (2006). Tolerance to shade, drought, and waterlogging of temperate Northern Hemisphere trees and shrubs. *Ecol. Monogr.*, 76, 521-547.

Oliver, C.D. & Larson, B.C. (1990). *Forest stand dynamics / by Chadwick Dearing Oliver and Bruce C. Larson*. New York : McGraw-Hill Pub. Co., 1990.
Oliver, C.D. & Larson, B.C. (1996). *Forest stand dynamics: updated edition*. John Wiley and sons.
Olson, D.M., Dinerstein, E., Wikramanayake, E.D., Burgess, N.D., Powell, G.V., Underwood, E.C., D'amico, J.A., Itoua, I., Strand, H.E. & Morrison, J.C. (2001). Terrestrial Ecoregions of the World: A New Map of Life on Earth: A new global map of terrestrial ecoregions provides an innovative tool for conserving biodiversity. *Bioscience*, 51, 933-938.
Pacala, S.W., Canham, C.D., Saponara, J., Silander, J.A., Kobe, R.K. & Ribbens, E. (1996). Forest models defined by field measurements: Estimation, error analysis and dynamics. *Ecol. Monogr.*, 66, 1-43.
Pan, Y., Birdsey, R.A., Fang, J., Houghton, R., Kauppi, P.E., Kurz, W.A., Phillips, O.L., Shvidenko, A., Lewis, S.L., Canadell, J.G., Ciais, P., Jackson, R.B., Pacala, S.W., McGuire, A.D., Piao, S., Rautiainen, A., Sitch, S. & Hayes, D. (2011a). A large and persistent carbon sink in the world's forests. *Science*, 333, 988-993.
Pan, Y., Chen, J.M., Birdsey, R., McCullough, K., He, L. & Deng, F. (2011b). Age structure and disturbance legacy of North American forests. *Biogeosciences*, 8, 715-732.
Paquette, A., Joly, S., Messier, C.J.E. & Evolution (2015). Explaining forest productivity using tree functional traits and phylogenetic information: two sides of the same coin over evolutionary scale? , 5, 1774-1783.
Parker, I.M., Saunders, M., Bontrager, M., Weitz, A.P., Hendricks, R., Magarey, R., Suiter, K. & Gilbert, G.S. (2015). Phylogenetic structure and host abundance drive disease pressure in communities. *Nature*, 520, 542-544.
Peng, C.H., Ma, Z.H., Lei, X.D., Zhu, Q., Chen, H., Wang, W.F., Liu, S.R., Li, W.Z., Fang, X.Q. & Zhou, X.L. (2011). A drought-induced pervasive increase in tree mortality across Canada's boreal forests. *Nature Climate Change*, 1, 467-471.
Poage, N.J. & Tappeiner, J.C. (2002). Long-term patterns of diameter and basal area growth of old-growth Douglas-fir trees in western Oregon. *Canadian Journal of Forest Research-Revue Canadienne De Recherche Forestiere*, 32, 1232-1243.
Poorter, L., Bongers, F., Aide, T.M., Almeyda Zambrano, A.M., Balvanera, P., Becknell, J.M., Boukili, V., Brancalion, P.H., Broadbent, E.N., Chazdon, R.L., Craven, D., de Almeida-Cortez, J.S., Cabral, G.A., de Jong, B.H., Denslow, J.S., Dent, D.H., DeWalt, S.J., Dupuy, J.M., Duran, S.M., Espirito-Santo, M.M., Fandino, M.C., Cesar, R.G., Hall, J.S., Hernandez-Stefanoni, J.L., Jakovac, C.C., Junqueira, A.B., Kennard, D., Letcher, S.G., Licona, J.C., Lohbeck, M., Marin-Spiotta, E., Martinez-Ramos, M., Massoca, P., Meave, J.A., Mesquita, R., Mora, F., Munoz, R., Muscarella, R., Nunes, Y.R., Ochoa-Gaona, S., de Oliveira, A.A., Orihuela-Belmonte, E., Pena-Claros, M., Perez-Garcia, E.A., Piotto, D., Powers, J.S., Rodriguez-Velazquez, J., Romero-Perez, I.E., Ruiz, J., Saldarriaga, J.G., Sanchez-Azofeifa, A., Schwartz, N.B., Steininger, M.K., Swenson, N.G., Toledo, M., Uriarte, M., van Breugel, M., van der Wal, H., Veloso, M.D., Vester, H.F., Vicentini, A., Vieira, I.C., Bentos, T.V., Williamson, G.B. & Rozendaal, D.M. (2016). Biomass resilience of Neotropical secondary forests. *Nature*, 530, 211-214.
Pretzsch, H. (2014). Canopy space filling and tree crown morphology in mixed-species stands compared with monocultures. *For. Ecol. Manage.*, 327, 251-264.

Pretzsch, H., Biber, P., Schutze, G., Uhl, E. & Rotzer, T. (2014). Forest stand growth dynamics in Central Europe have accelerated since 1870. *Nat Commun*, 5, 4967.

Prior, L.D. & Bowman, D.M. (2014). Big eucalypts grow more slowly in a warm climate: evidence of an interaction between tree size and temperature. *Glob Chang Biol*, 20, 2793-2799.

Pugh, T.A.M., Lindeskog, M., Smith, B., Poulter, B., Arneth, A., Haverd, V. & Calle, L. (2019). Role of forest regrowth in global carbon sink dynamics. *Proc Natl Acad Sci U S A*, 116, 4382-4387.

Pureswaran, D.S., De Grandpre, L., Pare, D., Taylor, A., Barrette, M., Morin, H., Regniere, J. & Kneeshaw, D.D. (2015). Climate-induced changes in host tree-insect phenology may drive ecological state-shift in boreal forests. *Ecology*, 96, 1480-1491.

Réginère, J., Saint-Amant, R. & Béchard, A. (2014). BioSIM 10 user's manual. In: *Information Report LAU-X-137E* Natural Resources Canada Sainte-Foy, QC.

Reich, P.B., Sendall, K.M., Rice, K., Rich, R.L., Stefanski, A., Hobbie, S.E. & Montgomery, R.A. (2015). Geographic range predicts photosynthetic and growth response to warming in co-occurring tree species. *Nature Climate Change*, 5, 148-152.

Robin, X., Turck, N., Hainard, A., Tiberti, N., Lisacek, F., Sanchez, J.C. & Muller, M. (2011). pROC: an open-source package for R and S+ to analyze and compare ROC curves. *BMC Bioinformatics*, 12, 77.

Rowland, L., da Costa, A.C., Galbraith, D.R., Oliveira, R.S., Binks, O.J., Oliveira, A.A., Pullen, A.M., Doughty, C.E., Metcalfe, D.B., Vasconcelos, S.S., Ferreira, L.V., Malhi, Y., Grace, J., Mencuccini, M. & Meir, P. (2015). Death from drought in tropical forests is triggered by hydraulics not carbon starvation. *Nature*, 528, 119-122.

Ryan, M.G., Phillips, N. & Bond, B.J. (2006). The hydraulic limitation hypothesis revisited. *Plant Cell Environ*, 29, 367-381.

Sapijanskas, J., Paquette, A., Potvin, C., Kunert, N. & Loreau, M. (2014). Tropical tree diversity enhances light capture through crown plasticity and spatial and temporal niche differences. *Ecology*, 95, 2479-2492.

Schmid-Siegert, E., Sarkar, N., Iseli, C., Calderon, S., Gouhier-Darimont, C., Chrast, J., Cattaneo, P., Schutz, F., Farinelli, L., Pagni, M., Schneider, M., Voumard, J., Jaboyedoff, M., Fankhauser, C., Hardtke, C.S., Keller, L., Pannell, J.R., Reymond, A., Robinson-Rechavi, M., Xenarios, I. & Reymond, P. (2017). Low number of fixed somatic mutations in a long-lived oak tree. *Nat Plants*, 3, 926-929.

Schulte-Uebbing, L. & de Vries, W. (2018). Global-scale impacts of nitrogen deposition on tree carbon sequestration in tropical, temperate, and boreal forests: A meta-analysis. *Glob Chang Biol*, 24, e416-e431.

Searle, E.B. & Chen, H.Y.H. (2017a). Climate change-associated trends in biomass dynamics are consistent across soil drainage classes in western boreal forests of Canada. *Forest Ecosystems*, 4, 18.

Searle, E.B. & Chen, H.Y.H. (2017b). Tree size thresholds produce biased estimates of forest biomass dynamics. *For. Ecol. Manage.*, 400, 468-474.

Sheffield, J., Wood, E.F. & Roderick, M.L. (2012). Little change in global drought over the past 60 years. *Nature*, 491, 435-438.

Stephenson, N.L., Das, A.J., Condit, R., Russo, S.E., Baker, P.J., Beckman, N.G., Coomes, D.A., Lines, E.R., Morris, W.K., Ruger, N., Alvarez, E., Blundo, C., Bunyavejchewin, S., Chuyong, G., Davies, S.J., Duque, A., Ewango, C.N., Flores, O., Franklin, J.F., Grau,

H.R., Hao, Z., Harmon, M.E., Hubbell, S.P., Kenfack, D., Lin, Y., Makana, J.R., Malizia, A., Malizia, L.R., Pabst, R.J., Pongpattananurak, N., Su, S.H., Sun, I.F., Tan, S., Thomas, D., van Mantgem, P.J., Wang, X., Wiser, S.K. & Zavala, M.A. (2014). Rate of tree carbon accumulation increases continuously with tree size. *Nature*, 507, 90-93.

Swenson, N.G. (2014). *Functional and phylogenetic ecology in R*. Springer.

Talbot, J., Lewis, S.L., Lopez-Gonzalez, G., Brienen, R.J.W., Monteagudo, A., Baker, T.R., Feldpausch, T.R., Malhi, Y., Vanderwel, M., Murakami, A.A., Arroyo, L.P., Chao, K.J., Erwin, T., van der Heijden, G., Keeling, H., Killeen, T., Neill, D., Vargas, P.N., Gutierrez, G.A.P., Pitman, N., Quesada, C.A., Silveira, M., Stropp, J. & Phillips, O.L. (2014). Methods to estimate aboveground wood productivity from long-term forest inventory plots. *For. Ecol. Manage.*, 320, 30-38.

Taylor, A.R., Seedre, M., Brassard, B.W. & Chen, H.Y.H. (2014). Decline in Net Ecosystem Productivity Following Canopy Transition to Late-Succession Forests. *Ecosystems*, 17, 778-791.

Thomas, H. (2013). Senescence, ageing and death of the whole plant. *New Phytol.*, 197, 696-711.

Toigo, M., Perot, T., Courbaud, B., Castagneyrol, B., Gegout, J.C., Longuetaud, F., Jactel, H. & Vallet, P. (2018). Difference in shade tolerance drives the mixture effect on oak productivity. *J. Ecol.*, 106, 1073-1082.

Trugman, A.T., Detto, M., Bartlett, M.K., Medvigy, D., Anderegg, W.R.L., Schwalm, C., Schaffer, B. & Pacala, S.W. (2018). Tree carbon allocation explains forest drought-kill and recovery patterns. *Ecol. Lett.*, 21, 1552-1560.

Trumbore, S., Brando, P. & Hartmann, H. (2015). Forest health and global change. *Science*, 349, 814-818.

USDA Forest Service (2010). Forest Inventory and Analysis National Program. Available at: http:// fia.fs.fed.us/.

van Mantgem, P.J., Stephenson, N.L., Byrne, J.C., Daniels, L.D., Franklin, J.F., Fule, P.Z., Harmon, M.E., Larson, A.J., Smith, J.M., Taylor, A.H. & Veblen, T.T. (2009). Widespread increase of tree mortality rates in the western United States. *Science*, 323, 521-524.

Vicente-Serrano, S.M., Begueria, S. & Lopez-Moreno, J.I. (2010). A Multiscalar Drought Index Sensitive to Global Warming: The Standardized Precipitation Evapotranspiration Index. *J. Clim.*, 23, 1696-1718.

Weir, J.M.H., Johnson, E.A. & Miyanishi, K. (2000). Fire frequency and the spatial age mosaic of the mixed-wood boreal forest in western Canada. *Ecol. Appl.*, 10, 1162-1177.

Westerling, A.L., Hidalgo, H.G., Cayan, D.R. & Swetnam, T.W. (2006). Warming and earlier spring increase western U.S. forest wildfire activity. *Science*, 313, 940-943.

Williams, L.J., Paquette, A., Cavender-Bares, J., Messier, C. & Reich, P.B. (2017). Spatial complementarity in tree crowns explains overyielding in species mixtures. *Nat Ecol Evol*, 1, 63.

Willmott, C.J., Matsuura, K. & Legates, D. (2001). Terrestrial air temperature and precipitation: monthly and annual time series (1950–1999). *Center for climate research version*, 1.

Zhang, J., Huang, S. & He, F. (2015). Half-century evidence from western Canada shows forest dynamics are primarily driven by competition followed by climate. *Proc Natl Acad Sci U S A*, 112, 4009-4014.

Zhang, T., Niinemets, U., Sheffield, J. & Lichstein, J.W. (2018). Shifts in tree functional composition amplify the response of forest biomass to climate. *Nature*, 556, 99-102.

Zhang, Y., Chen, H.Y.H. & Reich, P.B. (2012). Forest productivity increases with evenness, species richness and trait variation: a global meta-analysis. *J. Ecol.*, 100, 742-749.
Zhu, K., Zhang, J., Niu, S., Chu, C. & Luo, Y. (2018). Limits to growth of forest biomass carbon sink under climate change. *Nat Commun*, 9, 2709.
Zuur, A., Ieno, E.N., Walker, N., Saveliev, A.A. & Smith, G.M. (2009). *Mixed effects models and extensions in ecology with R*. Springer Science & Business Media.
Zuur, A.F., Ieno, E.N. & Elphick, C.S. (2010). A protocol for data exploration to avoid common statistical problems. *Methods in Ecology and Evolution*, 1, 3-14.

APPENDIX I: SUPPLEMENTAL INFORMATION FOR CHAPTER 2

Table A1-1: Coefficient values from fitted linear mixed effects model for each demographic rate. Values in the Table are mean values with the lower and upper 95% quantiles from bootstrapped distributions, created using 10,000 iterations using the bootMer function in the lme4 package, shown in brackets. Coefficients were considered significant when their 95% confidence intervals did not overlap zero. Significant values are shown in bold.

	Intercept	***A***	***A*^{2} (10^4)**	***A*^{3} (10^5)**	**log*A***	***Y***
Productivity						
No threshold	2.896 (2.747 - 3.050)	-0.063 (-0.086 - -0.040)	2.395 (0.807 - 3.950)			0.024 (0.008 - 0.040)
5 cm threshold	2.833 (2.682 - 2.989)	-0.058 (-0.081 - -0.034)	2.141 (0.538 - 3.709)			0.024 (0.008 - 0.041)
10 cm threshold	2.696 (2.474 - 2.922)	0.106 (0.024 - 0.186)	-18.843 (-30.118 - -7.510)	0.794 (0.327 - 1.263)		0.026 (0.005 - 0.047)
Growth						
No threshold	2.754 (2.606 - 2.907)	-0.051 (-0.074 - -0.028)	1.781 (0.216 - 3.298)			0.024 (0.009 - 0.040)
5 cm threshold	2.578 (2.409 - 2.751)	0.043 (-0.018 - 0.104)	-10.399 (-18.940 - -1.825)	0.467 (0.113 - 0.823)		0.023 (0.007 - 0.039)
10 cm threshold	1.732 (1.535 - 1.929)	0.202 (0.144 - 0.259)	-26.690 (-34.673 - -18.723)	0.987 (0.652 - 1.323)		0.020 (0.005 - 0.036)
Ingrowth						
No threshold	0.142 (0.073 - 0.214)				-0.240 (-0.427 - -0.059)	-0.000 (-0.007 - 0.007)
5 cm threshold	0.259 (0.197 - 0.322)	-0.065 (-0.090 - -0.041)	7.409 (4.002 - 10.780)	-0.258 (-0.400 - -0.119)		0.002 (-0.005 - 0.008)
10 cm threshold	0.960 (0.849 - 1.072)	-0.105 (-0.154 - -0.057)	9.256 (2.459 - 16.107)	-0.250 (-0.528 - 0.029)		0.007 (-0.008 - 0.021)
Mortality						
No threshold	1.486 (1.278 - 1.696) 1.189				0.290 (-0.281 - 0.844) 0.818	0.078 (0.052 - 0.104) 0.073

5 cm threshold	(0.986 - 1.395)		(0.260 - 1.359)	(0.048 - 0.099)
10 cm threshold	0.729 (0.558 - 0.902)		0.765 (0.295 - 1.221)	0.059 (0.037 - 0.080)

Table A1-2: AIC values for different age functions for each demographic rate.

Function of age	Demographic rate			
	Productivity	Growth	Ingrowth	Mortality
No DBH threshold				
Linear	1214.3	1178.1	483.3	1624.2
Quadratic	**1207.1**	**1174.8**	482.3	1625.3
Cubic	1208.5	1175.0	482.9	1626.7
Logarithmic	1211.1	1179.0	**480.6**	**1623.7**
5 cm threshold				
Linear	1214.8	1196.6	444.8	1607.5
Quadratic	**1209.6**	1198.0	431.0	1605.0
Cubic	1210.9	**1193.4**	**420.1**	1604.8
Logarithmic	1212.2	1203.6	427.3	**1604.1**
10 cm threshold				
Linear	1442.9	1166.7	1113.1	1455.3
Quadratic	1444.9	1152.9	1088.6	1452.9
Cubic	**1436.3**	**1122.6**	**1087.6**	1454.8
Logarithmic	1449.7	1160.7	1096.4	**1452.7**

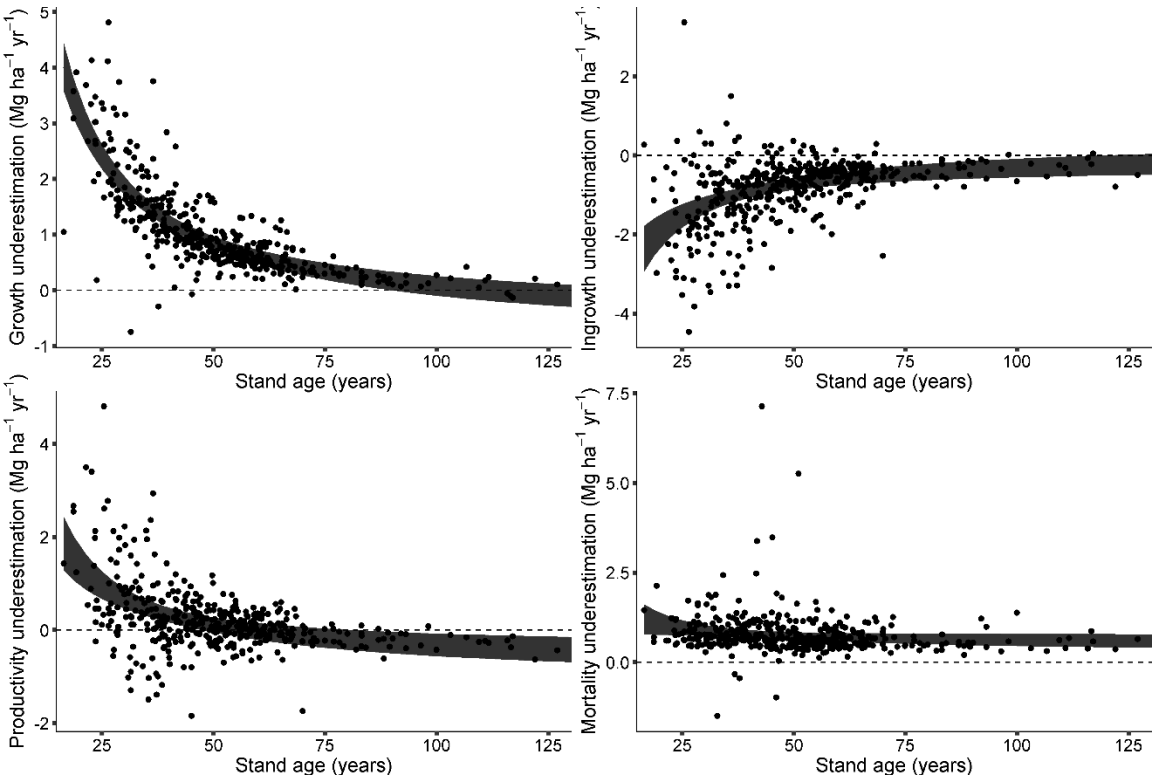

Figure A1-1: Models of underestimates of 10 cm threshold sampling versus 1.3m height threshold sampling of the four biomass dynamics along age gradients. Models are AGB_{No} – AGB_{10cm} related to the inverse of stand age and a plot random effect. Background points have plot-effects removed so may contain biologically unreasonable points (i.e., some mortality underestimation<0). Lines are upper and lower 95% confidence bands estimated from bootstrapping models 10,000 times.

Figure A1-2: Spatial locations of the 141 plots across the study region.

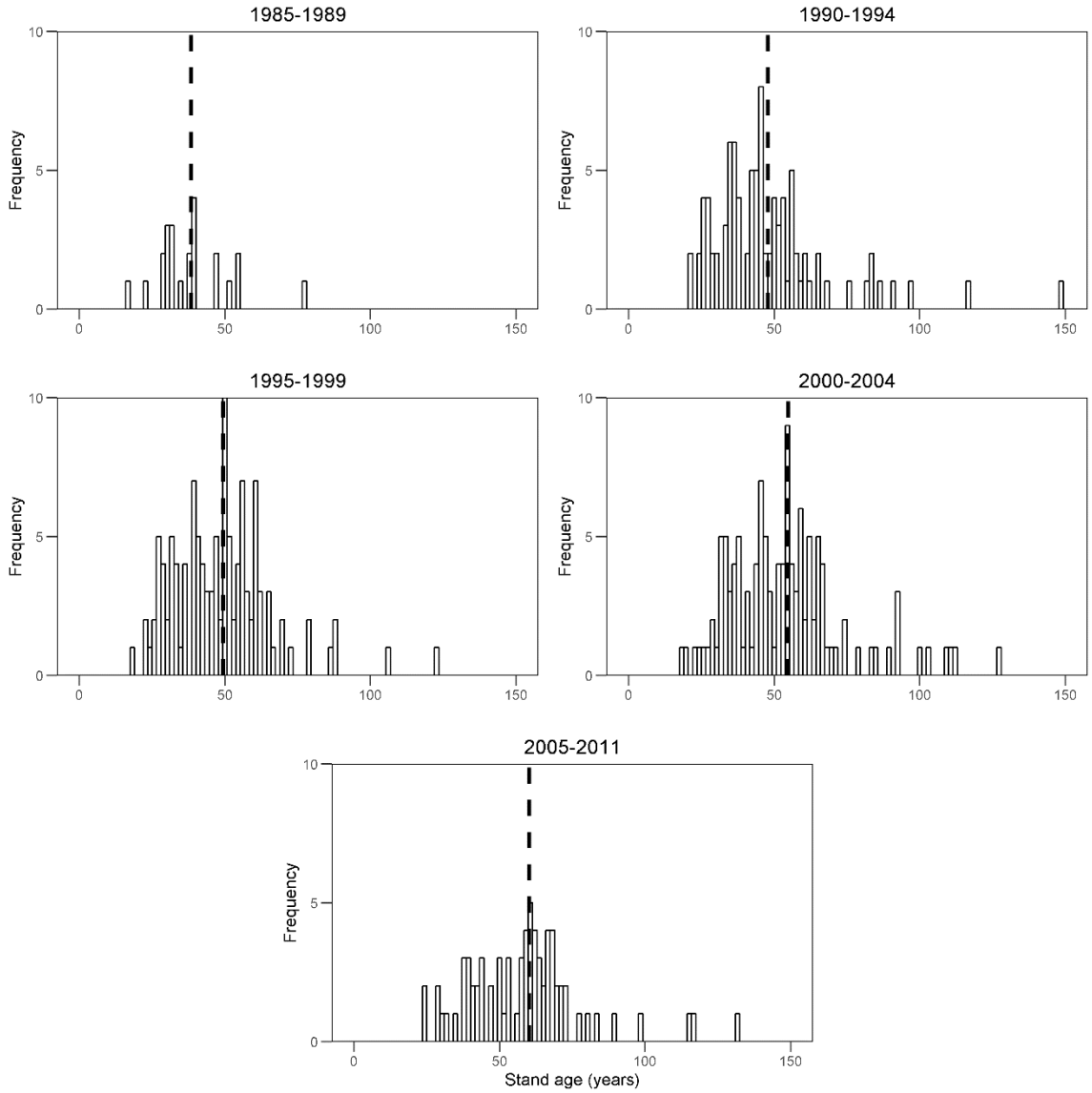

Figure A1-3: Histograms of stand age, binned by five year intervals over the study period. Dashed bold line is the mean stand age for each sampling period.

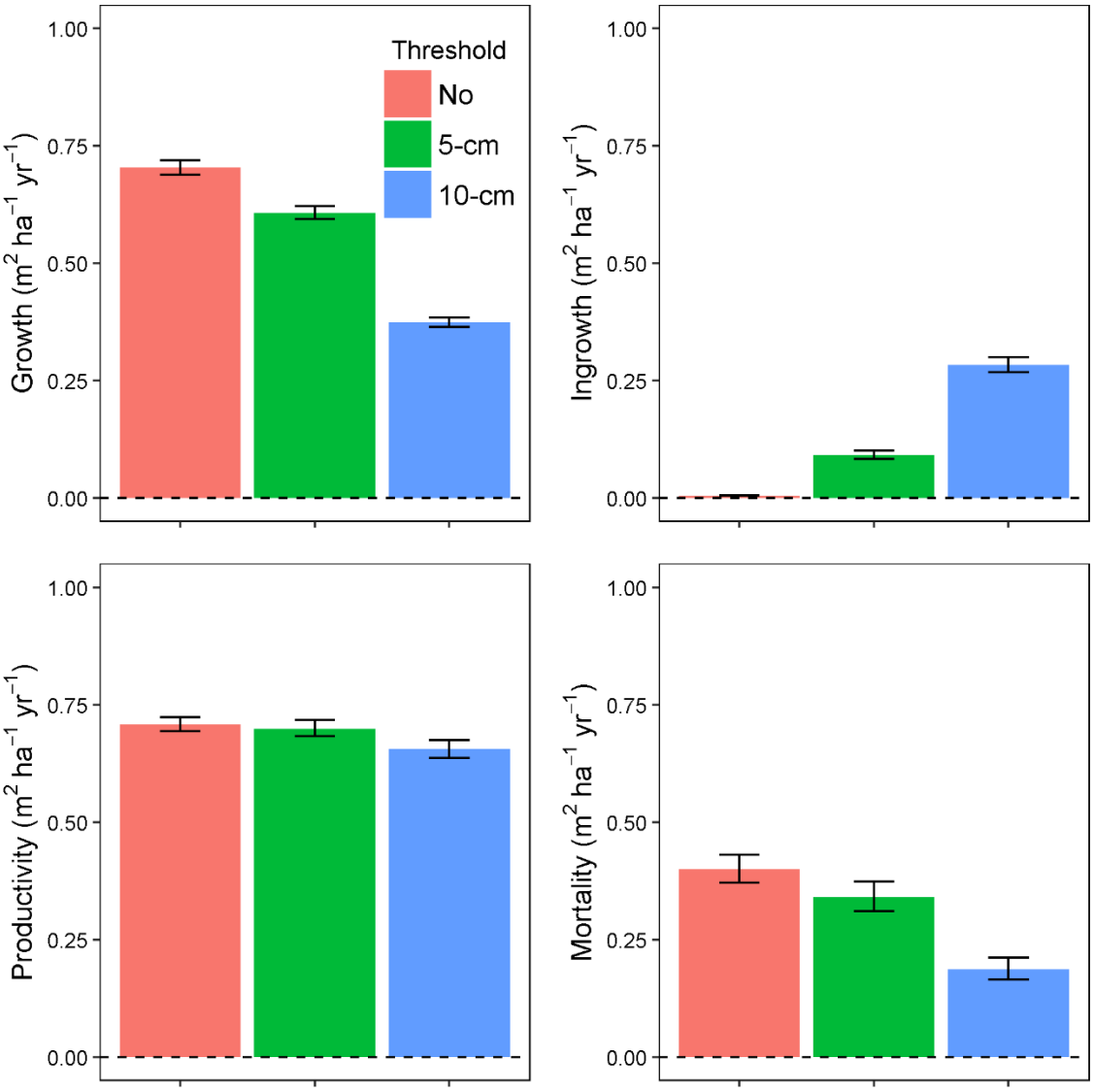

Figure A1-4: Bootstrapped mean and associated 95% confidence interval of each basal area component following the removal of the mean effects of age and calendar year.

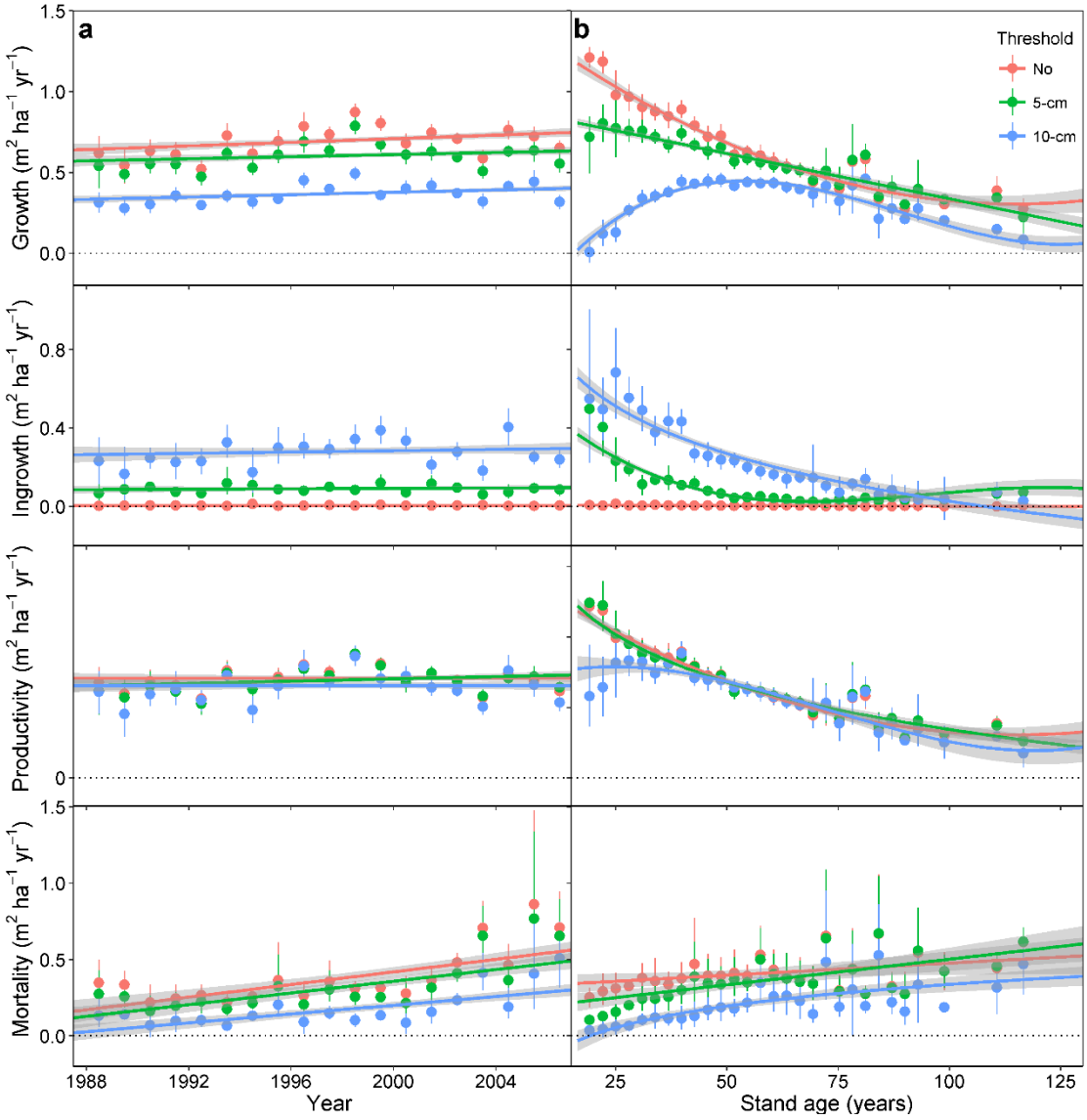

Figure A1-5: Partial regression plots of variables included in plot level analysis of basal area dynamics by threshold: (a) Calendar year effect; (b) Stand age effect. Shaded lines are 95% confidence intervals.

APPENDIX II: SUPPLEMENTAL INFORMATION FOR CHAPTER 3

Table A2-1. Numbers of stems, observations, plots, years measured, and ages measured of all individuals and by major species.

Species	Number of stems	Number of observations	Number of plots	Year of the first census	Year of the last census	Age of the first Census (years)	Age of the last Census (years)
All individuals	54680	129533	539	1960	2009	103	216
P. tremuloides	7193	16899	302	1961	2009	103	196
P. balsamifera	1623	4013	192	1961	2009	103	206
P. contorta	13470	32000	291	1960	2009	103	213
P. mariana	4029	9494	179	1962	2009	103	213
P. glauca	22920	53358	481	1964	2009	103	216
A. balsamea	4493	11803	171	1962	2009	105	216
All other	952	1966	185	1964	2009	103	209

Table A2-2: AIC values for models assessing whether best fit function of relative size (either logarithmic or linear), using eqn. (2).

	Fit function	
	Linear	Log
All species	95517.8	**95143.6**
P. tremuloides	15541.6	**15343.1**
P. balsamifera	3374.1	**3369.7**
P. contorta	24333.2	**24158.5**
P. mariana	5877.7	**5875.7**
P. glauca	35831.3	**35635.4**
A. balsamea	**9656.8**	9666.4

Table A2-3: Effects of relative size, year, and absolute size on annual tree mortality probability by species. Values are parameter estimates with 95% confidence interval in brackets. logR is natural log transformed relative tree basal area, Y is calendar year, D is diameter at breast height. Model is defined in eqn. 2.

	Populus tremuloides	*Populus balsamifera*	*Pinus contorta*	*Picea mariana*	*Picea glauca*	*Abies balsamea**
Intercept	-3.520 (-3.596 - -3.444)	-3.504 (-3.658 - -3.349)	-4.197 (-4.276 - -4.117)	-4.339 (-4.504 - -4.173)	-4.428 (-4.511 - -4.345)	-3.917 (-4.054 - -3.780)
logR	-0.456 (-0.494 - -0.419)	-0.315 (-0.410 - -0.221)	-0.587 (-0.619 - -0.556)	-0.127 (-0.202 - -0.052)	-0.309 (-0.336 - -0.282)	0.126 (0.079 - 0.173)
Y	0.445 (0.408 - 0.482)	0.410 (0.332 - 0.489)	0.702 (0.668 - 0.735)	0.392 (0.321 - 0.463)	0.515 (0.488 - 0.543)	0.324 (0.278 - 0.371)
logR x Y	0.202 (0.169 - 0.235)	0.135 (0.060 - 0.211)	0.200 (0.174 - 0.226)	0.107 (0.042 - 0.172)	0.034 (0.011 - 0.057)	-0.026 (-0.067 - 0.015)

*Note: Relative size was linear for *Abies balsamea*

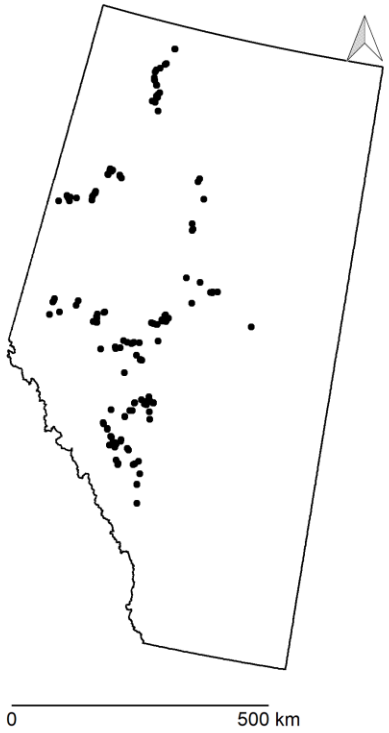

Fig. A2-1: Location of the 539 plots used in the study.

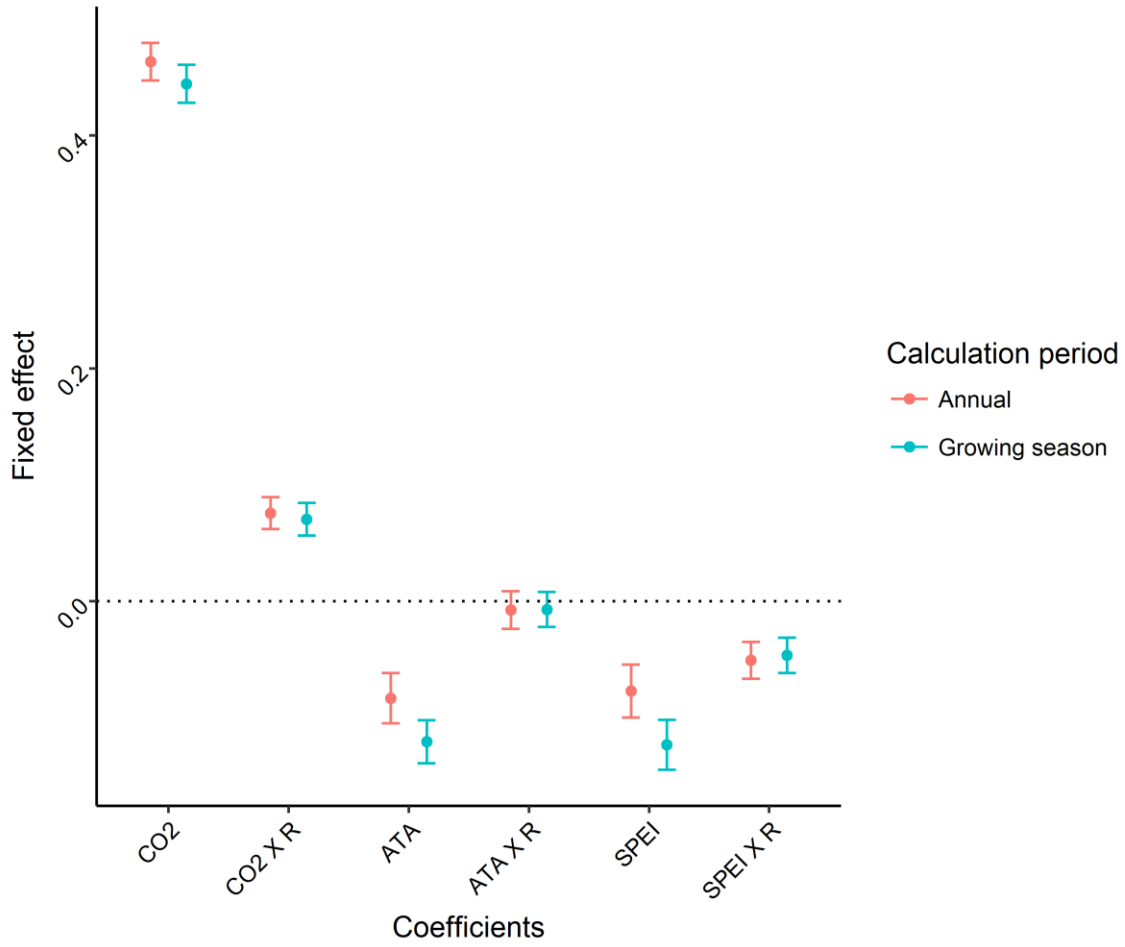

Fig. A2-2: Coefficients and 95% confidence intervals from the models using average annual and average growing season (May 1st to Sept 1st) temperature anomaly (ATA) and standardized precipitation-evapotranspiration index (SPEI). CO2 and R are described in Table 3-2

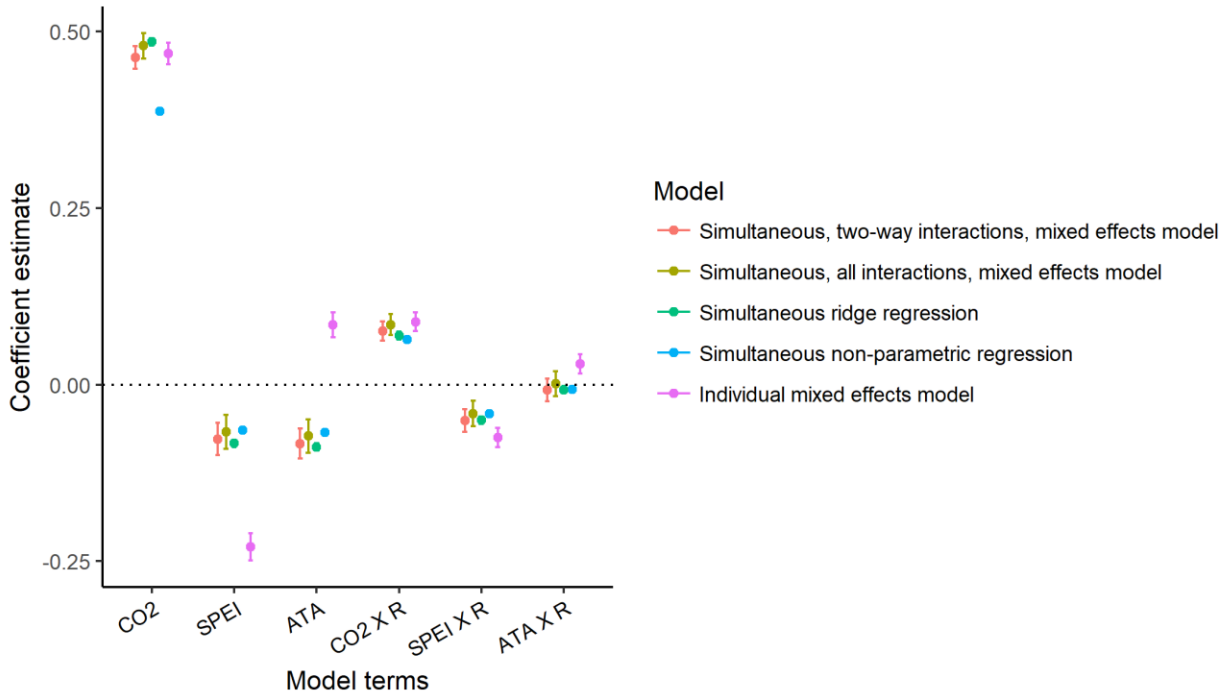

Fig. A2-3: Coefficient estimates of global change driver effects on annual tree mortality probability using five modelling approaches: simultaneous modelling of all drivers using generalised linear mixed effect model, simultaneous modelling of all drivers and all interactions using generalised linear mixed effect model, simultaneous ridge regression of all drivers, simultaneous non-parametric regression of all drivers, and individual modelling of drivers.

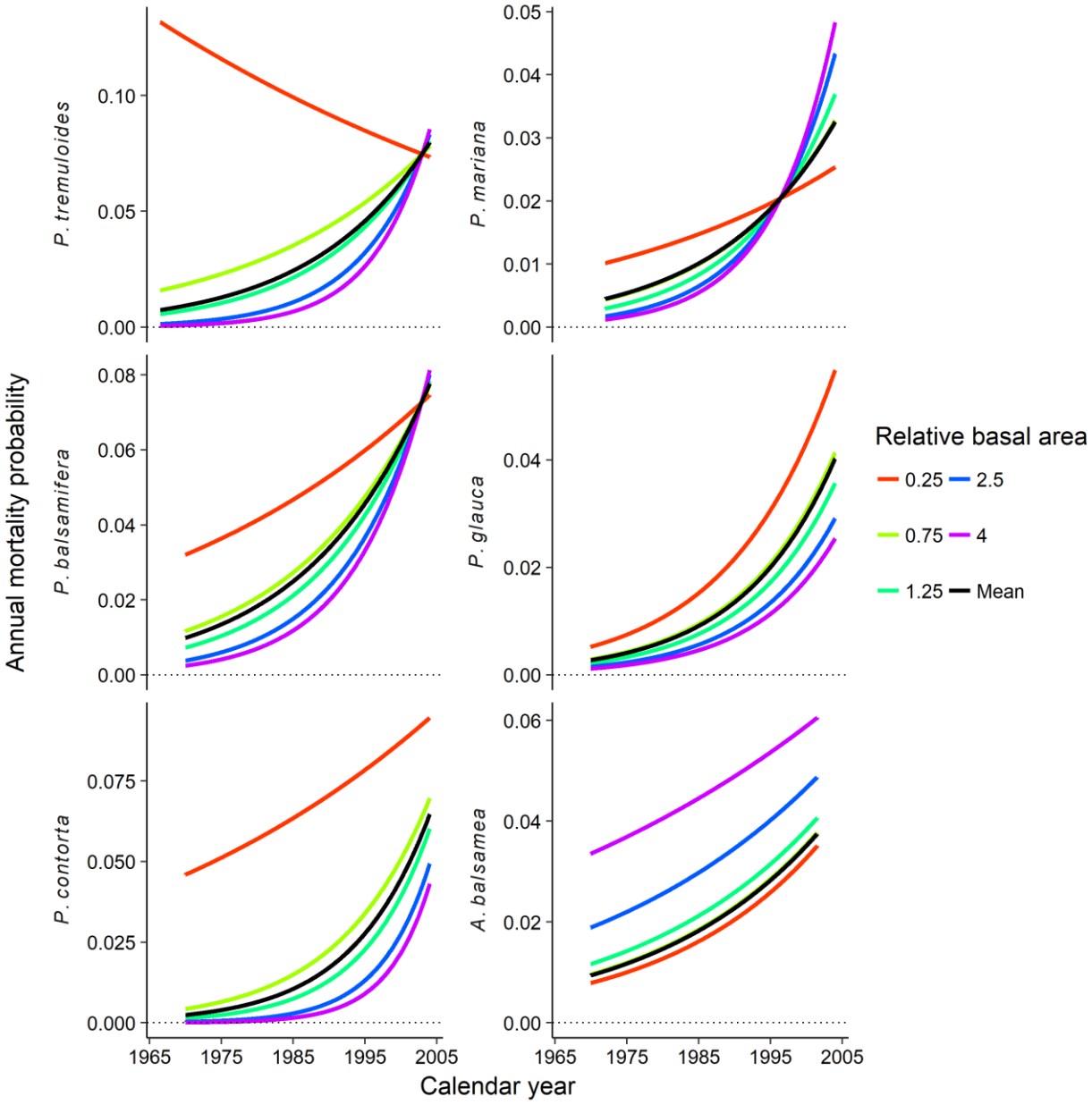

Fig. A2-4: Species-specific temporal trends in annual mortality probability by relative basal area. Black lines represent the responses at mean relative basal area. Only species with at least 1000 observations were modelled. Coefficient estimates and confidence intervals are presented in Table A2-3.

APPENDIX III: SUPPLEMENTAL INFORMATION FOR CHAPTER 4

Table A3-1: Effect of competition (*C*), year (*Y*), shade tolerance dissimilarity (*D*), phylogenetic dissimilarity (*P*), and stand age (*A*) on logarithmic basal area growth. Numbers are the mean coefficient estimate with bootstrapped 95% confidence intervals in brackets. Marginal R^2 (R^2m) refers to variation explained by the fixed effects alone and conditional R^2 (R^2c) refers to variation explained by both the fixed and random effects combined. Partial R^2 is estimated from the marginal R^2 times the relative sum of squares of fixed effects.

	Simultaneous model R^2m = 0.645, R^2c = 0.869			Shade tolerance dissimilarity only R^2m = 0.644, R^2c = 0.868			Phylogenetic dissimilarity only R^2m = 0.643, R^2c = 0.874		
Source	Estimate	Partial R^2	Sum of squares	Estimate	Partial R^2	Sum of squares	Estimate	Partial R^2	Sum of squares
Intercept	-0.613 (-0.678 - -0.550)	-	-	-0.600 (-0.663 - -0.538)	-	-	-0.541 (-0.608 - -0.475)	-	-
C	-1.414 (-1.422 - -1.405)	0.636	36018.8	-1.408 (-1.417 - -1.4)	0.623	36086.7	-1.394 (-1.402 - -1.385)	0.634	35428.8
Y	-0.018 (-0.027 - -0.009)	<0.001	4.7	-0.02 (-0.029 - -0.009)	<0.001	5.8	-0.032 (-0.042 - -0.023)	<0.001	16.0
D	0.093 (0.074 - 0.111)	<0.001	35.3	0.100 (0.084 - 0.117)	<0.001	51.0	-	-	-
P	0.013 (-0.004 - 0.031)	<0.001	0.7	-	-	-	0.010 (-0.007 - 0.027)	<0.001	0.5
C × *Y*	-0.006 (-0.011 - -0.002)	<0.001	2.6	-0.006 (-0.010 - -0.001)	<0.001	2.2	-0.022 (-0.026 - -0.018)	<0.001	35.6
D × *C*	0.151 (0.141 - 0.161)	0.006	351.7	0.160 (0.153 - 0.167)	0.011	633.6	-	-	-
D × *Y*	0.011 (0.004 - 0.017)	<0.001	3.6	0.035 (0.029 - 0.040)	0.001	66.2	-	-	-
P × *C*	0.011 (0.002 - 0.020)	<0.001	1.9	-	-	-	0.103 (0.095 - 0.110)	0.005	263.2
P × *Y*	0.037 (0.030 - 0.043)	<0.001	46.0	-	-	-	0.035 (0.030 - 0.039)	0.001	74.5
D × *C* × *Y*	-0.001 (-0.007 - 0.004)	<0.001	0.1	0.018 (0.014 - 0.022)	<0.001	29.0	-	-	-

P × *C* × *Y*	0.032 (0.027 - 0.038)	<0.001	43.3	-	-	-	0.026 (0.022 - 0.030)	<0.001	51.6
A	-0.139 (-0.164 - -0.11)	<0.001	30.4	-0.131 (-0.162 - -0.103)	<0.001	27.1	-0.135 (-0.165 - -0.107)	<0.001	29.3

Table A3-2: Effect of competition, climate drivers, neighbourhood diversity, and stand age on logarithmic basal area growth. Numbers are the mean coefficient estimate with bootstrapped 95% confidence intervals in brackets.

Coefficient	Estimate	Coefficient	Estimate	Coefficient	Estimate
Intercept	-0.647 (-0.721 - -0.577)	*Intercept*	-0.597 (-0.666 - -0.529)	*Intercept*	-0.553 (-0.621 - -0.487)
C	-1.415 (-1.424 - -1.407)	*C*	-1.421 (-1.43 - -1.412)	*C*	-1.407 (-1.416 - -1.399)
CO_2	-0.064 (-0.074 - -0.055)	*ATA*	-0.048 (-0.053 - -0.043)	*SPEI*	0.012 (0.007 - 0.016)
D	0.089 (0.070 - 0.108)	*D*	0.036 (0.019 - 0.055)	*D*	0.070 (0.052 - 0.087)
P	0.018 (-0.001 - 0.036)	*P*	0.026 (0.007 - 0.045)	*P*	-0.015 (-0.033 - 0.003)
C × CO_2	-0.018 (-0.022 - -0.013)	*C* × *ATA*	-0.037 (-0.041 - -0.033)	*C* × *SPEI*	-0.006 (-0.01 - -0.001)
D × *C*	0.152 (0.142 - 0.161)	*D* × *C*	0.118 (0.109 - 0.126)	*D* × *C*	0.138 (0.129 - 0.146)
D × CO_2	0.022 (0.015 - 0.028)	*D* × *ATA*	-0.007 (-0.012 - -0.001)	*D* × *SPEI*	0.016 (0.010 - 0.022)
P × *C*	0.012 (0.003 - 0.021)	*P* × *C*	0.027 (0.018 - 0.036)	*P* × *C*	0.001 (-0.007 - 0.010)
P × CO_2	0.039 (0.033 - 0.045)	*P* × *ATA*	0.043 (0.037 - 0.048)	*P* × *SPEI*	-0.007 (-0.012 - -0.001)
D × *C* × CO_2	-0.003 (-0.009 - 0.002)	*D* × *C* × *ATA*	-0.013 (-0.018 - -0.008)	*D* × *C* × *SPEI*	0.011 (0.005 - 0.016)
P × *C* × CO_2	0.037 (0.031 - 0.042)	*P* × *C* × *ATA*	0.041 (0.035 - 0.046)	*P* × *C* × *SPEI*	-0.001 (-0.006 - 0.005)

A	-0.016 (-0.044 - 0.015)	*A*	-0.109 (-0.124 - -0.093)	*A*	-0.194 (-0.211 - -0.179)

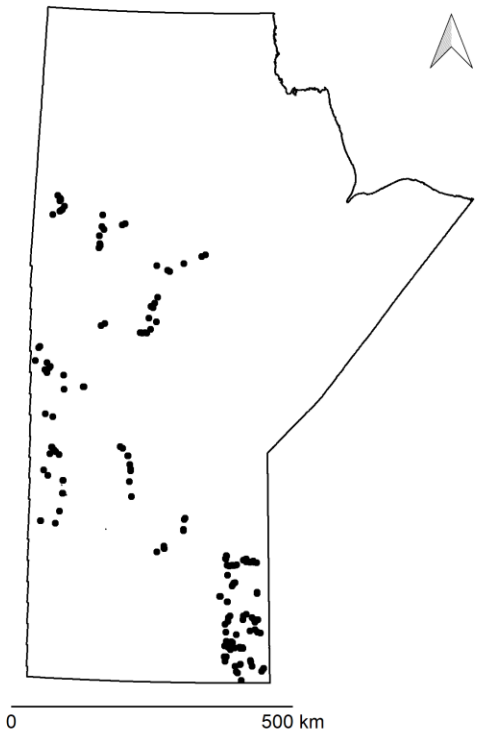

Fig. A3-1: Spatial location for all 180 permanent sample plots used in the study.

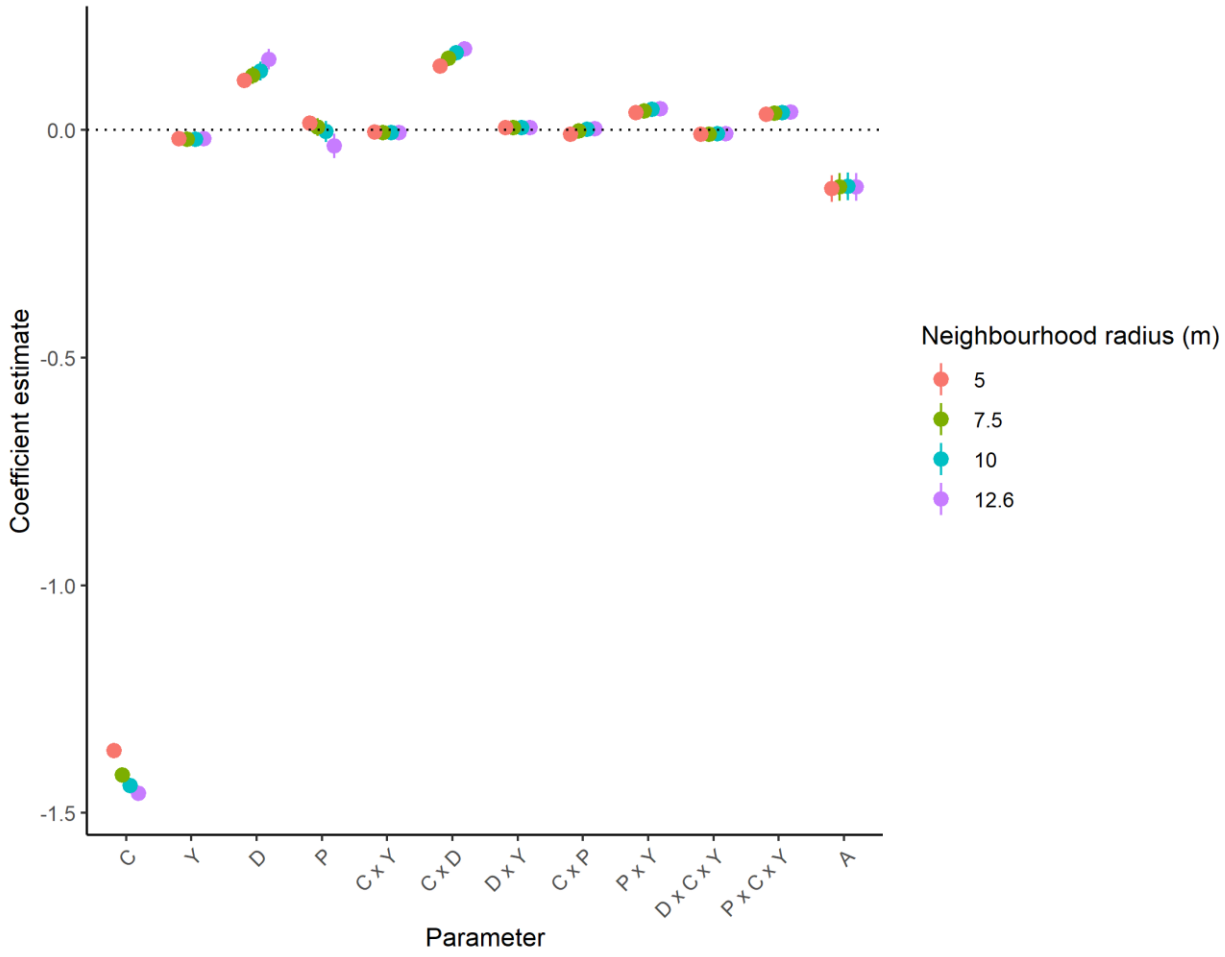

Fig. A3-4: Coefficient estimates and associated bootstrapped 95% confidence intervals from eqn. (3) using four neighbourhood radii to determine explanatory variables: 5, 7.5, 10, and the full plot radius of 12.6 metres.

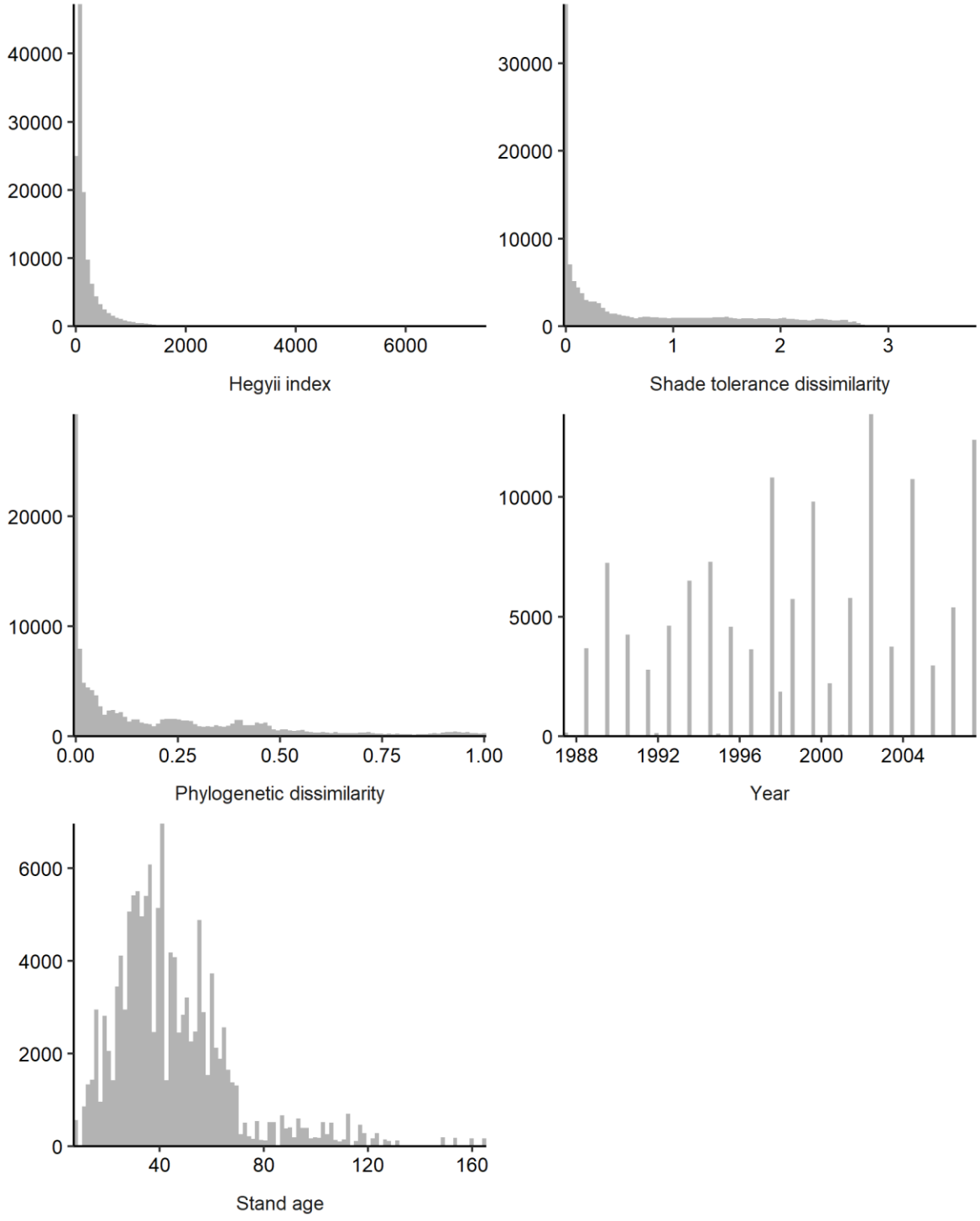

Fig. A3-3: Histograms of measured independent variables

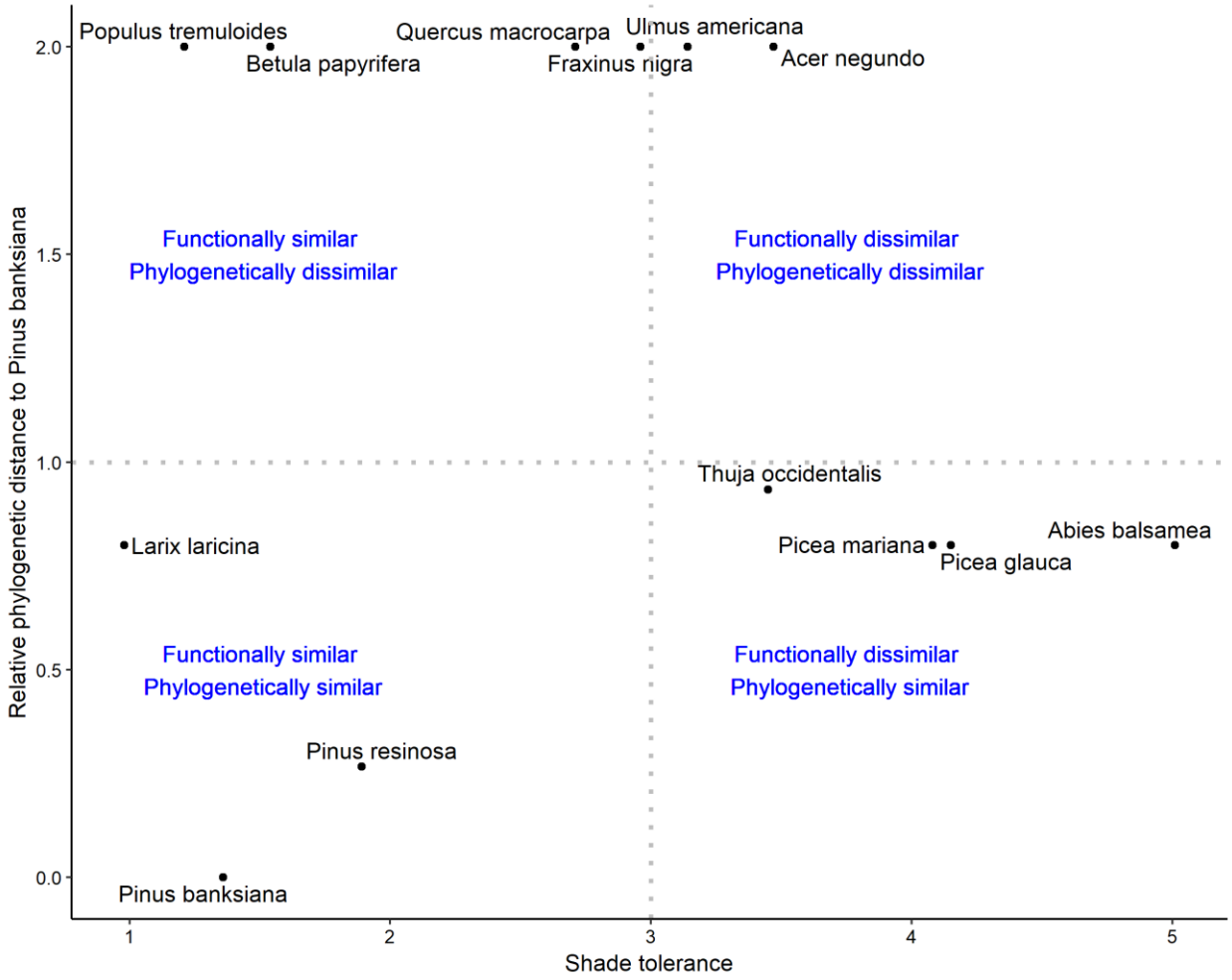

Fig. A3-4: Shade tolerance of each species *versus* phylogenetic similarity to *Pinus banksiana*. Species in the bottom left are functionally (i.e., similar shade tolerance values) and phylogenetically similar to *Pinus banksiana*; species in the top left are functionally similar but phylogenetically dissimilar to *Pinus banksiana*; species in the top right are functionally and phylogenetically dissimilar to *Pinus banksiana*; and, species in the bottom right are functionally dissimilar but phylogenetically similar to *Pinus banksiana*. The horizontal dotted line denotes the break between gymnosperms and angiosperms in the phylogeny while the vertical line is approximately the average shade tolerance observed in the dataset.

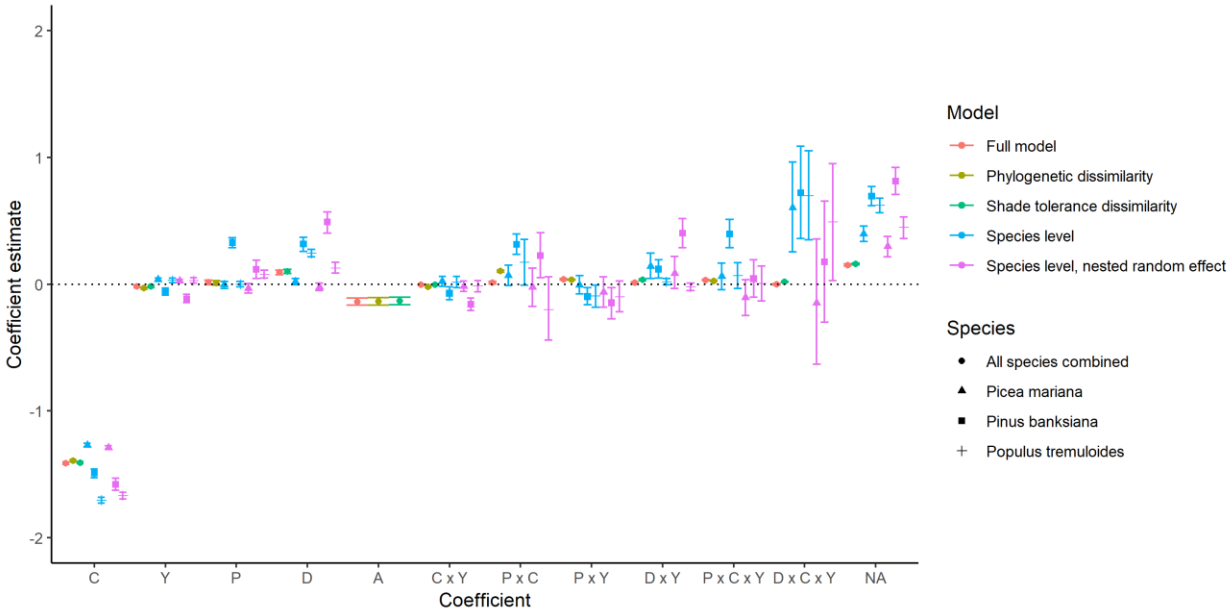

Fig. A3-5: Coefficient estimates and associated bootstrapped 95% confidence intervals from eqn. (3) using three different modelling approaches: full model with both shade tolerance and phylogenetic dissimilarity across all species, shade tolerance and phylogenetic dissimilarity modelled separately, and estimates from a nested species level model. The three major species (*Picea mariana*, *Pinus banksiana*, and *Populus tremuloides*) are shown for clarity, but models were fit including all species.

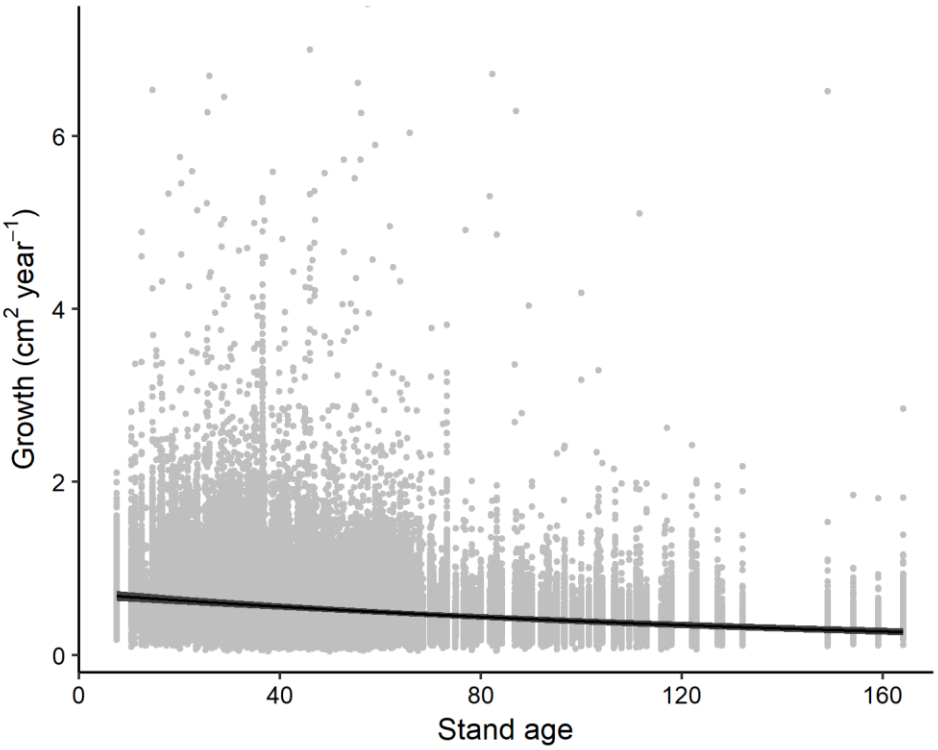

Fig. A3-6: Effect of stand age on individual focal tree growth. Solid black lines show average effects, with 95% confidence bands in grey. Background points are individual measurements of tree growth with the effects of all other predictors removed.

APPENDIX IV: SUPPLEMENTAL INFORMATION FOR CHAPTER 5

Table A4-1: Sampling intensity by biome. Biomes are a broad classification of ecosystems and forested regions can exist within biomes that are not designated as "forest". Forest area is calculated as the amount of area of each polygon in Figure 1 that contains at least 20% coverage of vegetation greater than 5m in height.

Biome	Plots	Observations	First Year of Census	Last Year of Census	Forest area (km^2)
Tropical and Subtropical Moist Broadleaf Forests	1531	1609	1985	2016	3321310
Tropical and Subtropical Dry Broadleaf Forests	79	98	2002	2016	720
Temperate Broadleaf and Mixed Forests	147696	180448	1925	2018	3834675
Temperate Conifer Forests	25763	36512	1955	2018	2023033
Boreal Forests/Taiga	14299	35084	1951	2016	5537113
Tropical and Subtropical Grasslands, Savannas and Shrublands	181	228	1985	2017	851208
Temperate Grasslands, Savannas and Shrublands	1862	2408	1986	2018	198615
Flooded Grasslands and Savannas	63	82	2002	2016	26916
Mediterranean Forests, Woodlands and Scrub	34024	34024	1916	2017	288511
Deserts and Xeric Shrublands	3056	3087	2000	2017	71518

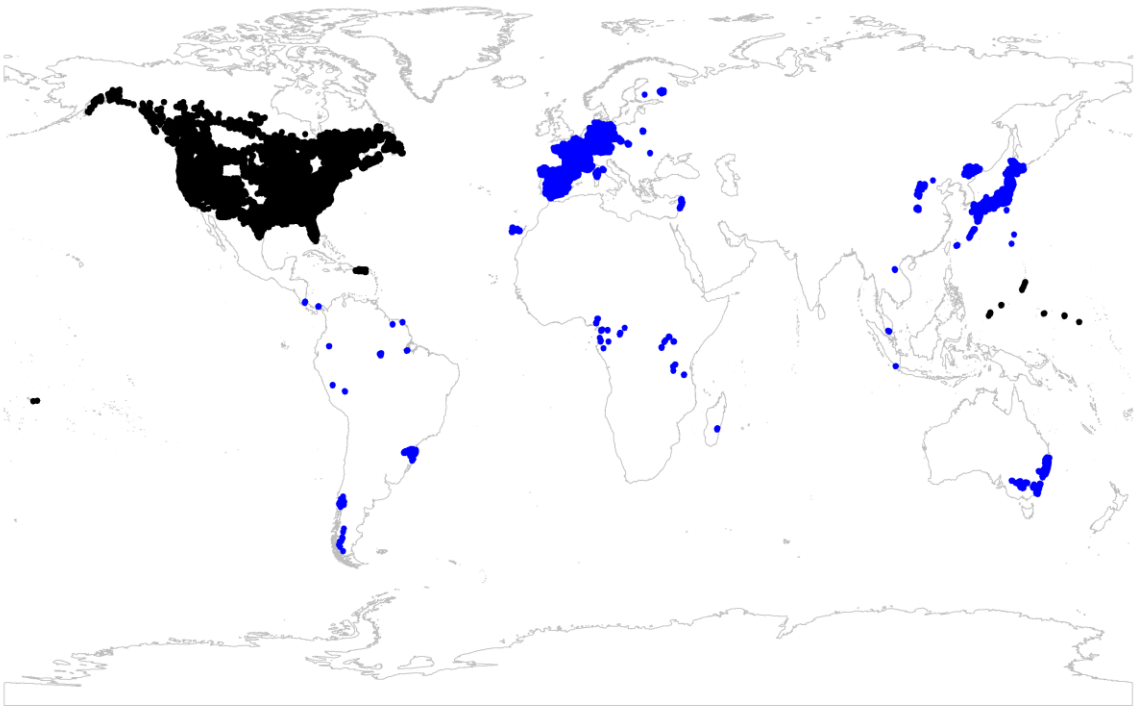

Fig. A4-1: Spatial location of all 228,554 plots included in the study. Tier 1 plots shown in black; Tier 2 plots shown in blue

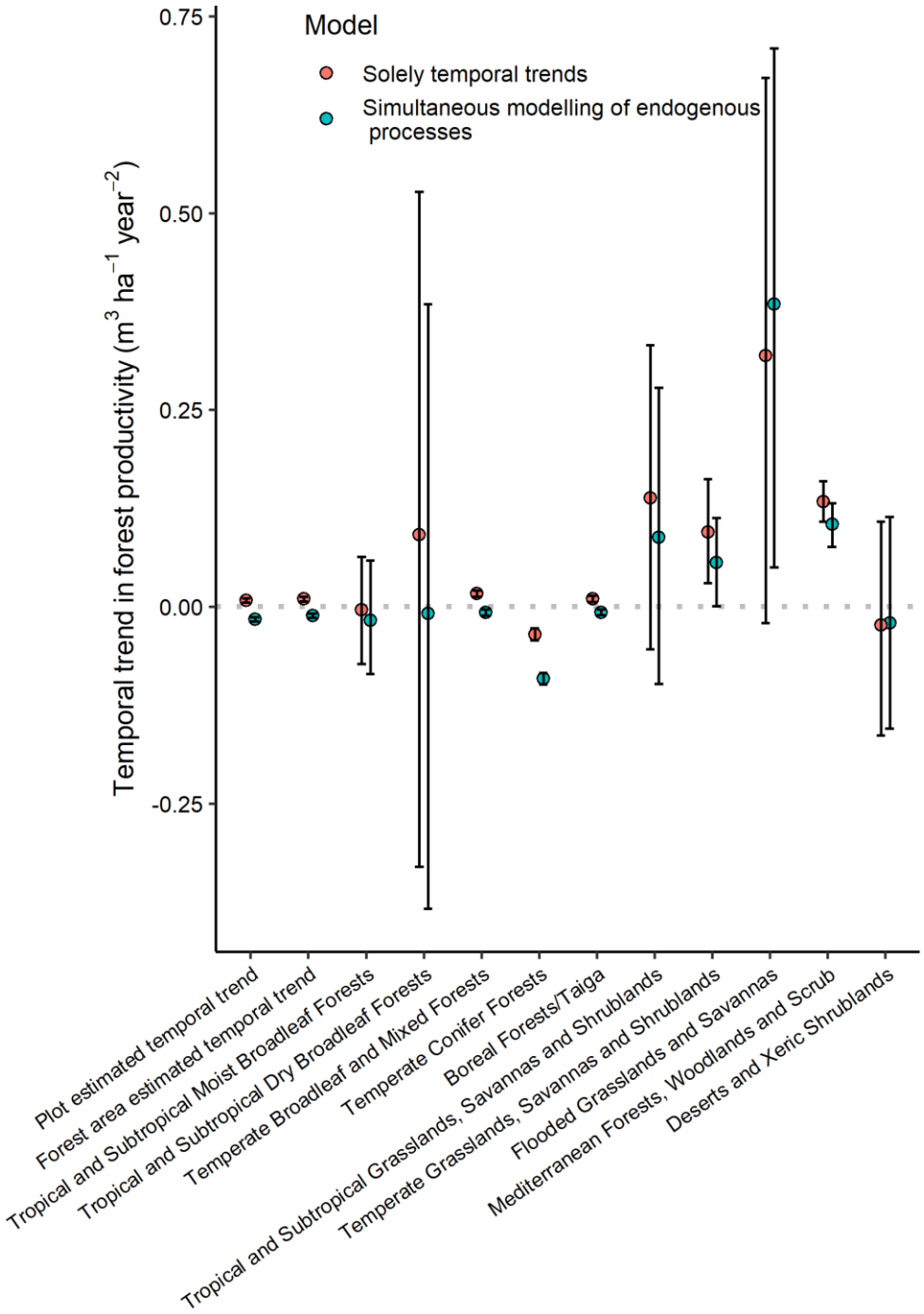

Fig. A4-2: Standardised coefficient estimates of temporal trend in forest productivity. Estimates are from overall temporal trend models and from models simultaneously modelling stand basal area. Points show mean estimate and bars represent bootstrapped 95% confidence intervals.

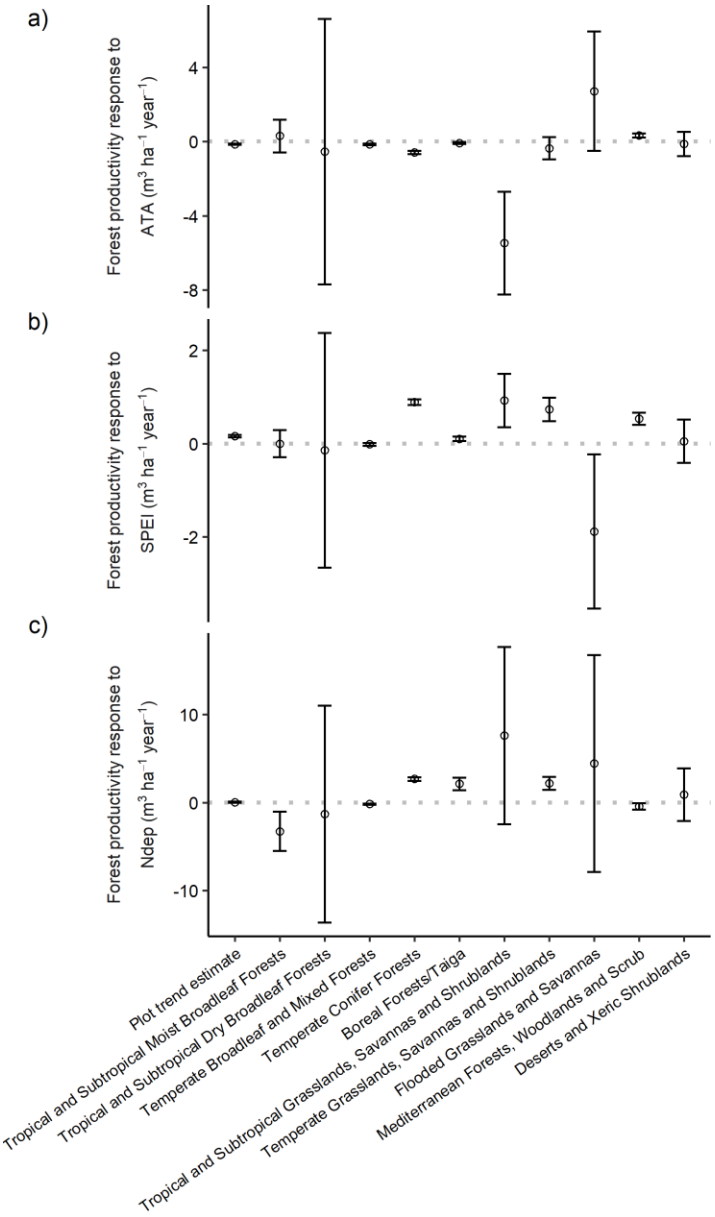

Fig. A4-3: Standardised coefficient estimates of climate driver trends in forest productivity. Response of forest productivity overall and by biome to: a) annual temperature anomaly; b) standardised precipitation-evapotranspiration index; and, c) Nitrogen deposition. Points show mean estimate and bars represent 95% confidence intervals determined using the Wald method from the *confint* function in the *lme4* package in R statistical software.

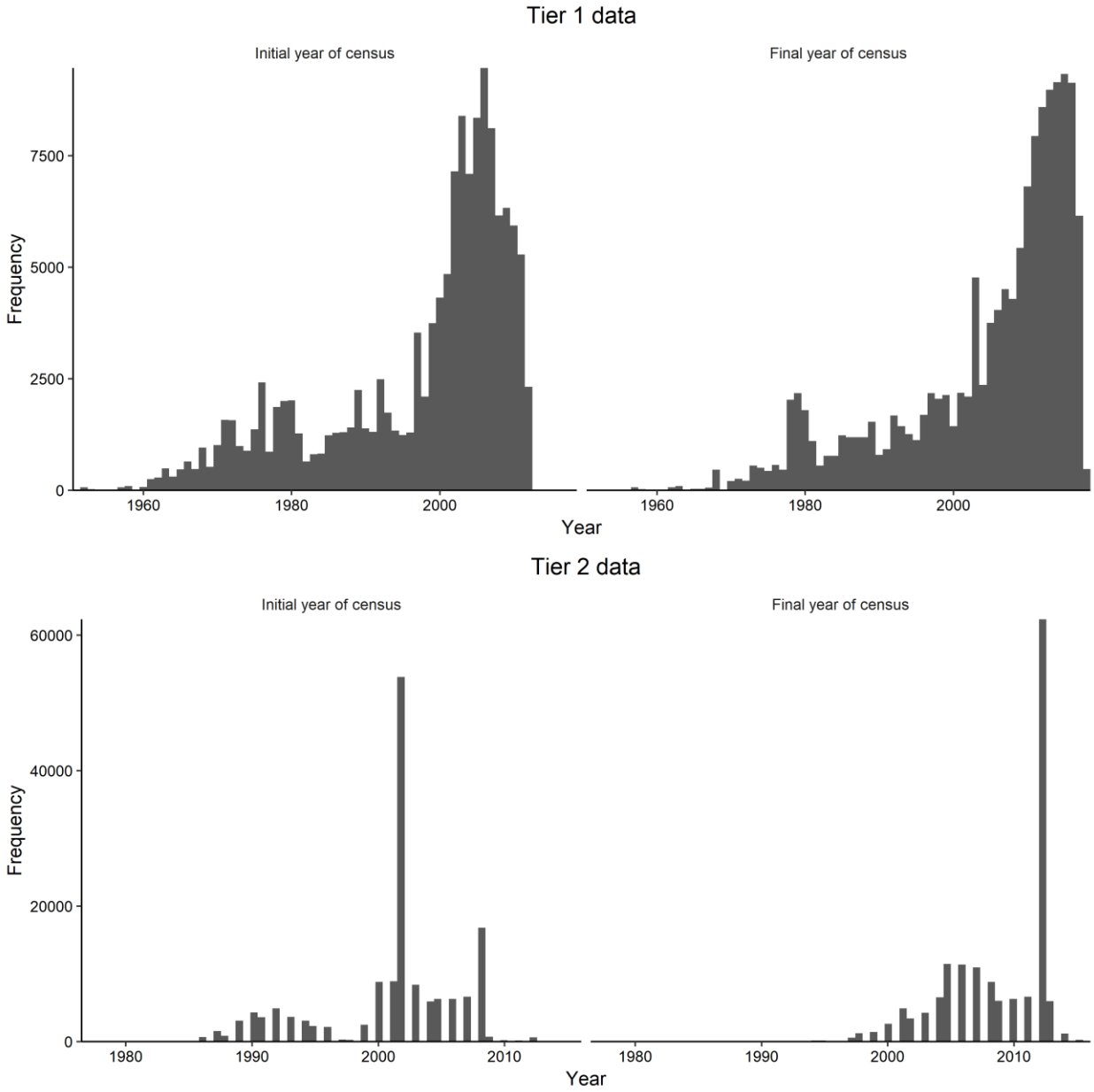

Fig. A4-4: First year and last year of census period for each plot measurement in Tier 1 and Tier 2 data.

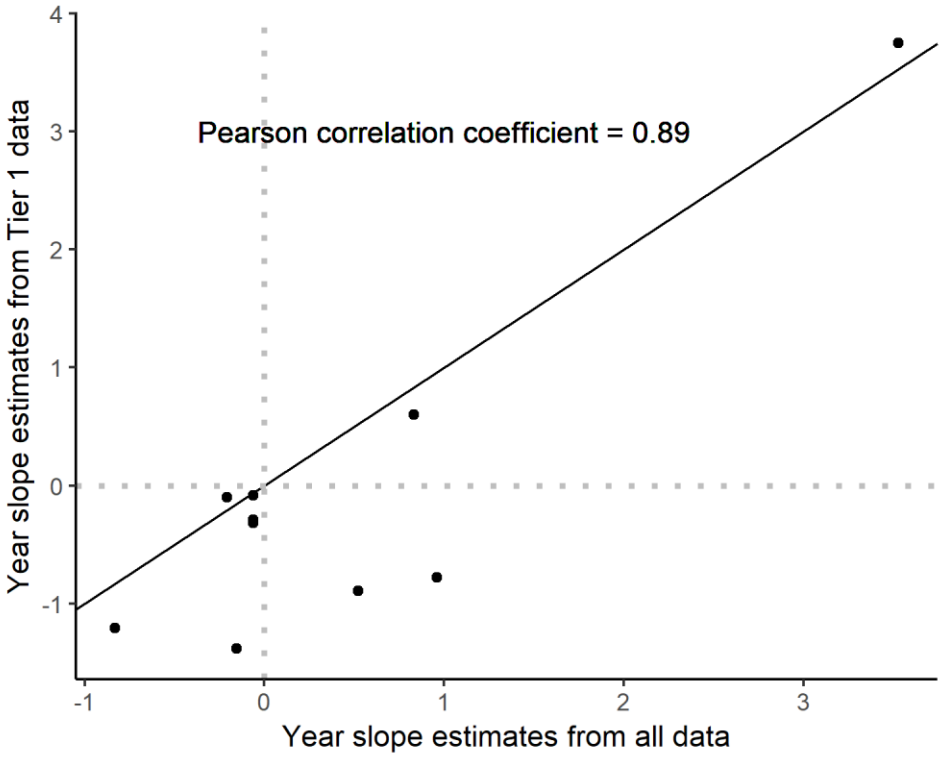

Fig. A4-5 Correlation between biome level temporal trend estimates fit by using Tier 1 data and fit with all data pooled. Background points represent estimates of temporal trends in forest productivity for each biome. Solid line is a 1 to 1 line, with dotted lines at x=0 and y=0.

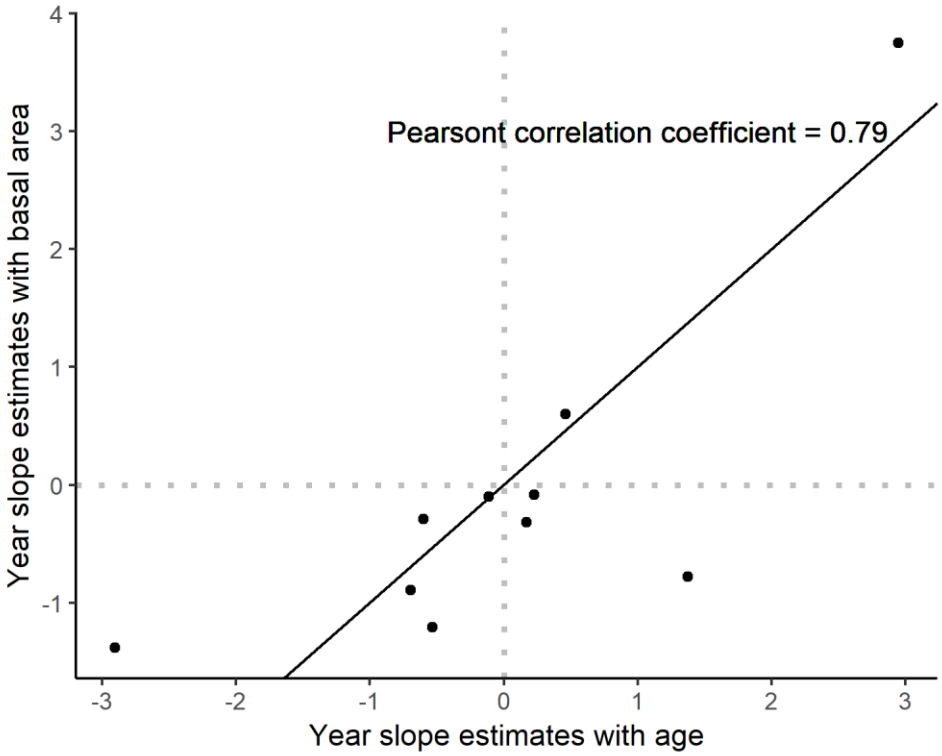

Fig. A4-6: Correlation between biome level temporal trend estimates in forest productivity while including stand basal area or stand age as a covariate. Background points represent estimates of temporal trends in forest productivity for each biome. Solid line has a slope of 1 and an intercept of 0 with dotted lines at x=0 and y=0.

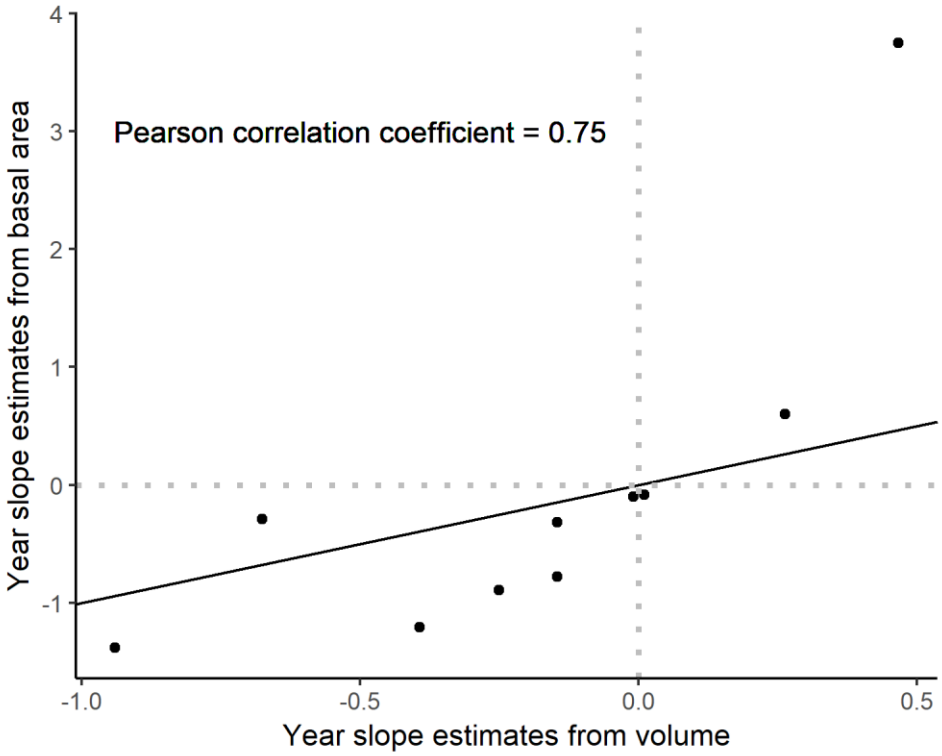

Fig. A4-7: Correlation between biome level temporal trend estimates in forest productivity estimated by volume and by basal area, using only Tier 1 data. Background points represent estimates of temporal trends in forest productivity for each biome estimated through use of volume or basal area. Solid line has a slope of 1 and an intercept of 0 with dotted lines at x=0 and y=0.